Novel Antimicrobial Restorative Materials for the Control of Dental Disease

A thesis submitted to Cardiff University

for the degree of Doctor of Philosophy

2018

Elen Pierce Everett

School of Dentistry

i fy Nhad

Acknowledgements

Pursuing my PhD has been an incredible challenge and it would not have been possible without the help and support of those around me. Firstly, I owe a huge deal of gratitude to my supervisors for giving me the opportunity to carry out this project: Prof. Alastair Sloan, Dr. Alison Paul, and Prof. Rachel Waddington. Their knowledge and advice has been invaluable in guiding my work and their door has always been open to me. Their encouragement and positivity has often been an antidote to my pessimism, and has inspired me to pursue a research career beyond my PhD.

I am grateful to my colleagues in the schools of Dentistry and Chemistry for all their support. In particular Dr. Wayne Ayre, for his training and advice; Dr. Genevieve Melling, for sharing my liposome-related woes; and Josh Twigg, who contributed clinical skill and expertise to part of this work. Hayley Pincott and Sue Wozniak have been of great help in the pathology lab, as has the advice of Dr. Adam Jones. I am also grateful for all the technical support from Lucy Marsh and Dr. Sarah Bamford in the microbiology lab, and from Dr. Rob Jenkins in the School of Chemistry. There have been many others who have lent a hand, an ear or a piece of equipment along the way, and I am very lucky to have worked with such a supportive group of people.

Daily life in the lab has been (mostly) made a joy by my wonderful friends: Dan, Emma, Clotilde, Josh, and of course my work wife Dally, who has never failed to brighten up my day through our 4 years of postgrad together. Together we've laughed (a lot), cried (a bit), and gotten through a ridiculous amount of coffee and crosswords.

Yr wyf wedi derbyn gymaint o gefnogaeth gan fy ffrindiau a fy nheulu. 'Rydych wedi codi fy nhgalon bob tro ddof adra, ac wedi tynnu fy sylw oddi wrth straen y PhD at bethau pwysicach fel cerdded y cŵn ar y traeth, croesawu babis newydd i'r byd, a gwario amser gwerthfawr hefo'n gilydd. In particular, thank you to Nain and Taid for their constant support; my sister Sarah and my brother Rhys, for never letting me get ideas above my station; Nigel, for his support and kindness; and to my Mam, whose strength inspires me every day. She has always encouraged me to be myself and to face life's challenges with determination and a sense of humour.

No words can express the contribution of my best friend and husband, Ali. Thank you for your endless love and patience, and for always believing in me, even when I don't. Dwi'n caru ti.

Funding & Presentations

This project was generously supported by a Health and Care Research Wales PhD studentship.

Work from this thesis has been presented at the following meetings:

Speaking of Science, Cardiff, May 2015
"Controlling Dental Disease with Jelly"
Elen P Everett, Rachel Waddington, Alison Paul, Alastair J Sloan

BSODR annual general meeting, Cardiff, September 2015
"Antimicrobial hydrogels for the control of pulpal disease"
Elen P Everett, Rachel Waddington, Alison Paul, Alastair J Sloan

CITER 3rd South West Regional Regenerative Medicine Meeting, Bristol, September 2015
"Antimicrobial hydrogels for the control of pulpal disease"
Elen P Everett, Rachel Waddington, Alison Paul, Alastair J Sloan

Cardiff Chemistry Conference, Cardiff, May 2016
"Antimicrobial Hydrogels For The Control Of Dental Disease"
Elen P Everett, Rachel Waddington, Alison Paul, Alastair J Sloan
Poster prize winner, 2nd place

TCES meeting, London, July 2016
"Antimicrobial hydrogels for the control of pulpal infection to facilitate regenerative endodontics"
Elen P Everett, Rachel Waddington, Alison Paul, Alastair J Sloan

M4 Colloids Symposium, Bath, July 2016
"Antimicrobial hydrogels for the control of pulpal infection to facilitate regenerative endodontics"
Elen P Everett, Rachel Waddington, Alison Paul, Alastair J Sloan

Chemistry: The science around us, Sheffield, July 2016
"Antimicrobial hydrogels for the control of dental disease"
Elen P Everett, Rachel Waddington, Alison Paul, Alastair J Sloan

CITER annual scientific meeting, Cardiff, September 2016
"Antimicrobial hydrogels for the control of dental disease"
Elen P Everett, Rachel Waddington, Alison Paul, Alastair J Sloan

School of Medicine and Dentistry Postgraduate Research Day, Cardiff, November 2016
"Development of an Antimicrobial Hydrogel to Manage Dental Disease"
Elen P Everett, Rachel Waddington, Alison Paul, Alastair J Sloan

IADR General Session, San Francisco, March 2017
"An antimicrobial hydrogel for the control of root canal infections"
Elen P Everett, Rachel Waddington, Alison Paul, Alastair J Sloan

IADR General Session, San Francisco, March 2017
"Physical analysis of an injectable hydrogel for endodontic drug delivery"
Elen P Everett, Rachel Waddington, Alison Paul, Alastair J Sloan

M4 Colloids Symposium, Cardiff, July 2017
"An injectable hydrogel for antimicrobial delivery to dental root canals"
Elen P Everett, Rachel Waddington, Alison Paul, Alastair J Sloan

BSODR annual general meeting, Plymouth, September 2017
"A novel, injectable hydrogel for endodontic antimicrobial delivery"
Elen P Everett, Rachel Waddington, Alison Paul, Alastair J Sloan

CITER annual scientific meeting, Cardiff, September 2017
"A novel, injectable hydrogel for endodontic antimicrobial delivery"
Elen P Everett, Rachel Waddington, Alison Paul, Alastair J Sloan
Winner, best oral presentation

Abstract

Recurrence and persistence of microbial infection is one of the main reasons for the revision of dental restorations in the clinic. Failure to control the pathogenic microbiota leads to the formation of caries, which in turn may lead to irreversible pulpal damage, resulting in the need for root canal (endodontic) therapy. Secondary endodontic infections can spread to the surrounding oral tissues and beyond, leaving the patient vulnerable to systemic infection. This project aimed to develop a novel, injectable hydrogel containing antimicrobial liposomes for use as an intracanal medicament in order to reduce the incidence of secondary endodontic infections.

Triclosan, a broad-spectrum, hydrophobic antimicrobial drug, was shown to have a bacteriostatic and bactericidal effect against two oral pathogens, *Enterococcus faecalis* and *Streptococcus anginosus*, which were grown planktonically and as a single-species biofilm. The bacteriostatic effect was also seen when triclosan was encapsulated in multilamellar vesicles (MLVs) and small unilamellar vesicles (SUVs) of phosphatidylcholine:cholesterol (PC:C) liposomes. Antimicrobial efficacy was associated with a high drug:lipid ratio in the liposomes.

The liposomes were incorporated into a methyl cellulose (MC) solution, and the rheological properties were measured. MC was a sheer-thinning, viscous solution at ambient temperature and formed a hydrogel as the temperature was increased above 30 °C. These properties were unaffected by the addition of liposomal MLVs or SUVs. The hydrogels containing triclosan-loaded liposomes had an antimicrobial effect when incubated in contact with suspensions of *E. faecalis* or *S. anginosus*, but MC containing triclosan only did not. A release assay showed the release of triclosan from MC loaded with triclosan liposomes, which was not seen when triclosan was incorporated into MC alone.

The liposomal hydrogel was injected into endodontically prepared extracted human teeth that had been inoculated with *E. faecalis* suspension to mimic endodontic infection. After 24 h treatment, histological analysis showed that triclosan solution, triclosan liposomes and triclosan liposomes in MC prevented the formation of a biofilm on the intraroot surface, which was observed in controls that underwent no treatment or treatment with MC hydrogel only.

The results of this work indicated that triclosan liposomes have potential to prevent secondary endodontic infections and may be loaded into a hydrogel suitable for injection into the root canal and subsequent gelation upon thermoequilibriation with the oral cavity. Triclosan release from this hydrogel may facilitate the prevention of bacterial colonisation of the root canal by *E. faecalis*, which has high prevalance in secondary endodontic infections.

List of Abbreviations

3D	3-dimensional
ALP	Alkaline phosphotase
BHI	Brain heart infusion
BLAST	Basic Local Alignment Search Tool
BMP	Bone morphogenic protein
C	Cholesterol
$Ca(OH)_2$	Calcium hydroxide
CEM	Calcium-enriched cement
DLS	Dynamic light scattering
DMP	Dentine matrix acidic phosphoprotein
DNA	Deoxyribonucleic acid
DS	Degree of substitution
DSPP	Dentine sialophosphoprotein
ECM	Extracellular matrix
EDTA	Ethylenediaminetetraacetic acid
EPS	Extracellular polysaccharide
FabI	Enoyl-acyl carrier protein reductase I
FabK	Enoyl-acyl carrier protein reductase K
GUV	Giant unilamellar vesicle
H&E	Haemotoxylin and eosin
H_2O	Water
HPLC	High performance liquid chromatography
IgG	Immunoglobulin G
IL	Interleukin

IPA	Propan-2-ol
LPS	Lipopolysaccharide
LUV	Large unilamellar vesicle
LVE	Linear viscoelastic
MAPK	Mitogen-activated protein kinase
MBC	Minimum bactericidal concentration
MBEC	Minimum biofilm eradicating concentration
MC	Methyl cellulose
MHC	Major histocompatibility complex
MI	Mechanical instrumentation
MIC	Minimum inhibitory concentration
Micro-CT	Micro-computed tomography
MLV	Multilamellar vesicle
MMP	Matrix metalloproteinases
MPS	Mononuclear phagocyte system
MTA	Mineral trioxide aggregate
MVV	Multivesicular vesicle
NaClO	Sodium hypochlorite
NHS	National Health Service
OD	Optical density
Pa.s	Pascal seconds
PBS	Phosphate-buffered saline
PC	Phosphatidylcholine
PCR	Polymerase chain reaction
PDI	Polydispersity index
rRNA	Ribosomal ribonucleic acid
RT	Retention time
SAG	*Streptococcus anginosus* group
SUV	Small unilamellar vesicle

TEM Transmission electron microscopy

TGF Transforming growth factor

TLR Toll-like receptor

TNF Tumour necrosis factor

TSA Tryptone soya agar

UV Ultraviolet

VPT Vital pulp therapy

VWD Variable wavelength detector

Contents

List of Figures

List of Tables

Chapter 1

General Introduction

1.1 Introduction

Persistence and recurrence of polymicrobial infections in the tooth are common reasons for the failure of dental restorations, including endodontic (root canal) fillings (Bernardo *et al.*, 2007; Tabassum and Khan, 2016). Most dental infection begins with the formation of caries (tooth decay) on the tooth's enamel, and this leads to the exposure of internal dental tissues to the oral cavity, which in turn can allow for the invasion of bacteria into the dental pulp. Pulpal infection leads to irreversible damage and necrosis of the pulpal tissue and the remaining cavity becomes a reservoir for bacteria and their by-products. Infection can spread to the surrounding periodontal tissues, leading to tooth loss and the risk of systemic infection. Tooth loss may have a significant impact on an individual's quality of life: causing social and aesthetic embarrassment, poorer diet, problems with speech and deterioration of the surrounding oral tissues (Saintrain and de Souza, 2012). Treatment of pulpal disease poses significant challenges and it is often necessary to perform endodontic treatment: removing the entirety of the dental pulp and replacing it with an inert material. This treatment is technically challenging, time-consuming and costly to the NHS and to individual patients. The NHS in England and Wales annually spend around £266 million providing around 12 million dental restorations, many of which are replacing failed restorations from previous treatment (Lynch and Wilson, 2013). The 10-year

survival rate of dental restorations is around 50 %, with root fillings having a shorter life span than other restorations (Burke *et al.*, 2005; Lucarotti *et al.*, 2014). Failure is usually due to the persistence of microbial infection that was not eradicated during treatment or the recurrence of infection (secondary infection) following bacterial leakage around the restoration. Currently, the use of antimicrobial materials is limited in dental treatment and systemic antibiotics are not effective in treating pulpitis or periodontitis. There is therefore a need to develop new therapeutic treatments that can control dental infection and prevent re-infection, thus extending the life of the restoration. This project aims to build on previous work in developing a dental restorative material that has effective antimicrobial properties. Ultimately, this material should aim to:

1. Limit bacterial re-infection following restorative dental treatment and reduce the number of restorations that fail due to secondary infection;

2. Reduce the need for further and more complex treatment or tooth extraction;

3. Reduce the need to use systemic antibiotics, which are often ineffective against the polymicrobial infections found in the tooth;

4. Reduce the cost of dental restorations to the NHS as well as individual patients.

Specifically, the project will aim to achieve controlled release of a broad-spectrum antimicrobial at a clinically significant dose from a novel restorative material. This material will be a biocompatible hydrogel that can incorporate liposomal triclosan, so a 2-tier delivery mechanism is employed, both from the liposomes and from the gel itself. Previous work has demonstrated that liposomes containing triclosan can prevent and treat infection by *Streptococcus anginosus* in an *ex vivo* rat pulp infection model and that liposomal triclosan is more effective than the drug alone. It has also been incorporated into glass ionomer cement, a material commonly used in dental restorations (unpublished). This project aims to build on this work by further characterising triclosan release from liposomes and assessing their effect on endodontic infections *ex vivo*, by developing a human root canal infection model. It will also aim

to introduce the liposome into hydrogel systems and assess the rheological and drug release properties of these formulations.

1.2 Dental function and anatomy

1.2.1 Function of teeth

Human teeth primarily function to mechanically prepare food for digestion, although they also play an important role in speech. Aesthetically, teeth are important and are often visually referred to in order to judge another persons attractiveness and general hygiene (liana Eli *et al.*, 2001). Humans develop 2 sets of teeth in their lifetime, and therefore the secondary, permanent dentition must have longevity. The tooth must be hard and well rooted in order to perform its function. Enamel, the outer layer of the tooth, is the hardest tissue in the body but is also very brittle. It is supported by the less mineralised dentine layer, which is produced and maintained by the dental pulp. The teeth are kept firmly attached to the jaw bones by the periodontal ligament, as shown in Figure 1.1 (Nanci, 2013).

1.2.2 Enamel

Enamel is the protective material of the crown of the tooth and its maintenance and/or repair is key to maintaining dental health (Featherstone, 2000). Enamel is produced by ameloblasts, which reside on the dentine-enamel junction of the developing tooth and regulate the secretion of a layer of proteins and proteinases, including amelogenin and enamelin (Gallon *et al.*, 2013). These proteins will then control the nucleation, growth and organisation of hydroxyapatite crystals, forming a highly ordered, mineralised tissue (Iijima *et al.*, 2010). Mature enamel is composed of around 96 % hydroxyapatite crystals, with the rest consisting of water and organic matter.

After enamel is formed, it cannot be regenerated naturally, due to the loss of ameloblasts after tooth development. Many ameloblasts undergo cell death by apoptosis and regression, and the remaining cells are either shed during tooth eruption,

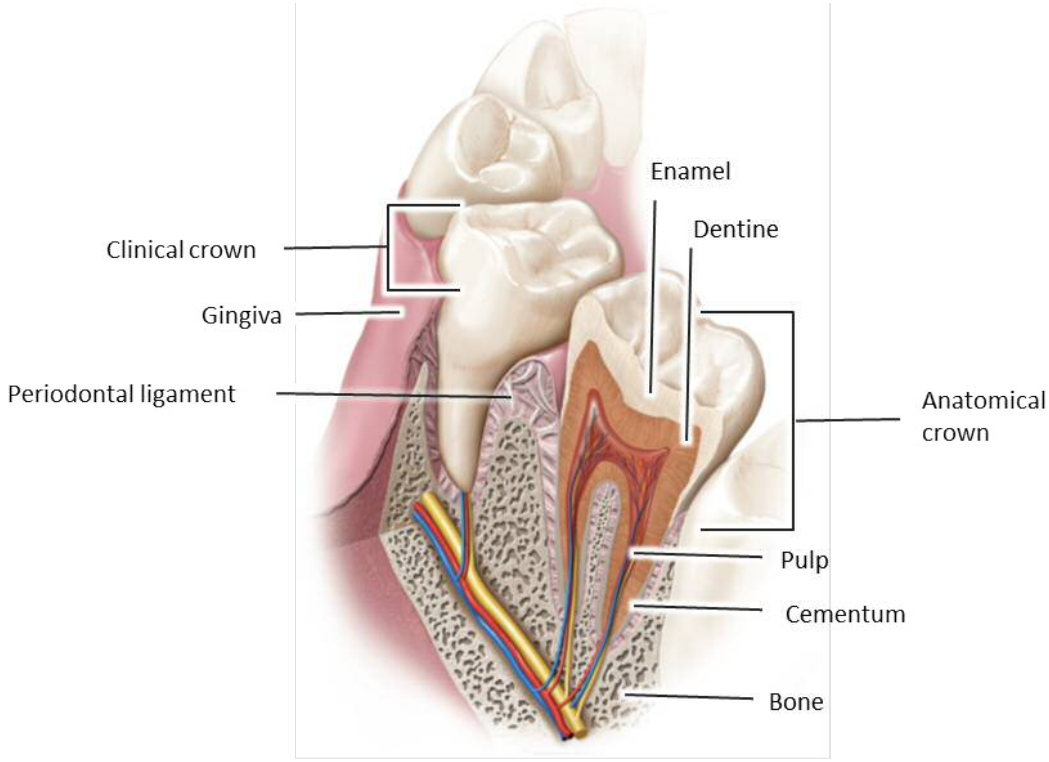

Figure 1.1: **Anatomy of human tooth and surrounding tissues.** Illustration adapted from Nanci (2013)

.

or incorporated into the tooth's epithelial attachment to the oral gingiva (Lacruz *et al.*, 2017). It has been shown that enamel can be produced *in vitro* from adult human gingival epithelial cells and contains ameloblast-like cells, confirmed by histology, micro-computed tomography (micro-CT) and immunohistochemistry for human major histocompatibility complex (MHC) class 1 protein (Angelova Volponi *et al.*, 2013).

Enamel is relatively impermeable but can be affected by acid produced by plaque-dwelling bacteria. The organic enamel matrix surrounding the apatite crystals has a relatively high water content and so it is permeable to hydrogen ions (Cawson and Odell, 2008). This causes acid erosion of enamel and the development of dental caries, which is one of the most prevalent chronic diseases of humans worldwide (Selwitz *et al.*, 2007).

1.2.3 Dentine

Below the enamel lies another mineralised layer, dentine, which forms the bulk of the tooth and provides structural support. Dentine is produced by pulpal cells, the odontoblasts, which unlike ameloblasts will remain as a constant source of dentine production for the lifespan of the tooth (Couve, 1986; Sloan *et al.*, 1998; Sloan and Waddington, 2009). Odontoblasts are tall, columnar cells located at the periphery of the dental pulp. They derive from ectomesenchymal cells originated by migration of neural crest cells during the early craniofacial development (Nanci, 2013). During dentine production (detinogenesis), they initially secrete a matrix (predentine) consisting of collagenous (primarily collagen type I) and non-collagenous proteins. The odontoblasts then control the mineralisation of this matrix, resulting in tissue composed of around 50 % v/v mineral (mainly hydroxyapatite); 30 % v/v organic matter (largely type I collagen); and about 20 % v/v fluid, which is similar to plasma and contains albumin, fibrinogen and immunoglobulin G (IgG) (Knutsson *et al.*, 1994; Marshall *et al.*, 1997). Primary dentinogenesis occurs during tooth development and involves relatively rapid dentine production. Secondary detinogenesis occurs after tooth eruption and is characterised by a lower rate of deposition and a different gene expression profile, including the up-regulation of matrix proteins osteocalin and dentine matrix acidic phosphoprotein-1 (DMP-1) and down-regulation of collagen type I and dentine sialophosphoprotein (DSPP), among others (Simon *et al.*, 2009).

As dentine is formed, the odontoblasts leave behind cell processes, which form the scaffold for tubule formation within the dentine. These long tubules follow the path of the progressing odontoblasts which make dentine a hard but highly porous tissue. Fibrillar structures are present within the tubules, which were originally posited to be branches or ramifications of the odontoblast processes (Szabo *et al.*, 1984), but have more recently been suggested to anchor the odontoblast processes inside the tubules (Garcés-Ortíz *et al.*, 2015). It has been observed that the odontoblast processes can extend through the entire thickness of the dentine, up to the dentine-enamel junction (Fox *et al.*, 1984) . The presence of the odontoblast process makes dentine

a vital tissue that can respond to external stimuli such as pressure and temperature (Pashley *et al.*, 1981; Camps and Pashley, 2003). The porous structure of dentine has important implications in pathogenesis. Without the protection of the enamel, the dentine is readily permeable to bacteria and their products, which can then progress to the pulp, causing inflammation and infection known clinically as pulpitis. The collagen-rich nature of both dentine and pulp allows for the attachment of bacteria posessing collagen-binding proteins, such as some *Streptococcus* species (Avilés-Reyes *et al.*, 2017).

1.2.4 Pulp

Pulp is a non-mineralised connective tissue that resides in the centre of the tooth in the pulpal chamber. It consists mainly of fibroblasts, with the dentine-forming odontoblasts lining the periphery. It also contains blood vessels, nerves and a number of other cell types, including immune cells and mesenchymal progenitor cells. The progenitor cells are pluripotent and can differentiate into a number of cell types including odontoblasts (Gronthos *et al.*, 2002).

Pulp fibroblasts secrete an extracellular matrix (ECM) consisting mainly of collagens type I and III and glycoproteins such as chondroitin sulphate and hyaluronic acid (Goldberg and Smith, 2004). The ECM acts as support for the fibroblasts and also mediates many of the cellular interactions, as cell metabolites, nutrients and waste pass through the matrix between the different cell types present in the pulp. In incidences of pulpitis, the matrix can act as a source of nutrients for invading bacteria, whilst the collagen components provide an anchor to which many bacteria can attach, as previously mentioned (Section 1.2.3). Roberts *et al.* (2013c) found that *Streptococcus anginosus* group bacteria could attach directly to dental pulp when co-cultured with rat tooth slices *ex vivo*. Additionally, the ECM directly adjacent to these showed signs of degradation, possibly due to the bacteria's synthesis of enzymes hyaluronidase and chondroitin sulfatase (Jacobs and Stobberingh, 1995). This highlights the importance of preventing bacterial infiltration into the pulpal chamber

in order to prevent destruction and necrosis of the tissue.

1.2.5 Dentine-pulp complex

Anatomically, dentine and pulp are distinguishable from one another due to differences in their structure and mineralisation, but they are functionally and embryologically considered together as the dentine-pulp complex. Pulp produces the dentine that surrounds it and also produces new dentine when required. The pulp also nourishes the avascular dentine and it is the nerves of the pulp that give the dentine its sensitivity in order to react to external stimuli. The odontoblasts act as the pulp's first line of defence, with processes that line the dentinal tubules able to sense the presence of bacteria and trigger an immune respose from the pulp before the bacteria have reached the pulpal chamber. This was investigated by Veerayutthwilai *et al.* (2007), who cultured tooth crowns with their odontoblasts *ex vivo* and observed that odontoblasts can identify and differentiate between Gram-positive and Gram-negative bacteria through toll-like receptors 2 and 4 (TLR2/TLR4) to initiate an immune response. One response is the rapid secretion of dentine, known as tertiary dentinogenesis.

1.2.5.1 Tertiary dentinogenesis

The dynamic nature of the dentine-pulp complex can be seen during pathogenesis. Injury or infection of the tooth leads to the exposure of the dentine-pulp complex to the oral cavity and leaves it susceptible to further infection and tissue damage. The pulp reacts by producing new dentine termed tertiary dentine. Tertiary dentine is different from primary and secondary dentine (Section 1.2.3) in that it is produced as a result of an environmental stimulus. Its structure depends on the severity of the stimulus and the speed at which the dentine matrix is secreted, with some examples being barely distinguishable from primary or secondary dentine, and other examples having a highly irregular, atubular structure, with cells trapped within it (Smith *et al.*, 2003). In cases of rapidly progressing dental caries, tertiary dentinogenesis

may not take place at all (Bjørndal, 2001).

There are 2 types of tertiary dentinogenesis, as defined by Smith *et al.* (1995):

Reactionary dentinogenesis is performed by post-mitotic odontoblasts that survive the initial injury or infection.

Reparative dentinogenesis occurs when a new generation of odontoblasts develop from progenitor cells in response to the death of the original odontoblasts.

Reactionary dentinogenesis is considered to be a similar process to primary dentinogenesis, as it is simply an up-regulation of the events that occur during tooth development (Smith and Lesot, 2001). It is only the source of the stimulus that is different between both events, however in some cases this may be similar too. The stimuli for reactionary dentinogenesis include growth factors such as transforming-growth factor β (TGFβ). TGFβ may be expressed by odontoblasts throughout the lifetime of the cells (Sloan *et al.*, 2000), and is believed to be sequestered by dentine as it has been found to be present using a bioassay (Finkelman *et al.*, 1990). Upon carious demineralisation of the dentine, this growth factor is solubilised and can act as a trigger for the up-regulation of dentine matrix secretion by the odontoblasts (Tziafas and Papadimitriou, 1998). As well as similar stimulatory molecules, it is also suggested that reactionary dentinogenesis is mediated by similar processes to primary dentinogensis. Simon *et al.* (2010) stimulated odontoblast-like cells with *Streptococcus mutans*, as well as growth factors known to stimulate reactionary dentinogenesis, to investigate this. They observed activation of the p53 mitogen-activated protein kinase (MAPK) pathway, which is also active during primary (but not secondary) dentinogenesis.

Reparative dentinogenesis is a more complex process than reactionary dentinogenesis: it requires division, migration and differentiation of pulp progenitor cells to occur, in order to replenish the odontoblast layer that is lost due to significant trauma (Cooper *et al.*, 2010). These processes are mediated by a host of signalling molecules, including members of the TGFβ family and bone morphogenic proteins (BMPs), as reviewed by (Kim, 2017). The range of regenerative responses is diverse

and dependent on the severity of the trauma, resulting in a range of dentine morphologies (Smith *et al.*, 2005). Reparative dentine is even disputed to be true dentine by some: Ricucci *et al.* (2014) histologically examined human teeth that had been exposed to different levels of trauma, and suggested that the reparative dentine was in fact more akin to a calcified scar tissue produced by pulpal fibroblasts, due to the lack of tubules and the absence of odontoblast-like cells adjacent to the calcified tissues.

Both reactionary and reparative dentinogenesis ultimately involve the rapid secretion of a dentine matrix in order to create a physical barrier between the pulp and the negative stimulus, such as microbial invasion. Where this process fails, the pulpal cells are exposed to infection and react to this in an inflammatory response.

1.2.5.2 Pulpal inflammation

Pulpal inflammation occurs as a result of the infiltration of bacteria and/or their products into the dentine-pulp complex. As previously stated (Section 1.2.3), molecular attachment to TLRs on the odontoblast processes induces an immune response but a response can also be induced before direct bacterial contact, through the acid erosion of dentine and the release of growth factors such as TGFβ (Section 1.2.5.1). Bacterial lipopolysaccharide (LPS) also plays a significant role in the dentine-pulp immune response. LPS is a major component of the bacterial cell wall and is found in almost all Gram-negative bacteria, including those associated with dental caries (e.g *Veillonella* spp.). It is released during cell multiplication and cell death, and has been shown to persist in dentine even after clinical disinfection of the tooth, where dentine is no longer positive for microbial growth (Vianna *et al.*, 2007). LPS induces the secretion of pro-inflammatory cytokines from the the pulpal cells, including tumour necrosis factor-α (TNF-α), interleukin-6 (IL-6) and interleukin-8 (IL-8) (Nagaoka *et al.*, 1996; Kent *et al.*, 1999; Fouad and Acosta, 2001).

Macrophages and neutrophils are the cells that mediate the innate immune response in pulp, as in other tissues (Hahn and Liewehr, 2007). B and T cells of the acquired immune system are later recruited as inflammation progresses. These cells

secrete pro-inflammatory cytokines as well as tissue degrading enzymes such as matrix metalloproteinases (MMPs), which mediate the destruction of pulpal tissues. This response is essential in driving repair processes such as tertiary dentinogenesis, as previously discussed (Section 1.2.5.1). A prolonged immune response, however, will lead to irreversible tissue necrosis, through accumulation of tissue-degrading enzymes (Colombo *et al.*, 2014). Additionally, it has been shown that tertiary dentinogenesis mediated by TGF-β and BMP-7 only occurs in the absence of LPS-induced inflammation in a ferret model of pulpitis, suggesting that the inflammatory response must be ameliorated before reparative processes can take place (Rutherford and Gu, 2000). As in most tissues, the balance between inflammation and repair in the dentine-pulp complex is a delicate one. Paula-Silva *et al.* (2009) showed that TNF-α promoted an odontoblastic phenotype in pulpal stem cells *in vitro* as well as down-regulating MMP-1 expression. Long-term TNF-α exposure, however, was suggested to inhibit tooth remineralisation long-term by Min *et al.* (2006), who cultured pulpal cells with TNF-α and observed initially high activity levels of the pro-mineralisation protein alkaline phosphatase (ALP), which then decreased with longer-term exposure. Clinically, it is therefore important that inflammation can be controlled by removal of the microbial presence at the site of infection in order to avoid long-term exposure of the pulp to a pro-inflammatory environment and allow regeneration to occur.

1.3 Microbiology of pulpitis and root canal infection

The oral cavity contains hundreds of bacterial, viral and fungal species, which normally exist as commensal organisms. Environmental changes induced by diet, oral hygiene habits, or the health status of an individual, however, can induce a pathogenic phenotype in some microbial species (Marsh, 1994). Specifically, it can lead to excessive secretion of acidic bacterial by-products, which erode the dental enamel and cause dental caries. This exposes the dentine-pulp complex to the oral cavity, its

bacteria and their by-products, causing pulpal inflammation (termed clinically as pulpitis).

The microbial population of an advancing carious lesion changes as infection progresses through the different environments of the enamel, dentine and pulpal tissues. Most notable is the transition from predominantly facultative Gram-positive bacteria in early caries to anaerobic Gram-positive bacilli and cocci, and Gram-negative bacilli in deep, carious lesions (Hoshino, 1985). The infection is difficult to treat due to its dynamic, polymicrobial nature, and failure to control this infection leads to it spreading to the periapical tissues and beyond (see Figure 1.2).

1.3.1 Dental plaque

The enamel is the only non-shedding tissue in the human body and so provides a uniquely stable surface for microorganisms to attach and adhere to. The presence of microorganisms as a surface-bound colony (as opposed to a planktonic suspension) is known as a biofilm and dental plaque is the biofilm that resides specifically on the enamel surface of a tooth. Plaque is composed of commensal bacteria and, in a healthy environment, acts to prevent colonisation by exogenous and/or pathogenic microorganisms (Marsh and Bradshaw, 1995). The development of caries depends on the formation of plaque and its modulation to allow for acid erosion of the enamel.

Plaque formation normally begins with the deposition of the pellicle: a cell-free layer of salivary proteins that will coat a clean tooth within 90-120 s (Marsh and Bradshaw, 1995). Its composition has been characterised using proteomic techniques such as mass spectrometry, and is found to contain antimicrobial molecules (lysozyme C), anti-inflammatory molecules (S100-A8, S100-A9), Ca^{2+} binding proteins (α-amylase 1, S100 proteins), and crosslinking enzymes (transglutaminase 3), amongst others (da Silva Ventura *et al.*, 2017; Delius *et al.*, 2017). The relative quantities of these proteins in the pellicle differs to those in the surrounding saliva and it has been suggested that proteins are selectively adsorbed to enamel, serving to promote healthy biofilm development, as well as protection of the enamel from acid erosion (Hannig

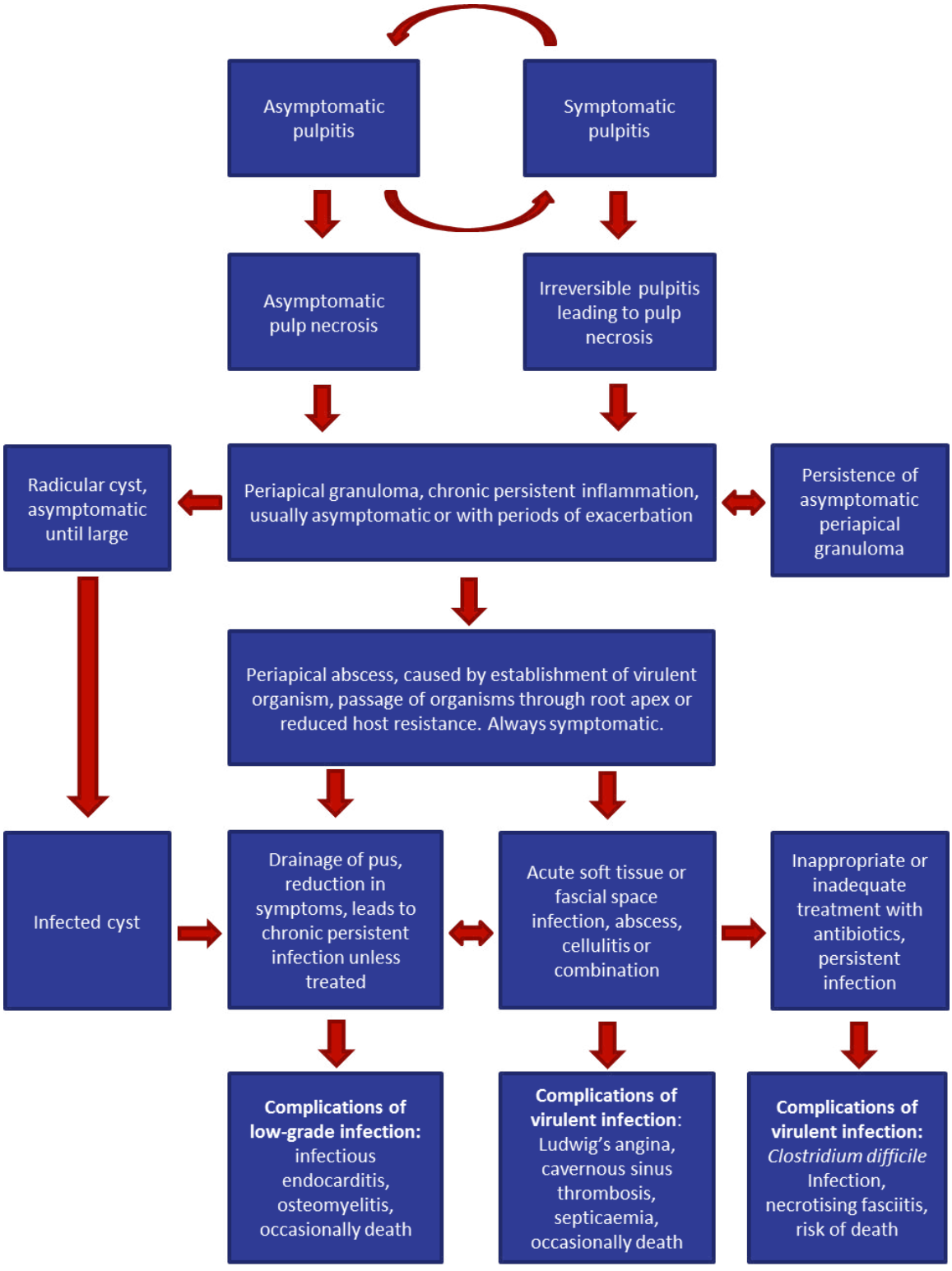

Figure 1.2: **Sequelae of pulpitis.** Adapted from Cawson and Odell (2008)

and Joiner, 2006).

Initial microbial pellicle colonisation is a passive process, with bacteria passing the pellicle through salivary flow and attaching via non-specific, reversible physico-chemical forces (Busscher *et al.*, 1992). The pellicle is then quickly colonised (within 24 h) by adherent bacteria posessing cell surface adhesins. (Cawson and Odell, 2008). It was observed by Nyvad and Kilian (1987) using biochemical identification, that non-mutans *Streptococcus* spp. dominated the early plaque formed on enamel pieces carried in the human oral cavity. The mechanism for their early adhesion is thought to be through lectin-like proteins on the bacterial cell wall that bind to pellicle-associated glycoproteins (Shibata *et al.*, 1980). Li *et al.* (2004) observed that *Actinomyces* species are the predominant plaque species after 2 h of biofilm formation, with *Streptococcus oralis* and *S. mitis* dominating after 6 h. The ability to interact with both the pellicle and other bacteria is crucial to the development and maturation of the biofilm. *Actinomyces* spp. possess cellular projections known as fimbriae, and Cisar *et al.* (1984) used adhesion and co-aggregation assays to show that there are 2 distinct functional types: type 1 fibrimae recognise and bind to salivary proteins and type 2 are associated with a lectin-like interaction with streptococci. Jenkinson *et al.* (1993) identified a large protein of *S. gordonii* that interacts with salivary proteins of the pellicle as well as a receptor on the surface of *A. naeslundii*. The function of the protein was confirmed by silencing the gene that encodes for the protein, and observing a decrease in adhesion to the 2 structures.

After initial attachment, bacteria continue to colonise the plaque, attaching to surfaces and each other. *Fusobacterium* spp. are considered to be critical in bridging the gap between early and late-colonising bacteria as they can adhere to and co-aggregate a wide range of bacterial species, although the mechanism for this is not fully known (Kolenbrander *et al.*, 2006). Late colonisers of dental plaque include *A. actinomycetemcomitans*, *Prevotella intermedia*, *Eubacterium* spp., *Treponema* spp., and *Porphyromonas gingivalis* (Kolenbrander *et al.*, 2002).

Plaque formation also involves the bacterial production of extracellular polysaccharides (EPS). Oral bacteria have been shown to synthesise dextrans (including

poorly water-soluble α-D-glucans) and levans using sucrose as a substrate (Sutherland, 2001). EPS contributes to the structural integrity of the biofilm, as well as its pathogenic properties. The increased pathogenicity of biofilms with higher EPS content was suggested by Dibdin and Shellis (1988), who observed that EPS-rich biofilms of *S. mutans* allowed for greater sucrose retention, and posited that this would allow for deeper sucrose penetration into dental plaque, resulting in a lower pH at the plaque-enamel interface. This was supported by a study comparing the effect of different ratios of *S. mutans* to EPS, which found that demineralisation of experimental enamel slides was greatest when the artificial plaque consisted of 95 % EPS and 5 % bacteria (Zero *et al.*, 1986).

The transition from health to pathology in the dental plaque is mediated by a number of factors, the most widely recognised being the intake of dietary sugars (Leme *et al.*, 2006). Increased sucrose in the oral cavity leads to an increase in EPS production and its previously mentioned caries-promoting effect. This is exacerbated by poor oral hygiene, where the absence of tooth brushing to disrupt the plaque allows for the formation of a mature, EPS-rich biofilm. An increase in biofilm density allows for the formation of microenvironments with lower pH and oxygen concentration than the oral cavity, which are protected from the buffering effects of saliva (Cawson and Odell, 2008). It is here that anaerobic, acid-tolerant bacteria may thrive and outcompete other plaque species, leading to a decrease in overall plaque biodiversity and an increase in caries-causing bacteria (Marsh and Zaura, 2017).

1.3.2 Dental caries

Dental caries is the demineralisation of enamel and/or dentine by bacterially-produced acid (primarily lactic acid). This depends on the presence of acidogenic bacteria within dental plaque, which are also tolerant of the low local pH in the biofilm. The dense structure of the dental plaque allows for the maintenance of an acidic environment that is not easily penetrated by salivary buffers, therefore exposing the enamel to a continuously low pH (Cawson and Odell, 2008). *S. mutans* and *Lactobacillus*

spp. survive better in low pH conditions than non-mutans *Streptococcus* spp. and *Actinomyces* spp. and so their presence becomes more prevalent in the carious biofilm (Horiuchi *et al.*, 2009). Some bacterial species, such as *Veillonella* spp. can utilise lactic acid and convert it to weaker acid: Van der Hoeven *et al.* (1978) observed a reduction in caries and lower plaque lactate in rats infected with *Veillonella alcalescens* and *S. mutans* compared with *S. mutans* alone.

The initial stages of caries are subsurface, with the topmost layer of enamel remaining intact and demineralisation occuring beneath the surface. This is known clinically as a white spot lesion and is believed to be a result of a higher degree of mineralisation in the surface of enamel compared to the subsurface, which results in the initial resistance of the surface enamel to demineralisation (Hallsworth *et al.*, 1972). As demineralisation progresses, the enamel becomes more porous and so acid can diffuse more freely into the matrix, thus accelerating the process.

Whereas *S. mutans* is prevalent in cavitated enamel lesions, the advancing front of dentine caries contains more *Lactobacillus* spp., *Prevotella* spp. and *Bifidobacterium* spp. (Takahashi and Nyvad, 2011). Despite the apparent importance of *S. mutans* and lactobacilli in the progression of dental caries, Boyar *et al.* (1989) found examples of carious lesions with no evidence of these species present in extracted teeth that were banded to allow plaque growth *ex vivo*, suggesting that these species are not essential to instigate caries formation. Simón-Soro *et al.* (2014) used metatranscriptomics to compare microbiomes sampled from enamel caries and dentine caries, and found that biodiversity increased in the dentine, although the reason for this is unclear. The presence of anaerobic bacteria in carious dentine of extracted teeth were detected by Martin *et al.* (2002) using real-time polymerase chain reaction (PCR), and the presence of *Micromonas micros* (now named *Parvimonas micra*) and *Porphyromonas endodontalis* correlated with the development of irreversible pulpitis and endodontic infections that occurred as a result of carious pulpitis. *P. endodontalis* is a virulent anaerobe, that was shown by Mirucki *et al.* (2014) to possess novel complex lipids that induce TNF-α expression in macrophages *in vitro*. *P. micra* is accociated with symptoms of throbbing pain in irreversible pulptitis (Rôças *et al.*, 2015) and some

strains have been shown, through biochemical testing, to produce collagenase, which could account for its destructive nature in the collagen-rich pulp tissue (Ota-Tsuzuki and Mayer, 2010).

Once caries has progressed to the dentine, the dentine-pulp complex is exposed to the oral cavity. As previously discussed (Section 1.2.5), odontoblasts and their processes recognise bacteria, bacterial LPS, and growth factors released from the demineralised dentine, and initiate an immune response. The dentine-pulp complex can also inhibit movement through the tubules by depositing minerals within the tubules to reduce their size and permeability in a process known as tubular sclerosis (Kidd and Fejerskov, 2004). This reaction may slow progression, but even sclerotic dentine is vulnerable to bacterial acid and can eventually be penetrated by bacteria.

1.3.3 Pulpal and periapical infection

Infection of the pulp triggers the production of tertiary dentine, as well as stimulation of the immune response, as previously discussed (Sections 1.2.5.1 and 1.2.5.2). Prolonged stimulation of the immune response alongside the destructive nature of certain microbial species (e.g. those that secrete collagenases), however, may lead to irreversible pulpal damage and necrosis.

Once necrosis of the pulp has occurred, it is possible for bacteria to colonise the internal dentine surfaces as a biofilm, as first observed by Nair (1987) using transmission elecron microscopy (TEM) on extracted carious teeth with periapical lesions. The composition of the biofilms are dependent upon the niche in which they reside and Chávez de Paz (2007) defined 3 of these niches as the coronal segment (nearest the crown), main canal, and the apical segment (tip) of the root canal (Figure 1.3). The microbial composition of these biofilms varies due to gradients in environmental conditions, such as oxygen concentration and nutrient levels, which both decrease from the coronal to the apical sections. Biofilms that colonise the apical section are of particular interest, as it is believed that this is the point of access for bacteria to the periapical tissues surrounding the tooth. Chugal *et al.* (2011) used molecular

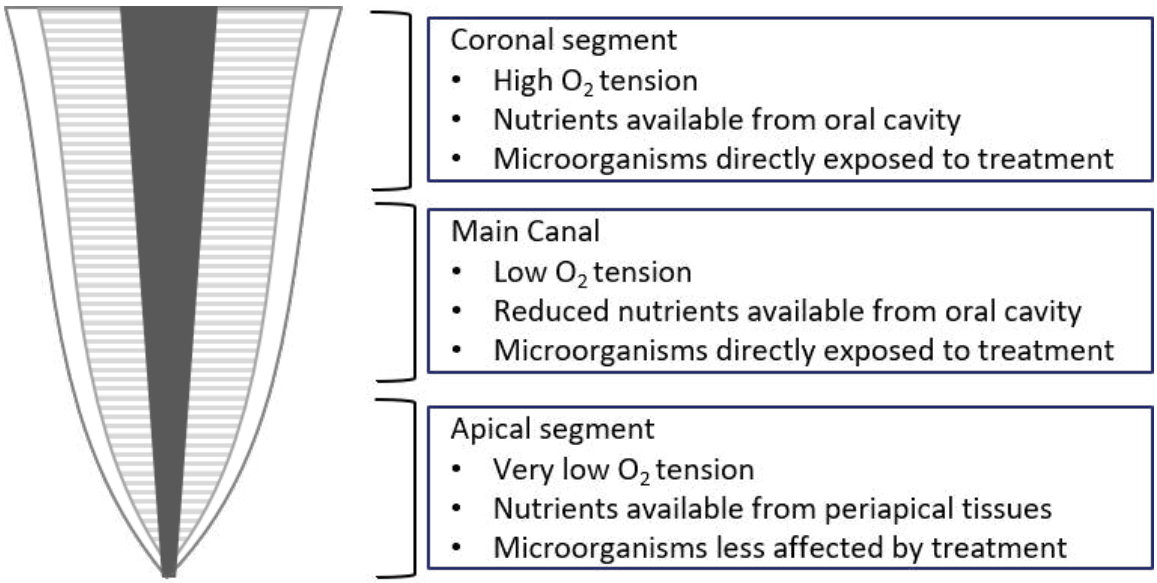

Figure 1.3: **Microbial niches of the dental root canal.** Modified from Chávez de Paz (2007).

sequencing techniques to characterise the microbiome of apical root sections of teeth with necrotic pulp and teeth that had undergone endodontic (root canal) therapy. They found *Fusobacterum* spp., *Actinomyces* spp., and oral *Anaeroglobus geminatus* in both types of infection and a general decrease in biodiversity in secondary infections. Many secondary infections contained *Burkholderiales* or *Pseudomonas* spp. as well as *Enterococcus faecalis*, all of which are opportunistic environmental pathogens that were not present in the primary infected tissue. This was in agreement with other similar studies (Siqueira and Rôças, 2005; Alves *et al.*, 2009). These studies suggest that primary and secondary endodontic infections are caused by distinct microbiomes. Additionally, clinical intervention may not eradicate infection, but rather modulate the microbiome to a less biodiverse, but selectively resilient community, that contains opportunistic environmental pathogens with the potential to cause further damage.

Further spread of infection causes a periapical lesion to develop, either in the form of a periapical granuloma or periapical abscess. This happens when bacteria within the root canal make contact with periapical tissue via apical foramina (holes in the root apex through which nerves and blood vessels enter the pulp) (Sasaki and Stashenko, 2012). These bacteria induce an immune response in the perapical tissues, leading to tissue liquefaction (through immune cell enzyme secretion) and formation

of a pus-filled cavity known as an abscess (Shweta, 2013). There is not a single pathogen that has been identified as causing periapical infection, although certain species are more prevalent (Robertson and Smith, 2009). The *Streptococcus anginosus* group of bacteria, for example, are commonly associated with periapical lesions (Iwu *et al.*, 1990; Fisher and Russell, 1993). The pathogenicity of *S. anginosus* is of great interest as these bacteria have been associated with a number of human infectious diseases. Asam and Spellerberg (2014) and Sitkiewicz (2017) recently reviewed the potential virulence factors of *S. anginosus* group bacteria, including their adhesion to host cells, β-haemolytic phenotype (the ability to destroy red blood cells), and secretion of toxic hydrogen sulphide.

Enterococcus spp. are often found in dental abscesses, most commonly *E. faecalis*, and particularly in secondary infection sites following dental treatment (Pinheiro *et al.*, 2003; Rôças *et al.*, 2004; Stuart *et al.*, 2006). This is due to its survival ability in high pH conditions, the introduction of which are often relied upon for disinfection during root canal treatments (i.e. using sodium hypochlorite irrigant or calcium hydroxide root dressings). It is not clear at what point *E. faeclis* enters the root canal. Some report that it is detectable neither as part of normal oral microflora, nor in advancing dental lesions (Zehnder and Guggenheim, 2009). Wang *et al.* (2012) cultured samples from the saliva and root canals of patients with apical periodontitis and found that the presence of *E. faecalis* in the root canal was more likely if it was also found in saliva, but not all patients with *E. faecalis* in the root canal also had it in their saliva. Vidana *et al.* (2011) performed a similar study but found no *E. faecalis* in any patients' saliva samples. Furthermore, the cultured isolates from the root canals of these patients were genetically compared to *E. faecalis* from the patients' gastrointestinal tract, and the bacteria isolated from the two sources were genetically distinct, suggesting that the root infection was not sourced from the patient's own microflora. Studies that use culture-independent molecular techniques, however, have found *E. faecalis* to be present at detectable, but not culturable quantities in the oral microflora, and suggest that it is a commensal organism that is selectively increased in cases of secondary root canal infection (Portenier *et al.*, 2003; Sedgley *et al.*, 2006).

Most recently, it has been hypothesised that *E. faecalis* is introduced to the oral cavity from food sources, due to shared genetic lineages between organisms isolated from root canals and food sources (Vidana, 2015; Chávez de Paz, 2018).

It is the dynamic and polymicrobial nature of pulpitis and associated conditions that makes treatment challenging. During the sequelae of pulpitis (Figure 1.2), there are several points for clinical intervention, although it is ultimately the successful eradication of microbial infection that determines the treatment efficacy, alongside other factors.

1.4 Pulpitis and root canal infection in the clinic

In 2010, the global prevalence of untreated dental caries in permanent teeth was 35 %, the most prevalent of all oral conditions (Marcenes *et al.*, 2013). It is this that leads to pulpitis, which is the most common cause of toothache and loss of teeth in younger people (Cawson and Odell, 2008). Pulpitis presents clinically as increased sensitivity in the tooth, discomfort or pain. Treatment depends on the severity of the condition, which has two clinical classifications. Reversible pulpitis describes inflammation that may be reversed upon the removal of the external stimulus, such as caries. In irreversible pulpitis, the damage is more severe and all the dental pulp must be removed in order to prevent further spread of infection. Recently, biomarkers for pulpal inflammation have been identified to aid in diagnosis of pulpitis, including IL-8, MMP-9, TNF-α, and a receptor for advanced glycation end products expression, according to a recent systematic review (Zanini *et al.*, 2017). Patients are diagnosed based on a number of factors, including radiographic evidence of caries, history of pain, sensitivity to hot and cold stimuli, sensitivity to tapping (percussive test) and sensitivity to electrical currents using an electric pulp test (Mejàre *et al.*, 2012). Both reversible and irreversible pulpitis, however, may also be asymptomatic. The mechanism of symptomless pulpitis is not fully understood, but has been associated with older patients (Farac *et al.*, 2012), with the suggestion that slower progression may result in the lack of symptoms (Michaelson and Holland, 2002).

1.4.1 Dental restorations

The treatment of pulpitis usually involves some form of dental restoration. The type of restoration performed will depend on a variety of factors including the severity of the condition, the type and position of the affected tooth (and surrounding teeth) and the age and health status of the patient. Preparation of the tooth prior to the placement of a restoration includes the removal of infected tissues and any portion of the tooth that may be structurally unsound. In cases of reversible pulpitis, this does not include pulp tissue. There are 2 types of dental restoration that may then be placed:

> **Direct restorations** involve the placement of a restorative material directly into the tooth. It is done as a single procedure, using a material such as amalgam, composite resin or glass ionomer cement. These can be moulded *in situ* to fill the prepared cavity and seal the tooth.
>
> **Indirect restorations** must be pre-formed before placement in the tooth and require multiple clinic visits by the patient. Crowns, inlays and onlays are examples of indirect restorations. Materials used include porcelain and gold.

The decision to place either direct or indirect restorations may be dictated by the clinical factors, such as lesion size and aetiology, however patient and dentist preference may also factor in (Smithson *et al.*, 2011). Indirect restorations are more costly than direct restoration, however indirect restorations generally last longer than direct restorations, as reviewed by Manhart *et al.* (2004). Despite their increased longevity, Kelly and Smales (2004) compared the cost-effectiveness of direct and indirect restorations and found that direct restorations remained the most cost-effective restorations over 15 years and recommended that these be placed in preference to indirect restorations where clinically applicable.

There are a range of materials that are used for dental restorations, each with advantages and disadvantages. The main criteria for a suitable material include biocompatibility, aesthetics and suitable physical properties (e.g. resistance to wear

and fracture, minimal shrinkage over time). The overall clinical success of a restoration, however, is multi-factorial and therefore difficult to predict based on physical properties alone (Ferracane, 2013).

Amalgam has traditionally been used for direct restorations, however it is now more common for composite resins to be used in its place. This is, in part, driven by the patients preference for a coloured filling that matches the tooth for a more aesthetically pleasing result. In anterior teeth, composite restorations are frequently used for aesthetic reasons, and the failure of these is commonly due to restoration or tooth fracture rather than secondary caries (Demarco *et al.*, 2015). Generally, however, secondary caries is the primary reason for composite restoration failure, and this is due to factors relating to the material itself as well as patient-related factors (Nedeljkovic *et al.*, 2015). A randomised control trial showed that composite posterior fillings have a lower survival rate than those of amalgam, although secondary caries was the main reason for failure in both cases (Bernardo *et al.*, 2007). Composite fillings are generally considered safer, due to the mercury content of amalgam fillings, however a recent Cochrane review concluded that there is no quality evidence to support or refute this (Rasines Alcaraz *et al.*, 2014).

1.4.2 Endodontic therapy

Endodontic therapy, more commonly termed root canal therapy, is performed where pulpitis has become irreversible. The purpose of the treatment is to remove all the pulp from the tooth, including the root canals, in order to eliminate bacteria and their nutrient source and prevent disease progression. The roots are then filled and the tooth sealed in order to prevent re-infection and maintain the tooth's structural integrity.

Typical endodontic preparation involves a combination of mechanical and chemical debridement (removal of infected tissue) and disinfection. Specialised tapered files are used to mechanically remove pulp and some dentine, widening the root canals. Following this, irrigation with sodium hypochlorite (NaClO) solution aims to dissolve

residual necrotic tissue and kill any remaining bacteria. NaClO is widely recognised as an effective biocide that also dissolves organic tissue (Siqueira *et al.*, 1997, 2000; Zehnder *et al.*, 2002), however it has also been shown to negatively affect the mechanical integrity of dentine (Grigoratos *et al.*, 2001), which may increase the risk of tooth fracture. Pladisai *et al.* (2016) assessed the efficacy of both mechanical instrumentation (MI) and irrigation on premolars with large root canals *ex vivo* and found that MI resulted in the lowest residual microbial burden of *E. faecalis* and that noninvasive irrigation could not substitute MI. Progressive widening of the canals, however, has been shown to correlate with the incidence of tooth fracture (Wilcox *et al.*, 1997), suggesting that a balance must be sought between effective debridement and maintenence of structural integrity.

The most widely used root filling material is gutta percha, which may be placed as pre-formed points or warmed in order to form a semi-solid that is mouldable to the shape of the cavity. Zinc oxide paste is used in conjunction with gutta percha in order to form a seal between the main filling material and the cavity walls.

Endodontic treatment may be performed in 1 or 2 stages, the 2-stage process involving the preparation and temporary filling of the tooth followed by a subsequent permanent filling and sealing of the tooth. The temporary filling may have antimicrobial properties: non-setting calcium hydroxide ($Ca(OH)_2$) paste is a common material used for this. The longevity of the temporary filling is dictated by the integrity of the restorative material used to seal the tooth: often this is a glass ionomer. Prolonged $Ca(OH)_2$ paste treatment has been shown to alter the physical properties of dentine (Grigoratos *et al.*, 2001; Andreasen *et al.*, 2002) and so, like other chemomechanical disinfection techniques, must be used in balance with the maintenance of the tooth's structural integrity.

A successful root canal restoration will leave the cavity completely free of pulpal tissue and have filled all the space within the cavity, forming a tight seal in order to prevent bacterial leakage and re-colonisation.

1.4.3 Vital pulp therapy

Endodontic therapy ultimately results in a non-vital tooth that is susceptible to structural damage and microbial infection: both of which would be naturally resisted by the reactionary mechanisms of the living dentine-pulp complex (Section 1.2.5). Vital pulp therapy (VPT) has therefore been proposed as an alternative to endodontic surgery (Witherspoon 2008). This treatment aims to leave some of the remaining pulp in the tooth and encourage pulpal regeneration whilst limiting microbial activity. Antimicrobial treatment in VPT is challenging as many biocides are cytotoxic to the pulpal cells, including NaOCl (Essner *et al.*, 2011). Most VPT procedures use materials containing $Ca(OH)_2$ or mineral trioxide aggregate (MTA).

A systematic literature review by Aguilar and Linsuwanont (2011) concluded that VPT using $Ca(OH)_2$ or MTA had a high reported success rate in permanent teeth (>97 % after 3 years). Asgary *et al.* (2013) reported the 12-month outcome of VPT with calcium-enriched cement (CEM) to be non-inferior to standard root canal therapy and the pain-relief outcome over 7 days was reported to be better. Other studies report worse outcomes, however, particularly in a process known as "pulp capping", where the coronal portion of the pulp is not removed. Barthel *et al.* (2000) reported a 45 % failure rate after 5 years and 80 % failure rate after 10 years with pulp capping.

A recent survey of dental practitioners in Wales found that VPT was performed in low numbers of patients, and that the expense and poor handling properties of MTA were cited prohibitive factors (Chin *et al.*, 2016). This highlights the need to develop affordable materials with desirable handling properties for this procedure.

1.4.4 Tooth extraction

In certain cases, the tooth may be removed altogether. This may be due to caries, failed root canal treatment or periapical infection (Chestnutt *et al.*, 2000; Richards *et al.*, 2005). Tooth loss is not a desirable outcome for many patients: low self-esteem; difficulty forming relationships; restriction in diet, and reluctance to smile or laugh in public have been reported as emotional outcomes of tooth loss (Fiske *et al.*,

1998; Davis *et al.*, 2001). Other physical problems may arise after extraction such as infection, problems with mastication or jaw damage (Lodi *et al.*, 2012).

1.4.5 The efficacy and survival of dental restorations and endodontic treatments

The reasons that dental restorations fail include secondary caries, fracture of the restoration or tooth, lost restorations and pain (Kopperud *et al.*, 2012). This leads to the need for re-intervention, including enlarging the cavity, performing endodontic therapy or tooth extraction.

In England and Wales, the survival rate of dental restorations before re-intervention has been reported to be 38-58 % over 10 years, depending on the type and size of the restoration (Burke and Lucarotti, 2009). Restorations where root canal treatment has been performed have a lower survival rate than those without root canal fillings, with an estimated 10-year survival rate of 34-60 % (Lucarotti *et al.*, 2014).

Persistence and recurrence of bacteria is recognised to be one of the foremost reasons for endodontic failure. In persistent infections, bacteria may evade disinfection and obturation when residing in isthmuses (narrow "ribbons" of pulp between canals) and dentine tubules, as well as root canals that may have been left untreated (Tabassum and Khan, 2016). The persistence of some microbial species such as *E. faecalis* can cause re-infection of the cavity and further periapical infection. Eradication of pathogens and necrotic pulp may be particularly challenging in older patients, where root canals may be narrow and difficult to negotiate. Tooth retention, however, may be critical for a number of reasons including the preservation of an intact dental arch and as a retainer for prostheses (Allen and Whitworth, 2004). Poor technique may be a cause of endodontic failure, however teeth that are well treated can still fail and the primary cause in both cases remains to be persistent microbial infection (Siqueira, 2001).

Recurrent infection refers to a secondary infection, i.e. the contamination of the cavity during treatment or bacterial leakage around the restoration after treatment

(Siqueira, 2002). Endodontic failure has been linked to the quality of the restoration of the tooth rather than the root treatment itself, as the majority of re-treated root canals are as a result of secondary caries rather than a root canal or periapical infection (Mannocci and Cowie, 2014).

Endodontically treated teeth are more prone to fracture due to tissue loss during treatment and this risk is increased when roots must be re-treated due to secondary infection (Er *et al.*, 2011). This highlights the importance of reducing incidence of endodontic failure and the need to develop non-invasive techniques for root disinfection that do not rely on mechanical instrumentation.

1.4.6 Antimicrobial treatments

The use of systemic antibiotics is not considered to be an effective treatment for irreversible pulpitis or periodontal infection (Keenan *et al.*, 2006; Cope *et al.*, 2014). This is for a number of reasons, including the polymicrobial and topical nature of dental infections. Additionally, infection as a result of caries requires mechanical intervention to prevent further bacterial infiltration as well as treat the current infection as the dental tissues have limited self-healing ability, particularly if the pulp is compromised. It is therefore advantageous to consider the development and use of topical antimicrobial agents to be used in conjunction with restorative materials in order to prevent and manage dental infection.

Products used to maintain general oral hygiene include toothpastes and mouthwashes. These are designed to prevent and inhibit plaque formation, alongside mechanical plaque removal by brushing and flossing. Chlorhexidine, triclosan and sodium lauryl sulphate are all examples of broad-spectrum antimicrobial agents used in these products (Marsh, 2010). One study found that mouthwashes containing triclosan had greater antimicrobial effect against *S. mutans*, *Escherichia coli* and *Candida albicans* when compared to mouthwashes containing chlorhexidine gluconate and potassium nitrate formulations (Prasanth and Capoor, 2013).

Antimicrobials are also used in management of disease and during treatment procedures. A typical chemomechanical preparation for endodontic treatment is the irrigation of the prepared root canal with NaOCl, followed by temporary filling with $Ca(OH)_2$ paste. $Ca(OH)_2$ has been shown to have good antimicrobial effects *in vitro*, including the ability to eradicate *E. faecalis* from root canals that were incubated with the baterium for 3 weeks, treated with $Ca(OH)_2$ paste for 7 days, and the resulting dentine broken down into chips, which were incubated and observed for bacterial growth (Han *et al.*, 2001). Its effect against multi-species biofilms, however, is disputed (Mohammadi *et al.*, 2012). An *in vivo* study looked at the microbial presence in teeth following a typical root canal preparation and found that, although significantly lowered, a bacterial presence still persisted in the root canals, suggesting that there is still a need for more effective treatment (Rôças and Siqueira, 2011).

1.5 Liposomal drug delivery

Liposomes are artificially produced, self-assembling spherical vesicles comprising of one or more phospholipid bilayers surrounding an aqueous core. Phospholipids have a hydrophilic head group and two hydrophobic tails, making them poorly soluble in water unless they self-assemble to form a bilayer. The perimeter of the bilayer has an energy associated with it where the hydrophobic tails are exposed to water. This energy can be minimised if the bilayer bends and closes to form a vesicle, and it is this that drives the self-assembly of phospholipids into liposomes (see Figure 1.4). These vesicles, initially named 'bangosomes', were first described in 1965, when it was observed that phospholipids spontaneously formed large, multilamellar vesicles in water (Bangham *et al.*, 1965). Liposomes composed of naturally occurring phospholipids were used as models of the cell membrane due to their similarity in structure (Papahadjopoulos and Watkins, 1967), and it is this structural similarity and biocompatibility that makes them ideal for use in the biomedical field. Additionally, their ampiphilic nature means they can be used to encapsulate both hydrophilic and hydrophobic drugs for therapeutic delivery.

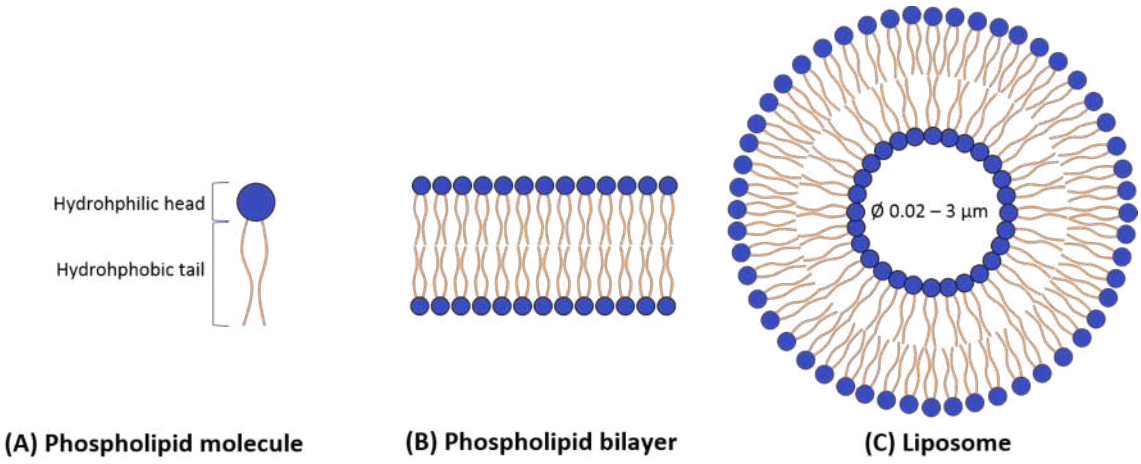

Figure 1.4: **Schematic illustrating phospholipid self assembly involved in liposome formation.** A phospholipid molecule with hydrophilic and hydrophobic regions (A) will self-assemble as a bilayer (B) under certain conditions. A liposome (C) is formed when the bilayer folds and closes upon itself to form a spherical vesicle. *Schematic is not to scale.*

The first commercially available liposomes, AmBisome®, contain the antifungal drug amphotericin B and continue to be used to treat serious fungal infections (Adler-Moore, 1993). Currently, 15 liposomal formulations are in clinical use (Table 1.1), 7 of which are used in cancer therapy (Bulbake *et al.*, 2017). There are currently no liposomal formulations used in treating bacterial infections, and particularly not for oral infections.

The physical characteristics of liposomes, such as size, charge and lamellarity, can be adapted for their intended application. These characteristics are dependent on the lipid composition and the method used for preparation, as well as the characteristics of the compound they are used to encapsulate.

1.5.1 Liposome composition

Phospholipids used for liposome preparation are usually naturally derived, biodegradable and have a molecular shape that will favourably form bilayers in aqueous environments (in contrast to phospholipids that form micellar structures). They typically consist of a polar head group linked to two fatty acid chains by a glycerol molecule. Changing the headgroup of the phospholipid can change the overall charge of the

Table 1.1: **Summary of liposomal formulations approved for clinical use.**

	Product (year approved)	Active agent	Phospholipids/other components	Indication	Company
Cancer therapy	Doxil® (1995)	Doxorubicin	HSPC, Cholesterol, PEG 2000-DSPE	Ovarian, breast cancer, Kaposi's sarcoma	Sequus Pharmaceuticals
	DaunoXome® (1996)	Daunorubicin	DSPC, Cholesterol	AIDS-related Kaposi's sarcoma	NeXstar Pharmaceuticals
	Depocyt® (1999)	Cytarabine/Ara-C	DOPC, DPPG, Cholesterol, Triolein	Neoplastic meningitis	SkyPharma Inc.
	Myocet® (2000)	Doxorubicin	EPC, Cholesterol	Metastatic breast cancer (combination therapy with cyclophosphamide)	Elan Pharmaceuticals
	Mepact® (2004)	Mifamurtide	DOPS, POPC	High-grade, resectable, non-metastatic osteosarcoma	Takeda Pharmaceutical Limited
	Marqibo® (2012)	Vincristine	SM, Cholesterol	Acute lymphoblastic leukaemia	Talon Therapeutics, Inc.
	Onivyde™ (2015)	Irinotecan	DSPC, MPEG-2000:DSPE	Metastatic adenocarcinoma of the pancreas (combination therapy with fluorouracil and leucovorin)	Merrimack Pharmaceuticals Inc.
Fungal Diseases	Abelcet® (1995)	Amphotericin B	DMPC, DMPG	Invasive severe fungal infections	Sigma-Tau Pharmaceuticals
	Ambisome® (1997)	Amphotericin B	HSPC, DSPG, Cholesterol	Presumed fungal infections	Astellas Pharma
	Amphotec® (1996)	Amphotericin B	Cholesteryl sulphate	Severe fungal infections	Ben Venue Laboratories Inc
Pain management	DepoDur™ (2004)	Morphine sulfate	DOPC, DPPG, Cholesterol, Triolein	Pain management (epidural)	SkyPharma Inc.
	Exparel® (2011)	Bupivacane	DEPC, DPPG, Cholesterol , Tricaprylin	Pain management (intravenous)	Pacira Pharmaceuticals, Inc.
Viral vaccines	Epaxal® (1993)	Inactivated hepatitis A virus (strain RGSB)	DOPC, DOPE	Hepatitis A	Crucell, Berna Biotech
	Inflexal® V (1997)	Inactivated haemagglutinin of Influenza virus strains A and B	DOPC, DOPE	Influenza	Crucell, Berna Biotech
Photodynamic therapy	Visudyne® (2000)	Verteporphin	Verteporphin, DMPC, EPG	Choroidal neovascularisation	Novartis

HSPC (hydrogenated soy phosphatidylcholine); PEG (polyethylene glycol); DSPE (distearoyl-sn-glycero-phosphoethanolamine); DSPC (distearoylphosphatidylcholine); DOPC (dioleoylphosphatidylcholine); DPPG (dipalmitoylphosphatidylglycerol); EPC (egg phosphatidylcholine); DOPS (dioleoylphosphatidylserine); POPC (palmitoyloleoylphosphatidylcholine); SM (sphingomyelin); MPEG (methoxy polyethylene glycol); DMPC (dimyristoyl phosphatidylcholine); DMPG (dimyristoyl phosphatidylglycerol); DSPG (distearoylphosphatidylglycerol); DEPC (dierucoylphosphatidylcholine); DOPE (dioleoly-sn-glycero-phophoethanolamine). Table adapted from (Bulbake et al., *2017)*

liposome. Liposomes that are highly cationic or anionic will repel each other in an aqueous suspension and therefore are more stable as they are less likely to aggregate. Neutral or cationic liposomes, however, are more stable than anionic liposomes *in vivo*, as they are less likely to bind to blood proteins and therefore stay in circulation longer (Hernández-Caselles *et al.*, 1993). Liposomes containing phosphatidylserine have been observed to induce apoptosis in some cell types as they are thought to mimic the serine-rich cell membrane of an apoptotic cell (Hosseini *et al.*, 2015).

Many commercial liposome formulations contain cholesterol, as it is used to optimise the stability and release characteristics of liposomes. Demel and De Kruyff (1976) observed that cholesterol increases the packing density of phospholipid molecules in the bilayer and therefore reduces the permeability of the membrane, which would allow for slower drug release. It can also improve the physical stability of the liposome and its resistance to shear stress because the membrane has higher rigidity when cholesterol is added (Liu *et al.*, 2000). Aramaki *et al.* (2016) found that cholesterol increased the charge of cationic liposomes, therefore reducing the concentration of cytotoxic cationic surfactant required to obtain the same charge. Cholesterol addition may, however, reduce the encapsulation efficiency of liposomes, as was found by Mohammed *et al.* (2004) when incorporating ibuprofen into phosphatidylcholine liposomes.

1.5.2 Liposome preparation methods

Several methods have been developed for the production of liposomes, a summary of which are shown in Table 1.2. Different preparation techniques result in different liposome sizes, ranging from tens of nanometres to tens of microns in diameter. In addition, liposomes may have different lamellarity, as summarised in Figure 1.5.

Most liposome preparation methods produce multilamellar and/or large liposome sizes, and so post-production modifications such as extrusion, homogenisation or sonication are employed to reduce liposome size and polydispersity, usually resulting in dispersions of small unilamellar vesicles (SUVs) for clinical use. Liposomes may

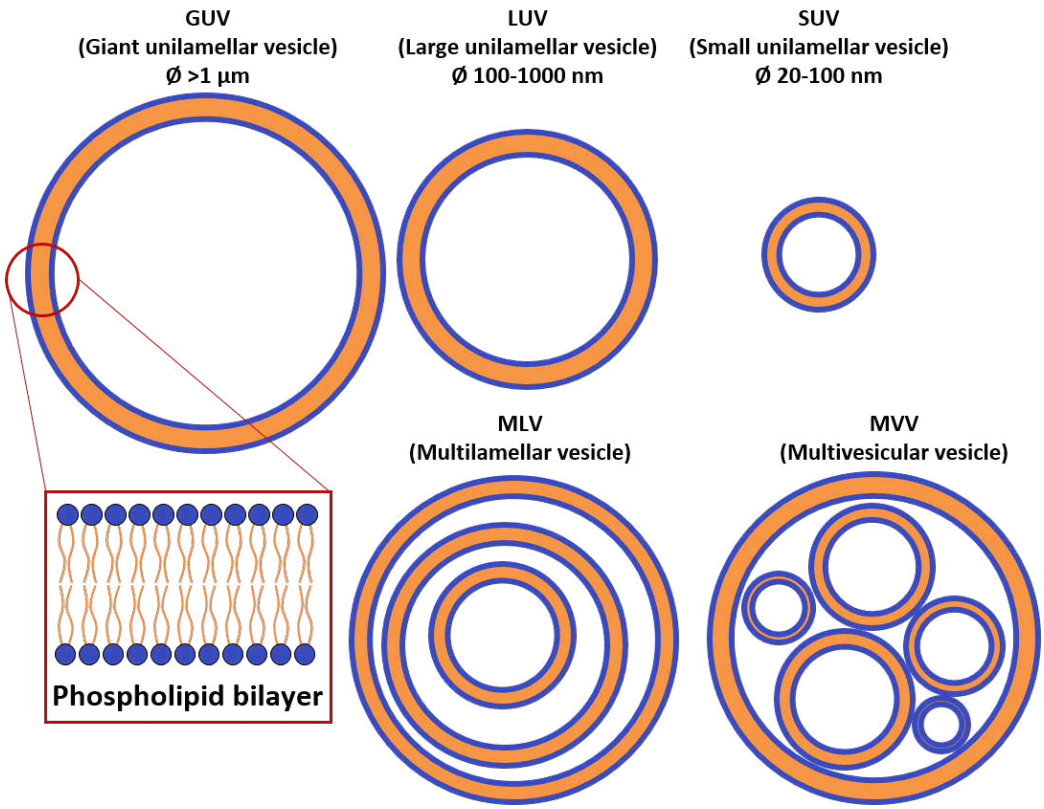

Figure 1.5: **Schematic showing liposome classification by size and lamellarity.** Phospholipid bilayers will form spherical vesicles that may be classed as giant, large, or small unilamellar vesicles. Vesicles containing more than 1 membrane, or lamella, are classed as multilamellar vesicles (with many concentric lamellae) or multivesicular vesicles (with mulitple vesicles contained in the same large vesicle). *Schematic is not to scale.*

Table 1.2: **Summary of liposome preparation methods.**

Method	Brief description	Liposomes obtained
Thin film hydration	Phospholipids are dissolved in organic solvent and subsequent solvent removal. To deposit phospholipid bilayer film onto substrate. Film is hydrated in aqueous solution with no hydrodynamic flow over long time period (days).	GUVs MLVs
Thin film hydration with hydrodynamic flow	Similar to above, but film is hydrated under hydrodynamic flow over shorter time period.	MLVs
Electro-formation	Phospholipid film is deposited onto electrodes and hydrated in the presence of an electric field.	GUVs
Solvent-spherule method	Aqueous phase is vigorously shaken under vacuum with an organic phase containing phospholipids to form an oil-in-water emulsion containing small spherules of lipid-containing solvents. Organic phase is subsequently removed using evaporation.	MLVs
Hydration of proliposomes	Proliposomes are formed by drying an organic solution of phospholipids and a carrier/drug resulting in particles comprising of crystalline carrier/drug at the core encapsulated by a phospholipid shell. This will form liposomes when dispersed in an aqueous phase.	MLVs
Reverse phase evaporation	Similar to solvent-spherule method , but a water-in-oil emulsion is formed.	LUVs MLVs
Detergent dialysis	Phospholipids are solubilised by detergent micelles in an aqueous phase. Detergent is then removed by dialysis, resulting in coalescence of the phospholipid rich micelles and formation of liposomes.	LUVs
Ethanol injection	Ethanol containing dissolved phospholipids is injected into an aqueous phase.	SUVs
Microfluidics	Similar to ethanol injection, but the phases are mixed in a microfluidics cell allowing for more controlled mixing.	SUVs

GUV (giant unilamellar vesicle); MLV (multilamellar vesivle); LUV (large unilamellar vesicle); SUV (small unilamellar vesicle). Adapted from (Patil and Jadhav, 2014)

also be lyophilised for long-term storage, with some formulation modifications (Chen *et al.*, 2010).

Multilamellar vesicles (MLVs) and multivesicular vesicles (MVVs) have a larger lipidic surface area and have a propensity to carry a higher concentration of drugs. Maestrelli *et al.* (2006) prepared MLVs, LUVs and SUVs using various methods and measured their encapsulation efficiency of the anti-inflammatroy drug ketoprofen. They found that MLVs had the highest encapsulation efficiency, followed by LUVs and then SUVs. Berger *et al.* (2001) extruded MLVs containing the hydrophilic dye calcein through different pore sizes and found that the encapsulation efficiency correlated with particle size. A larger particle size, however, makes them easier for

the body's mononuclear phagocyte system (MPS) to detect and eradicate (Malam *et al.*, 2009). SUVs are therefore preferred in a clinical setting, as they will stay in circulation longer and are more likely to reach their therapeutic target, if they are administered systemically (Gubernator, 2011).

1.5.3 Liposomes for antimicrobial drug delivery

As previously discussed, liposomes are often employed in the delivery of therapeutics, as they can improve the solubility of hydrophobic drugs and are highly biocompatible. Liposomes have not yet been utilised for the control of dental infections, however some research has been done on this possibility.

Cationic and anionic liposomes have been shown to be adsorbed into single and 2-species biofilms *in vitro* and can effectively deliver triclosan to inhibit growth of *S. sanguis* but not *S. salivarius* (Robinson *et al.*, 2001b). Anionic liposomes can be adsorbed into hydroxyapatite (a model for dental enamel), although they also interact with salivary components, which reduces their efficacy (Nguyen *et al.*, 2011). Recent work within the Cardiff University Mineralised Tissue Group has also found that neutral triclosan loaded liposomes are more effective than free drug against *S. anginosus* using an *ex vivo* model of rat pulpal infection (Roberts *et al.*, 2013a,b). Additionally, liposomes could be incorporated into glass ionomer cements/MTA for the successful delivery of antimicrobials without compromising mechanical and material properties. This was not the case for composite resins, which do not absorb water, hence did not release triclosan. Furthermore, light activation of materials was found to degrade triclosan, rendering it inactive against bacteria (unpublished data). This work shows promise for triclosan liposomes to be used in a non light-activated composite system for dental antimicrobial delivery. In particular, it suggests that a material with a high aqueous content would best allow liposome release, such as a hydrogel.

1.6 Hydrogels for drug delivery

1.6.1 Hydrogels

Hydrogels can be described as 3-dimensional (3D) structures of hydrophilic polymers that retain a large amount of water. Despite their significant aqueous component, they possess a solid-like structure, provided by the supporting network of polymers. Hydrogels are said to be chemically similar but physically distinct from gels in that they have differing swelling properties. Hydrogels maintain their 3D structure upon the addition of water whereas a gel will become more dilute. This is due to the level of cross-linking between the polymers: a hydrogel inherently contains a high level of cross-linking whereas the polymers in a gel display only weak physical entanglements that will not inhibit their dilution in water (Gupta *et al.*, 2002). Hydrogels may be classified according to several features, including their source (natural or synthetic), cross-linking bond type (ionic, hydrogen, covalent, etc.), charge (ionic, non-ionic), polymeric composition (homopolymeric, copolymeric), or the environmental stimuli that initiate gel formation.

1.6.2 Physical and chemical hydrogels

Cross-links that form the hydrogel structure may be in the form of physical bonds or chemical bonds. Physical, or reversible hydrogels, include those formed by ionic, hydrophobic or hydrogen bonding. Physical hydrogels often do not have uniform pore sizes due to the non-homogenous nature of bond formation. Chemical hydrogels are formed by covalent bonding and are irreversible due to the configurational changes they undergo upon gelation. Chemically cross-linked polymers are considered to be strong hydrogels. They generally form more solid structures, have more controllable pore sizes and their gelation mechanism cannot be reversed. Some examples of physical and chemical hydrogels are shown in Table 1.3.

Table 1.3: **Examples of physical and chemical cross-linking in hydrogels.** Table adapted from Omidian and Park (2012)

Physical hydrogels	Chemical hydrogels
Hydrophobic interactions	**Covalent cross-links formed:**
Methyl groups in methyl cellulose	**Simultaneous polymerisation and cross-linking**
Isopropyl groups in poly(N-isopropyl acrylamide)	Acrylic acid or acrylamide, cross-linked with methylene bisacrylamide
Ionic interactions	
Ion-polymer interactions e.g. poly(vinyl alcohol) treated with borax, sodium alginate treated with calcium and aluminium.	**Post-polymerisation chemical cross-linking**
Polymer-polymer complexation e.g. alginate and chitosan	Acrylic-based hydrogel, cross-linked with glycerine
	Gelatin cross-linked with glutaraldehyde
Hydrogen Bonding	
Poly (acrylic acid)/polyacrylamide chains	
Chain aggregation	
Hydrocolloids e.g agar, gelatin	

1.6.3 Responsive hydrogels

A hydrogel may exhibit changes in structure as a response to an environmental change, such as temperature, pH or ionic strength. Different polymers are responsive to different environmental factors. For example, polymers containing hydrophobic groups become less soluble and form hydrophobic cross-links at high temperatures. Inversely, hydrocolloids such as agar, once heat-treated, will form a gel as the temperature decreases due to chain aggregation of the polymers double helical structures. Whereas non-ionic hydrogels show no sensitivity to pH changes, ionic hydrogels are more readily influenced by pH conditions, with the type of response depending if they are cationic or anionic. Cationic hydrogels swell in low pH conditions, leading to a more open structure, whereas anionic hydrogels have the opposite reaction, where the structure will swell at a higher pH value. This is as a response to ionic interractions between the polymers and the H^+ or OH^- ions in the solvent (Gupta *et al.*, 2002).

1.6.4 Hydrogels for drug delivery

Hydrogels were first described for biological use by Wichterle and Lim (1960), who suggested the use of poly-glycolmonomethacrylate hydrogels for making contact lenses.

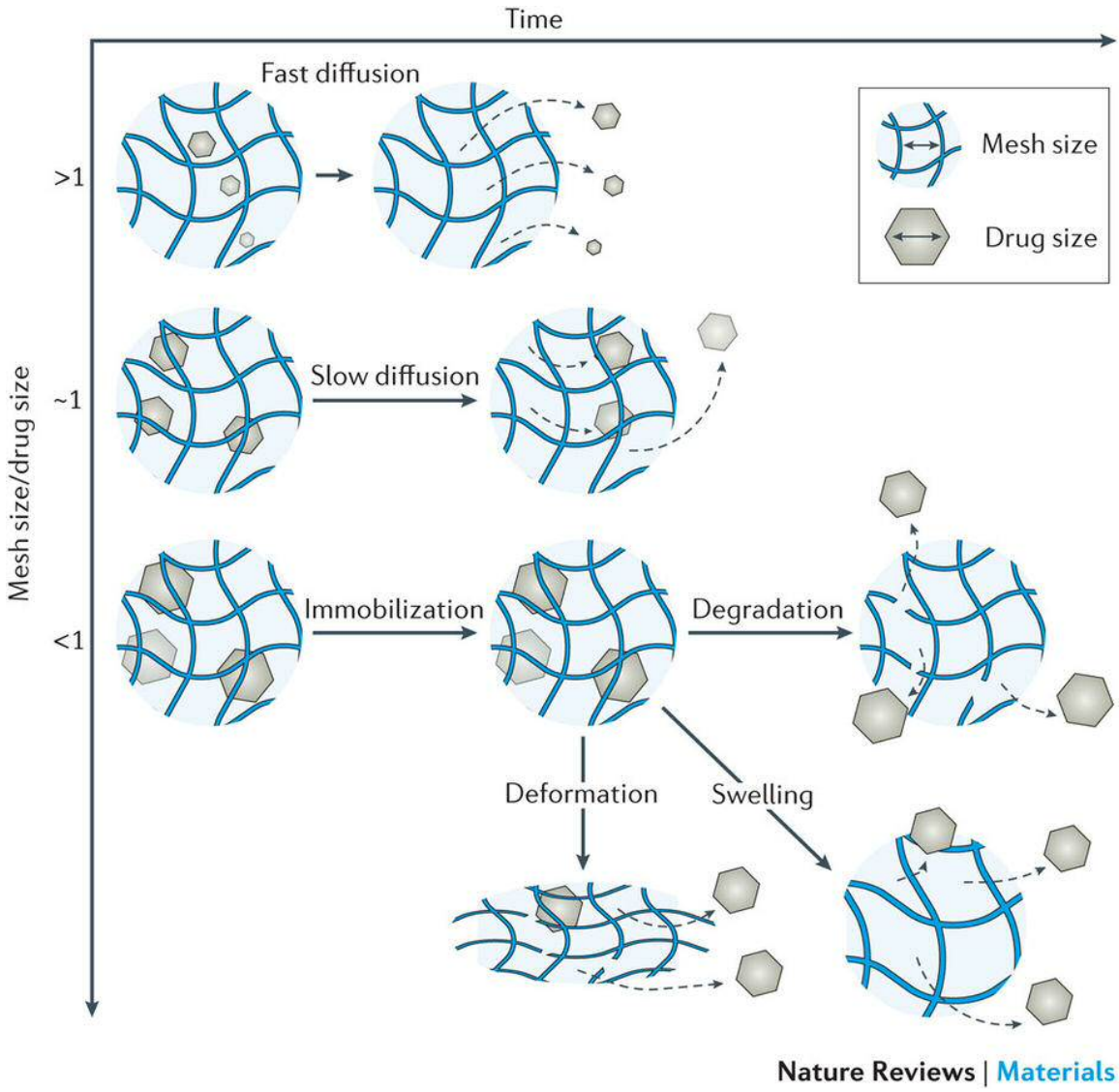

Figure 1.6: **Hydrogel mesh size mediates drug diffusion.** A small drug to mesh size ratio allows for rapid drug diffusion whereas diffusion slows as the ratio approaches 1. A size ratio >1 results in drug immobilisation, unless the mesh is enlarged through degradation, deformation or swelling of the hydrogel, which then allows drug release. Image from Li and Mooney (2016).

Since then, their biocompatibility and tuneable mechanical properties make them suitable for a range of biological and biomedical uses, including as carriers for the delivery of drugs.

Drug loading into hydrogels allows for local drug delivery, bypassing the systemic administration route and therefore reducing the risk of off-target effects. For example, collagen type I hydrogels containing the cytokines BMP-2 and BMP-7 are used clinically for treatment of long bone fracture and spinal fusion (Bessa *et al.*, 2008). The cytokines induce bone and cartilage growth and local delivery allows for a reduced concentration to be administered, which may reduce undesirable side-effects, including tumorigenesis (James *et al.*, 2016).

Spatial and temporal control of drug release is achieved by tuning the hydrogel's physical properties. The size of the open spaces between polymer chains (mesh size) relative to the drug size dictates the rate of drug diffusion, and the hydrogel response to its environment, such as swelling, deformation or degradation, results in modification of the mesh size and therefore the diffusion of the drug (summarised in Figure 1.6). Drug release may also be mediated through drug-polymer interactions, such as covalent conjugation, electrostatic interactions or hydrophobic associations (Li and Mooney, 2016).

Chemically cross-linked hydrogels generally have a more controllable mesh size than physical hydrogels, through changing the concentration of the cross-linkers, which allows for a greater level of control over drug release properties (Hoare and Kohane, 2008). A limitation of this is the potential cytotoxicity of residual, unbound cross-linking molecules. Glutaraldehyde is often used to form carbohydrate-based hydrogels, but is also a tissue fixative (Balakrishnan and Jayakrishnan, 2005). Using multiple cross-linking agents may overcome this problem: for example a chitosan/gelatin blend was used with a covalent cross-linker (glutaraldehyde) and an ionic cross-linking agent with the intention of reducing the amount of toxic glutaraldehyde required to form the gel but retain its stability (Jatariu Cadinoiu *et al.*, 2011; Ciobanu *et al.*, 2014).

1.6.4.1 Injectable hydrogels for drug delivery

Local drug delivery can be achieved by implanting a pre-formed hydrogel to the delivery site, however in some cases this may require surgery to access the site. Additionally, the gel would have to be pre-formed to fit the desired spacial parameters. Injectable hydrogels have gained interest in the biomedical field as they offer an alternative method of hydrogel delivery that eliminates the need for invasive surgery and allows the gel to take up the shape of the cavity it is injected into.

Injectable hydrogels are so-called because of the relatively low viscosity of the initial material, usually in the form of a polymer/drug solution. This can then be injected into the body and will have a physiological trigger resulting in the *in situ* formation of the hydrogel. Temperature is often used as the trigger for *in situ* formation, for example a hydrogel based on the thermo-responsive polymer methyl cellulose (MC) has been developed for the controlled delivery of Neurotrophin-3 to the injured spinal cord (Gupta *et al.*, 2006; Elliott Donaghue *et al.*, 2014).

1.6.4.2 Hydrogels for liposomal drug delivery

Due to the aqueous environment within the polymer network of a hydrogel, there is a limited capacity to carry hydrophobic drugs. As such, composite gel systems have been developed that include loading hydrophobic drugs into aqueous colloidal suspensions, such as micelles or liposomes, for hydrogel incorporation (Hoare and Kohane, 2008; McKenzie *et al.*, 2015). There are also examples of hydrophilic drugs being encapsulated in liposomes before addition to the hydrogel in order to allow for more controlled drug release. Ingebrigtsen *et al.* (2017) loaded the antibiotic chloramphenicol into liposomes for incorporation into a chitosan hydrogel for topical, dermal delivery and its *in vitro* antimicrobial activity was greater than that of chloramphenicol solutions alone. Mao *et al.* (2016) used an injectable hydrogel to deliver liposomes containing the hydrophobic chemotherapeutic drug paclitaxel in a mouse model of pancreatic cancer. They found that intratumoural injection of the hydrogel resulted in a high local paclitaxel concentration, sustained and stable drug release,

extend drug retention inside the tumour, and low toxicity to normal tissues.

A composite liposomal/hydrogel system could potentially combine the advantages of liposomal drug encapsulation (Section 1.5) and hydrogel drug delivery to develop a medicament for effective, local antimicrobial delivery to sites of potential dental infection.

1.7 Aims and objectives

The primary aim of this thesis is to develop a material with antimicrobial properties that has a use in dental restorations in order to control pulpitis and root canal infection. It will:

- Determine the suitability of liposomes to encapsulate and release the antimicrobial triclosan;
- Investigate the ability of polymer hydrogels to carry and deliver liposomes;
  - Hydrogels will be assessed for their suitability as dental restoration materials that can carry liposomes and deliver their contents. Rheological studies will assess the handling properties of the hydrogel and any effect that liposome incorporation will have on these properties;
- Investigate the effects of antimicrobial agents released on common pathogenic bacteria implicated in the development of pulpitis and root canal disease;
  - The effect of liposomal triclosan released from the gel will be measured using *in vitro* assays and a root canal infection model.

Chapter 2

Characterisation of Bacterial Isolates and Assessment of the Antimicrobial Efficacy of Triclosan

2.1 Introduction

Microbial infections following endodontic surgery are difficult to treat and, if allowed to progress, can lead to irreversible tissue damage and systemic infection. Studies that have isolated bacteria from root canals following endodontic failure have found that failure is not associated with a single species alone, however some species are more commonly isolated than others. Gomes *et al.* (2004) found a significant association between teeth that had previously undergone endodontic treatment and the presence of *Enterococcus* and *Streptococcus* species in root canal isolates.

Streptococcus anginosus, alongside *Streptococcus constelatus* and *Streptococcus mutans*, are part of the *Streptococcus anginosus* group (SAG) of bacteria, which have clinical similarities and are implicated in early colonisation and secondary infection of the dental pulp (Lamothe, 1990; Jenkinson and Demuth, 1997). *Enterocoocus faecalis* is commonly isolated from filled root canals, however it is not often found in advancing carious lesions and its mode of infiltration into the root canal system is unknown (Zehnder and Guggenheim, 2009).

Despite the predominance of *E. faecalis*, root infections are generally polymicrobial, and therefore antimicrobial selection must take this into account. Triclosan is a broad-spectrum antimicrobial agent that is used in a variety of dental hygiene products, including mouthwash and toothpaste. Its mode of action is concentration-dependent, with high concentrations being bactericidal and lower concentrations being bacteriostatic. Its bacteriostatic effect comes from inhibition of fatty acid production at the enoyl-acyl carrier protein reductase (FabI) step (Heath *et al.*, 1999). As a biocide, it has multiple cytoplasmic and membrane targets (Russell, 2004).

A recent Cochrane review showed that the use of triclosan toothpaste reduced plaque, gingivitis, bleeding gums and caries in patients when the triclosan was delivered in combination with a copolymer to reduce the dilution of the drug with mouth rinsing or saliva (Riley and Lamont, 2013). Triclosan is not currently used for the treatment pulpitis or endodontic infection, however there is some evidence to suggest its potential efficacy. Nudera *et al.* (2007a) showed triclosan efficacy against 5 endodontic pathogens, including *E. faecalis in vitro* and Roberts *et al.* (2013c) demonstrated triclosan efficacy against *S. anginosus* in an *ex vivo* rat model of pulpal infection.

This chapter characterises strains of *E. faecalis* and *S. anginosus* for modelling endodontic infection. It also assesses the antimicrobial efficacy of triclosan against these bacteria and considers its use as a model antimicrobial for further incorporation into a dental filling material.

2.2 Materials and methods

2.2.1 Preparation of bacterial stocks and growing conditions

Clinical isolates *E. faecalis* RB17 (origin: gastrointestinal tract) and *S. anginosus* 39/2/14A (origin unknown) were selected from the culture collection of the Cardiff School of Dentistry. Swabs were taken from samples stored at -80 °C and streaked onto tryptone soya agar (TSA) plates, which were then incubated at 37 °C in 5 %

CO_2 for 18 h.

For growth inhibition experiments, overnight broth cultures were prepared: brain heart infusion (BHI) broth was inoculated with a single colony of bacteria taken from a TSA plate and this was incubated at 37 °C in 5 % CO_2 for 18 h prior to further use. All growth inhibition experiments were performed on 3 separate occasions with a fresh overnight broth culture.

2.2.2 Confirmation of bacterial species

2.2.2.1 Gram stain

Bacteria were Gram-stained in order to assess their morphology and check for contamination. Using a sterile wire loop, a swab was taken from a TSA plate culture and smeared on a glass slide with a drop of sterile water. The slide was air-dried and then heat-fixed over a bunsen flame. The slide was then flushed with crystal violet solution for 60 s, rinsed with tap water and then flushed with Lugoli's iodine solution for 60 s. Acetone was used to rinse the slide, before Carbol fuchsin solution was applied for 60 s. The slide was then rinsed with tap water and air-dried before it was viewed using oil-immersion light microscopy.

2.2.2.2 Genetic sequencing

DNA was extracted from the bacteria and the 16S ribosomal RNA (rRNA) region was sequenced to confirm correct species identification. *E. faecalis* and *S. anginosus* were collected from an overnight culture grown on TSA. DNA was extracted using a QIAamp DNA Mini Kit (Qiagen, Manchester, UK) according to the manufacturer's protocol (see Appendix A). DNA samples were then amplified at the 16S rRNA region using forward and reverse primers D88 and E94 and this DNA region was sequenced (amplification and sequencing was performed by Cardiff University Central Biotechnology Services). The resulting sequences were entered into the Basic Local Alignment Search Tool (BLAST) to assess how similar the sequences were to known

bacterial strains (National Center for Biotechnology Information, U.S. National Library of Medicine, Bethesda MD). A match of 95 % or above to the correct bacterial species was considered adequate.

2.2.3 Bacterial growth with triclosan

2.2.3.1 Preparation of triclosan solutions

Triclosan was dissolved in propan-2-ol (IPA) at 10 mg/mL and 6 subsequent 2-fold dilutions were done in IPA to obtain a range of triclosan concentrations (0.3125-20 mg/mL). BHI was then added dropwise to obtain a final IPA concentration of 1 % (v/v) and final triclosan concentrations of 3.125-200 µg/mL. Control solutions contained only 1 % (v/v) IPA in BHI.

2.2.3.2 Growth of bacteria with triclosan and determination of the minimum inhibitory concentration (MIC)

Triclosan solutions (0-200 µg/mL) in 1 % IPA (v/v) were pipetted into a 96-well plate (100 µL/well). Overnight broth cultures of *E. faecalis* and *S. anginosus* were diluted in BHI to obtain an optical density of 0.08-0.1 at 600 nm. Two further 10-fold dilutions in BHI were then done and 100 µL/well of the resulting bacterial suspension was pipetted onto the wells containing the triclosan solutions. The plate was incubated in a plate reader (FLUOstar Omega, BMG Labtech, Ortenberg, Germany) at 37 °C in 5 % CO_2 for 20 h. The absorbance at 600 nm was measured every 1 h and the plate was shaken at 40 RPM for 30 s before each measurement.

The MIC was considered to be the concentration at which no growth was observed after 20 h.

2.2.3.3 Analysis of bacterial growth curves

Bacterial growth curves from Section 2.2.3.2 were analysed using the statistical package R (R Core Team, 2013). The growth analysis package "Grofit" was used to analyse the growth curves produced from the obtained absorbance measurements

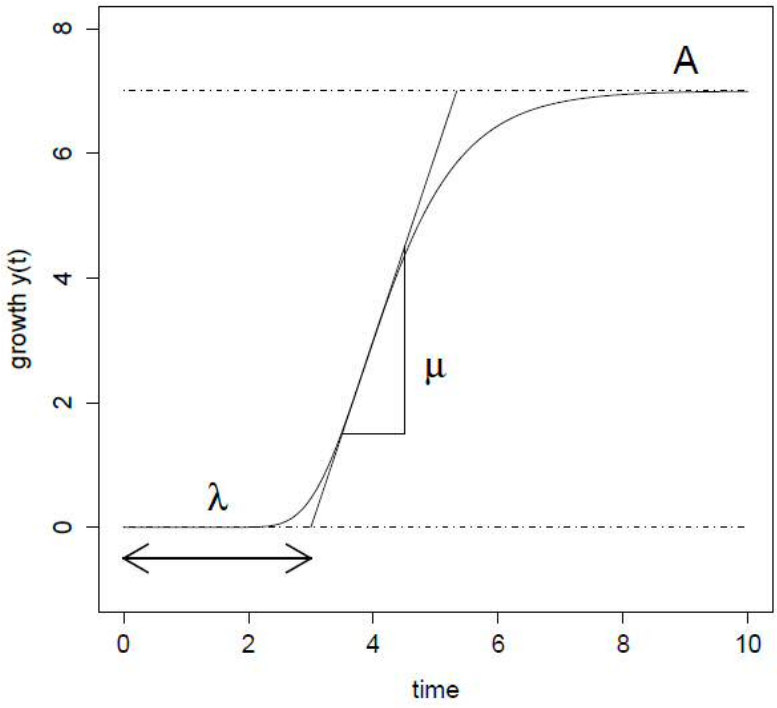

Figure 2.1: **Example of parameters derived from bacterial growth curves.** Example growth curve showing length of lag phase (λ), growth rate represented by the maximum slope (μ) and maximum growth (A). Taken from (Kahm *et al.*, 2010)

(Kahm *et al.*, 2010). Grofit fits a model-free spline to experimental data and the length of lag phase (λ), maximum growth rate (μ) and maximum absorbance value (A) are derived from this fit (example shown in Figure 2.1). Where a value of λ was less than 0 h or more than 20 h, it was assumed that there was no distinguishable lag phase for that particular growth curve, and therefore λ and μ were excluded from further analyses since no measurable growth had occured under these experimental conditions.

A difference in the mean values of λ, μ and A was tested for using ANOVA with post-hoc Tukey's test. A P value of 0.05 or less was considered statistically significant ("ns"=$P > 0.05$, *=$P < 0.05$, **=$P < 0.01$, ***=$P < 0.001$).

2.2.3.4 Minimum bactericidal concentration (MBC) of triclosan

To determine the MBC of triclosan, the bacterial/triclosan suspensions from the 96-well plate of the previous experiment (Section 2.2.3.2) were used. Concentrations

of triclosan were selected where no growth had been observed, in addition to the two concentrations above this value. Bacteria-only and broth-only controls were also included. The contents of the selected wells (200 µL/well) were removed and diluted in 20 mL of BHI. This suspension was incubated for 20 h at 37 °C in 5 % CO_2. Where growth was visually observed (indicated by an increase in broth turbidity compared to broth-only controls), a positive growth result was noted. Where the broth had remained clear, these suspensions, alongside the control suspensions, were centrifuged at 4000 $\times g$ for 5 min and the supernatant was poured off. The remaining pellet was resuspended in 50 µL of BHI and then spread onto a TSA plate using a spiral plater (Don Whitley Scientific Limited, Shipley, UK). The TSA plates were then incubated for 20 h, as previously described and inspected for growth. The MBC was considered to be the lowest triclosan concentration at which no growth had been observed.

2.2.3.5 Minimum biofilm eradicating concentration (MBEC) of triclosan

Overnight broth cultures of *E. faecalis* or *S. anginosus* were diluted in BHI to obtain an optical density of 0.08-0.1 at 600 nm. Two further 10-fold dilutions were then done and the resulting bacterial suspension was pipetted into a 96-well plate (200 µL/well). A biofilm was allowed to grow by incubating the plate at 37 °C in 5 % CO_2 for 24 h. The wells were aspirated and washed with sterile phosphate-buffered saline (PBS, 200 µL/well) to to remove unattached cells. Triclosan solutions (0-200 µg/mL, 1 % IPA in BHI v/v, 200 µL/well) were pipetted onto the remaining biofilms and the plate was incubated for a further 24 h (37 °C, 5 % CO_2). The triclosan solutions were aspirated and the wells were washed with 200 µL of sterile PBS before 200 µL of BHI was then added to the wells. The absorbance at 600 nm was read on a plate reader (FLUOstar Omega, BMG Labtech, Ortenberg, Germany) and then the plate was incubated for a further 24 h (37 °C, 5 % CO_2) before the absorbance was read as before.

All absorbance values were standardised to a blank well containing 200 µL BHI and the standardised absorbance values of the first reading were subtracted from those

of the second reading to determine the relative growth of the bacteria. The mean value was calculated from triplicate samples on each plate and the MBEC recorded as the lowest concentration of triclosan that demonstrated a $\geq$ 80 % reduction in absorbance compared to the control.

2.2.3.6 Growth inhibition on agar plates

Bacterial lawn plates were prepared by evenly swabbing an overnight broth culture of *E. faecalis* or *S. anginosus* over the surface of a TSA plate using a sterile, cotton swab. Wells were then punched into the agar using a sterile 6 mm biopsy punch. Triclosan solutions (50 µL, 0-500 µg/mL in 1 % IPA) were then pipetted into the wells and the plates were incubated at 37 °C in 5 % CO_2 for 20 h. Growth of bacteria was believed to be inhibited where a clear area of agar was observed around the innoculation site, in contrast to the bacterial growth covering the rest of the plate.

2.3 Results

2.3.1 Bacterial appearance, morphology and genetic identification.

E. faecalis and *S. anginosus* were cultured from previously isolated bacterial stocks. Both species grew on TSA and colonies were visible after incubation for 18 h. Figure 2.2 shows the appearance of both species on TSA. *E. faecalis* colonies were larger than those of *S. anginosus* and had a glossy appearance.

Visual inspection of Gram-stained bacteria (Figure 2.3) confirmed that both *E. faecalis* and *S. anginosus* were Gram-positive cocci, with no other cell morphologies identified. Cells appeared in pairs, short chains, or clusters and *E. faecalis* cells were larger than those of *S. anginosus*.

Genetic analysis of the bacterial species used confirmed that the 16S rRNA region of DNA matched with that of *E. faecalis* (D88: 97 %, E94: 99 %) and *S. anginosus* (D88: 98 %, E94: 97 %), according to the BLAST database. This gave further

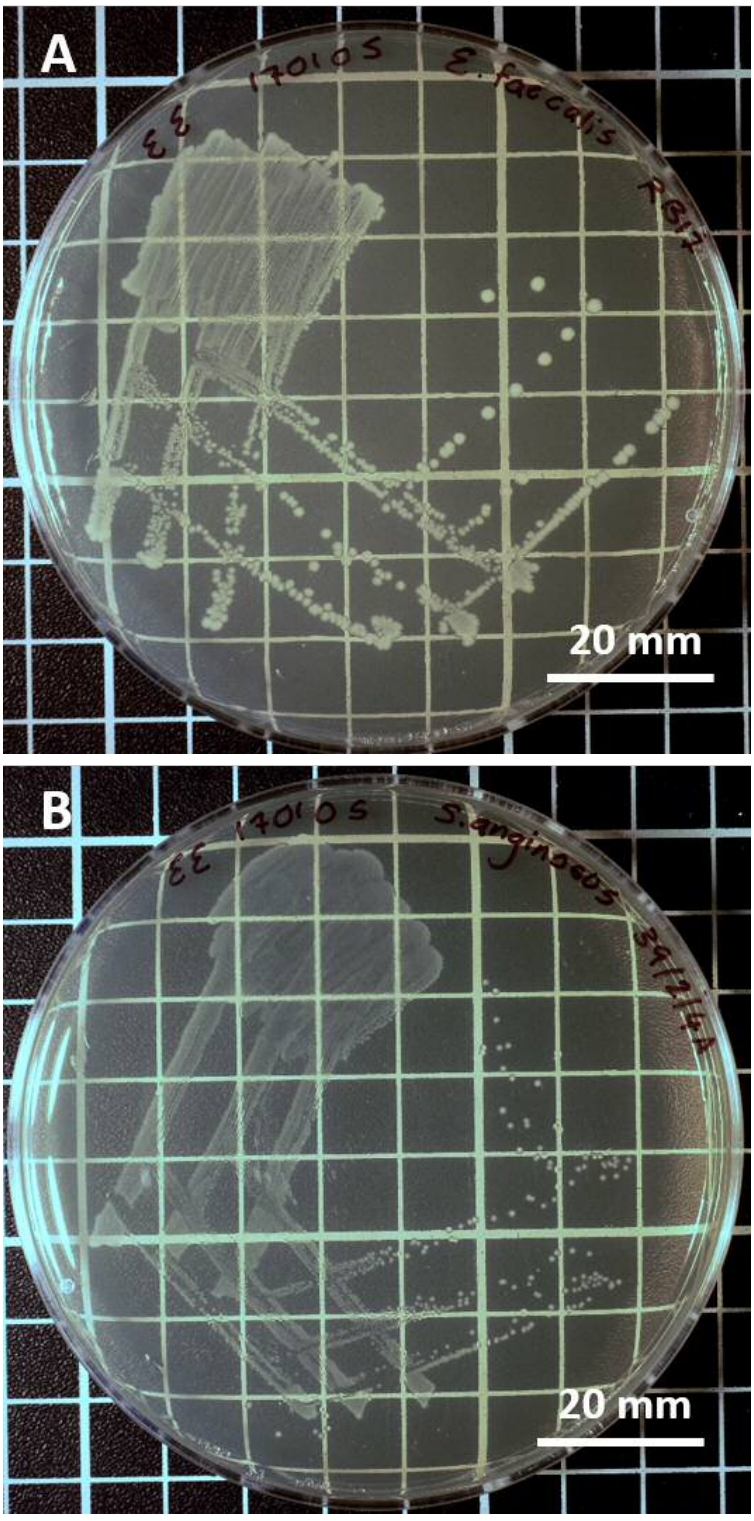

Figure 2.2: **Bacteria used for assessment of antimicrobial efficacy.** Streak plates of *Enterococcus faecalis* (A) and *Streptococcus anginosus* (B) show growth on TSA after 18 h incubation at 37 °C in 5 % CO_2.

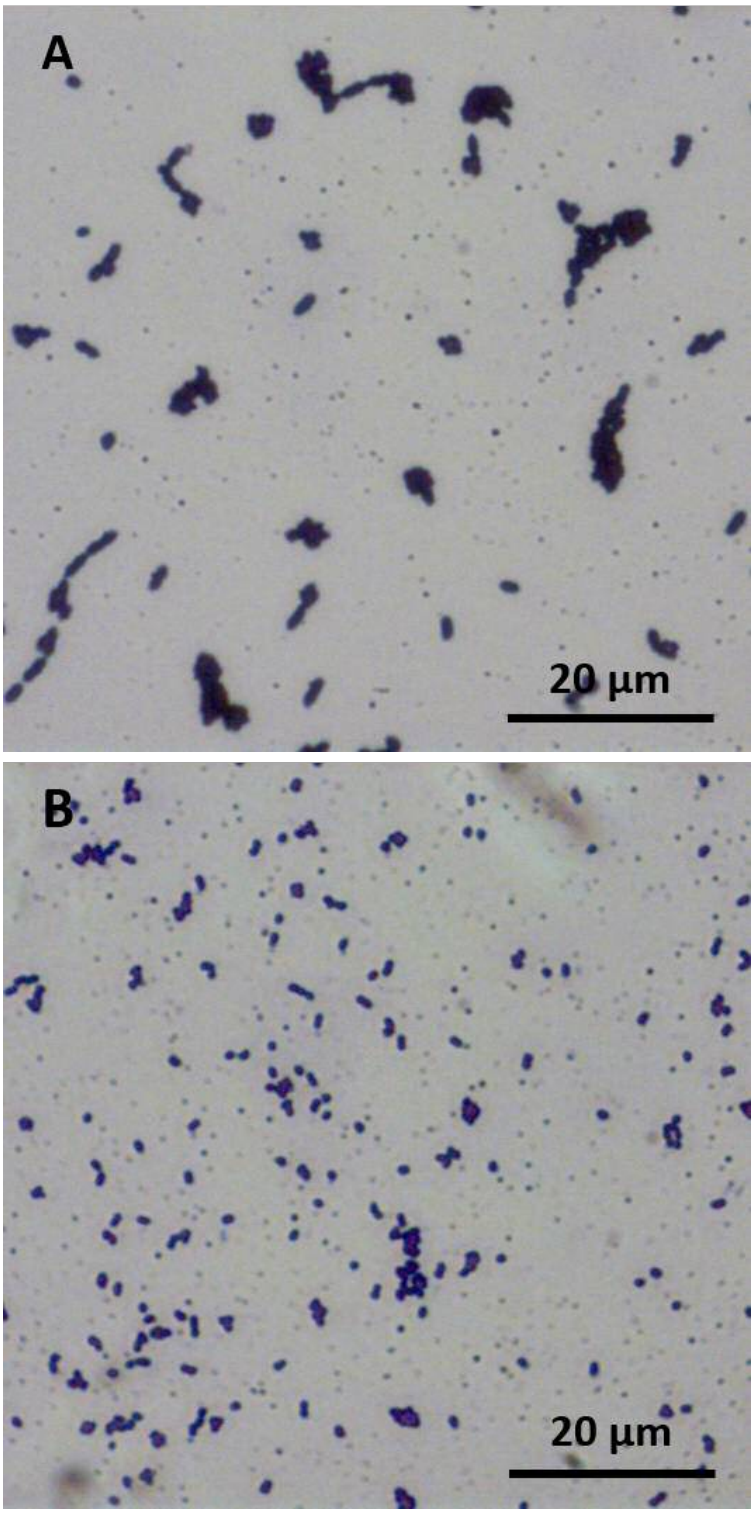

Figure 2.3: **Gram stain of bacteria used for assessment of antimicrobial efficacy.** Gram stains of *Enterococcus faecalis* (A) and *Streptococcus anginosus* (B) shown at 100 X magnification under oil immersion.

confirmation that the correct species of bacteria were used in this work. The full sequences are included in Appendix B.

2.3.2 Bacterial growth with triclosan

2.3.2.1 Growth curves for minimum inhibitory concentration (MIC) determination

Bacteria were incubated for 20 h with triclosan solutions in order to assess the antimicrobial efficacy of triclosan against these bacterial strains. Growth curves (Figure 2.4) showed that *E. faecalis* and *S. anginosus* growth was inhibited by triclosan compared to the untreated control and no growth was observed in either bacterial strain with concentrations of 6.25 µg/mL or above. Bacterial growth was not affected by addition of 1 % IPA, which was used as the diluent for triclosan.

Table 2.1 shows the characteristic parameters derived from the growth curves using a spline fit of the experimental data. For both bacterial species, values for λ (length of lag phase) and μ (maximum growth rate) for triclosan concentrations of 6.25 µg/mL and above were excluded from analyses for reasons set out in Section 2.2.3.3. The maximum absorbance value (A) for these concentrations was significantly lower than that of the bacteria in BHI alone (P¿0.001), indicating that the turbidity of the suspension had not increased as much as the control and therefore bacterial growth had been inhibited. For a triclosan concentration of 3.125 µg/mL, λ of *E. faecalis* was not significantly different. Values of μ and A, however, were significantly lower than those of bacteria alone (μ:P=0.0012, A:P¡0.001), suggesting a partial, but not complete, inhibition of growth. A similar result is seen for *S. anginosus*, with the exception that the reduction in A was not statistically significant (P=0.13).

Analysis of these bacterial growth curves therefore indicated that inhibition of both *E. faecalis* RB17 and *S. anginosus* 39/2/4A growth was achieved with triclosan and that the minimum inhibitory concentration was 6.25 µg/mL for both bacterial strains, with partial inhibition observed with 3.125 µg/mL.

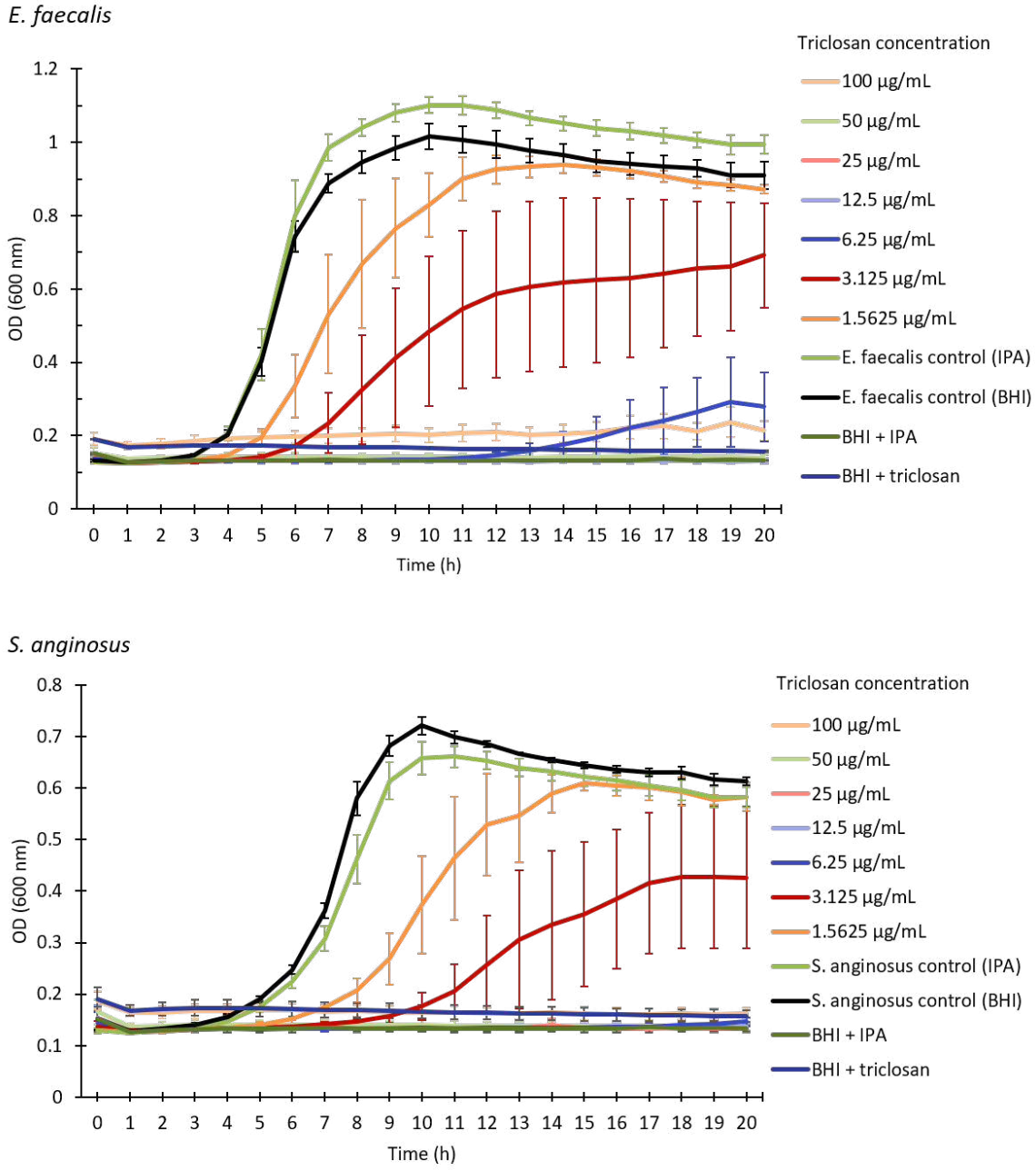

Figure 2.4: **Growth of *Enterococcus faecalis* (top) and *Streptococcus anginosus* (bottom) with triclosan.** Bacteria were grown in BHI with triclosan in a 96-well plate and the absorbance was measured over 20 h. Graphs show optical density at 600 nm. Error bars show standard error of the mean of 3 independent experiments.

Table 2.1: **Growth parameters of *Enterococcus faecalis* (top) and *Streptococcus anginosus* (bottom) with triclosan.**

Triclosan conc. (µg/mL)	λ (h)			µ			A (Abs_{600})		
	Mean	SEM	*sig.*	**Mean**	SEM	*sig.*	**Mean**	SEM	*sig.*
0 (*E. faecalis* in BHI)	**2.64**	0.20	-	**0.21**	0.01	-	**1.11**	0.02	-
0 (*E. faecalis* in BHI+IPA)	**2.64**	0.20	*ns*	**0.21**	0.01	*ns*	**1.11**	0.02	*ns*
1.56	**3.99**	0.72	*ns*	**0.16**	0.01	*ns*	**0.95**	0.02	*ns*
3.13	**7.79**	2.72	*ns*	**0.11**	0.03	***	**0.70**	0.16	**
6.25	**NA**	NA	-	**NA**	NA	-	**0.29**	0.11	***
12.50	**NA**	NA	-	**NA**	NA	-	**0.13**	0.01	***
25.00	**NA**	NA	-	**NA**	NA	-	**0.14**	0.01	***
50.00	**NA**	NA	-	**NA**	NA	-	**0.15**	0.01	***
100.00	**NA**	NA	-	**NA**	NA	-	**0.22**	0.03	***
BHI + IPA	**NA**	NA	-	**NA**	NA	-	**0.14**	0.02	***
BHI + triclosan (100 µg/mL)	**NA**	NA	-	**NA**	NA	-	**0.18**	0.02	***

Triclosan conc. (µg/mL)	λ (h)			µ			A (Abs_{600})		
	Mean	SEM	*sig.*	**Mean**	SEM	*sig.*	**Mean**	SEM	*sig.*
0 (*S. anginosus* in BHI)	**3.74**	0.20	-	**0.11**	0.01	-	**0.66**	0.02	-
0 (*S. anginosus* in BHI+IPA)	**3.74**	0.66	*ns*	0.11	0.01	*ns*	**0.20**	0.02	*ns*
1.56	**6.45**	0.96	*ns*	**0.10**	0.00	*ns*	**0.63**	0.01	*ns*
3.13	**9.05**	1.73	*ns*	**0.06**	0.03	*	**0.45**	0.15	*ns*
6.25	**NA**	NA	-	**NA**	NA	-	**0.15**	0.01	***
12.50	**NA**	NA	-	**NA**	NA	-	**0.15**	0.02	***
25.00	**NA**	NA	-	**NA**	NA	-	**0.14**	0.02	***
50.00	**NA**	NA	-	**NA**	NA	-	**0.16**	0.02	***
100.00	**NA**	NA	-	**NA**	NA	-	**0.18**	0.01	***
BHI + IPA	**NA**	NA	-	**NA**	NA	-	**0.14**	0.02	***
BHI + triclosan (100 µg/mL)	**NA**	NA	-	**NA**	NA	-	**0.18**	0.02	***

Bacteria were grown in BHI with triclosan in a 96-well plate for 20 h. Length of lag phase (λ), maximum growth rate (μ) and maximum absorbance value (A) of growth curves (shown in Figure 2.4) are shown. (*"SEM"= standard error of the mean, "sig."= significance of difference in means compared to bacteria in BHI:"ns"*= $P > 0.05$, *= $P < 0.05$, ** =$P < 0.01$, ***=$P < 0.001$)

2.3.2.2 Minimum bactericidal concentration (MBC) of triclosan

The MBC of triclosan was determined from cultures of *E. faecalis* and *S. anginosus* that had been incubated with 0-100 µg/mL of triclosan for 20 h, diluted to reduce the triclosan concentration below the MIC, and then transferred to a TSA plate to allow further growth, should any live bacteria still be present in the suspension. Growth of *E. faecalis* was observed from cultures grown with 12.5 µg/mL triclosan and below, but not with 25 µg/mL and above. Growth of *S. anginosus* was observed from cultures grown with 6.25 µg/mL of triclosan, but not with 12.5 µg/mL and above. Table 2.2 shows a summary of these results.

2.3.2.3 Minimum biofilm eradicating concentration (MBEC) of triclosan

Bacteria were grown as biofilms and treated with triclosan solutions to determine the MBEC of triclosan. By the conditions set out in Section 2.2.3.5, the MBEC of triclosan was 50 µg/mL against both bacterial species, as this was the concentration at which a $\geq$80 % reduction in absorbance was observed compared to the BHI-only control (Figure 2.5).

The results of the MIC, MBC and MBEC analyses suggested that triclosan was bacteriostatic, but not bactericidal at concentrations between 6.25-25 µg/mL against *E. faecalis* and 6.25-12.5 µg/mL for *S. anginosus*. Triclosan was bactericidal above these ranges, however a triclosan concentration of 50 µg/mL or more was needed to eradicate biofilms of both these bacteria.

2.3.2.4 Zones of inhibition on bacterial lawn plates

Bacterial lawn plates that had been inoculated with triclosan solutions showed zones of inhibition with all triclosan solutions tested, but not with negative controls. Figure 2.6 shows a representative image of the results obtained, which were similar for all 3 independent experiments. Growth of *S. anginosus* was visible by eye but the contrast was low between areas of growth and areas of no growth, making it difficult to identify clear zones of inhibition. *E. faecalis* growth was more evident and zones of inhibition

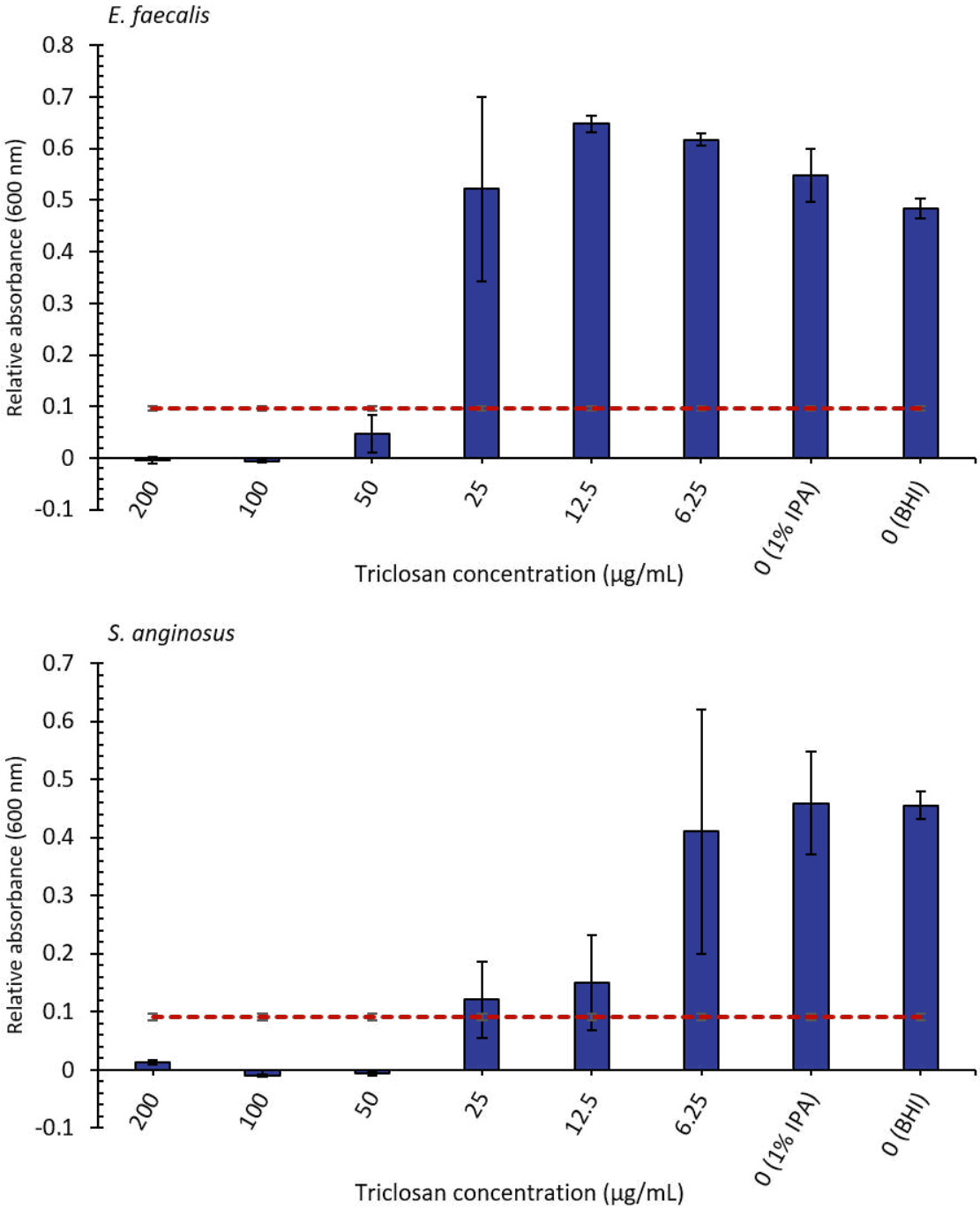

Figure 2.5: **Minimum biofilm eradicating concentration of triclosan.** Biofilms of *E. faecalis* or *S. anginosus* were grown and treated with triclosan solutions. Graphs show relative absorbance over 24 h of the remaining bacterial suspensions after the triclosan solutions had been removed. Dotted red line shows theoretical value of an 80 % reduction in relative absorbance of the BHI-only control (error is within the line thickness). Error bars show standard error of 3 independently performed experiments.

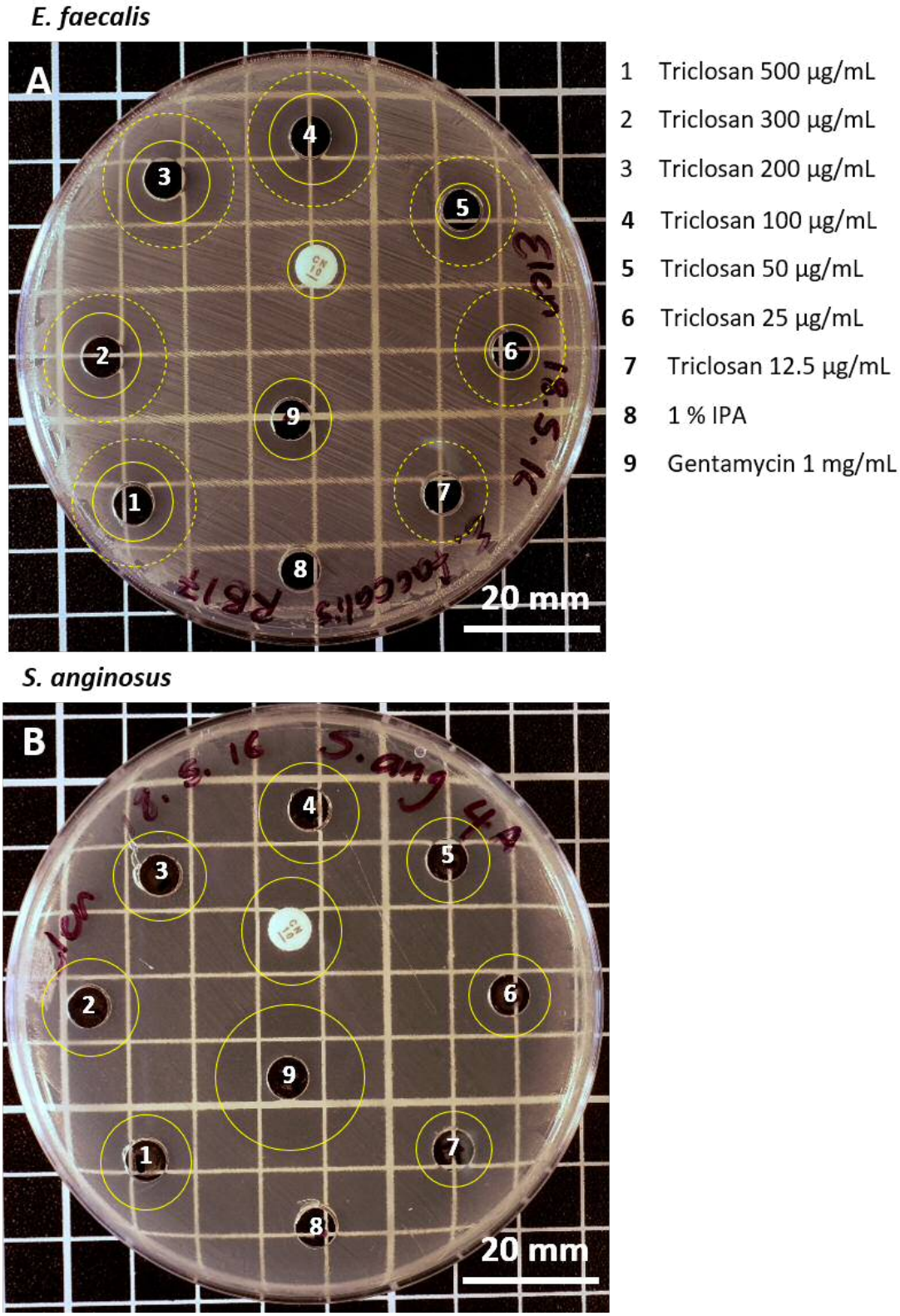

Figure 2.6: **Bacterial lawn plates with triclosan.** TSA plates were swabbed with cultures of *Enterococcus faecalis* **(A)** and *Streptococcus anginosus* **(B)** and inoculated with triclosan before incubating for 20 h. Representative images of 1 of 3 independent experiments are shown. Yellow lines are a visual aid to show areas of observed growth inhibition. Dashed lines show areas of observed reduced growth (*E. faecalis* only).

Table 2.2: Growth of *Enterococcus faecalis* and *Streptococcus anginosus* for the determination of triclosan MBC.

Triclosan conc.	Growth observed (+/-)	
(µg/mL)	E. faecalis	S. anginosus
0 (bacteria in BHI)	+ + +	+ + +
6.25	+ + +	+ + +
12.5	+ + +	+ - -
25	- - -	- - -
BHI only	- - -	- - -

Bacteria were grown in BHI with triclosan in a 96-well plate for 20 h. Suspensions were subsequently diluted to reduce triclosan concentration to sub-MIC levels and then re-cultured on TSA plates. Table shows whether growth had occurred, with each '+' or '-' indicating the result of one independent experiment.

were clearly identified. Gentamycin was included as a positive control, and the zones of inhibition observed were very clear-cut, whereas zones seen with triclosan showed a region of lower growth, giving a 'halo' effect on the plate. This may be due to the bacteriostatic effect of the drug acting on areas further away from the areas of complete inhibition.

2.4 Discussion

The bacterial strains used for this work conformed with UK Standards for Microbiology Investigations in terms of colony morphology and microscopic appearance for both *E. faecalis* and *S. anginosus* (Public Health England, 2014) and no contamination was present in the previously isolated stocks. Additionally, 16S rRNA sequence analyses confirmed that the species used were correctly identified.

Triclosan is a commonly used, broad-spectrum antimicrobial, which is used in mouthrinses and toothpastes for the control of oral bacteria. Its efficacy against *E. faecalis* is well documented, however there are some discrepancies in the literature regarding the effective concentration. Some studies report the MIC against *E. faecalis* to be between 1-7 µg/mL (Suller and Russell, 1999; Jones *et al.*, 2005; Williams and Stickler, 2008; Sun and Song, 2011), however others report a MIC of 16 µg/mL (Koburger *et al.*, 2010; Morrissey *et al.*, 2014) and one study found the MIC to be

s high as 94 µg/mL (Nudera *et al.*, 2007b). There is less evidence in the literature on triclosan efficacy against *S. anginosus*, despite the prevalance of this bacterium in oral diseases, and its importance in the advancing carious lesions that result in pulpitis and endodontic infections. Cullinan *et al.* (2014) assessed the efficacy of triclosan against dental plaque isolates of *S. anginosus* and found the MIC to be 125-250 µg/mL. Another study by Ledder *et al.* (2006), however, reported a much lower MIC of 4 µg/mL against *S. anginosus* isolated from a similar source. The variability in these reported results may be due to a number of factors, including differences in *in vitro* experimental conditions and potential acquired resistance of the bacteria, particularly from clinically obtained isolates. Both *Enterococcus* and *Streptococcus* species have the potential to develop resistance to triclosan, as they contain not only FabI (the target of triclosan), but also FabK, an alternative enoyl-acyl carrier protein reductase that has been shown to counter resistance to triclosan in *Streptococcus pneumoniae* (Heath and Rock, 2000; Cullinan *et al.*, 2014).

The variability in reported MICs therefore illustrates the importance of ascertaining the effective concentration of triclosan against the specific strains of bacteria used in this work in order to relate the efficacy of liposomal and hydrogel formulations developed in the following chapters to that of triclosan solution. The triclosan MIC against *E. faecalis* obtained in this chapter (6.25 µg/mL) is in agreement with the majority of the literature and shows that triclosan has an inhibitory effect on the tested strain of *E. faecalis* at relatively low concentrations, considering that the concentration allowed in antimicrobial products is 300 µg/mL (Scientific Committee on Consumer Safety, 2010). The same MIC was seen against *S. anginosus*, which suggests that triclosan is an appropriate choice of antimicrobial for the development of a material and may have potential for inhibiting primary colonisation or preventing secondary infection of the pulpal chamber and root canals.

The R package "grofit" was used to obtain a quantitative description of the bacterial growth curves and the conclusions drawn from analysis of these data agreed with those obtained from visual inspection of the growth curves themselves. This mode of analysis is therefore appropriate for analysing further antimicrobial efficacy

data (Chapters 3 and 4).

The MBC of triclosan was 4-times higher than the MIC against *E. faecalis*. Other studies have reported an MBC as 2-fold greater (Morrissey *et al.*, 2014) or equal to the MBC (Nudera *et al.*, 2007b; Koburger *et al.*, 2010). For *S. anginosus*, the MBC was 2-fold higher than the MIC: a result which was also observed by Ledder *et al.* (2006). These data, along with results found in the literature suggest that triclosan is bacteriostatic against the two strains tested, but is also an effective bactericide at relatively low concentrations, which is promising for its application in preventing recurrence of infection.

For determining the MBC, it was assumed that residual triclosan activity in the samples would be halted by the dilution to sub-MIC levels and subsequent centrifugation and resuspension of bacteria. The standards for antimicrobial testing suggest a neutraliser should be used to inhibit any residual antimicrobial activity, in order to obtain the MBC (McDonnell *et al.*, 1998; British Standards Institution, 2005), therefore the true MBC of triclosan for these bacterial strains may be higher than those reported here. This work, however, serves as an estimate and the efficacy is further assessed in a more clinically relavent setting for the intended application (Chapter 5).

Oral bacteria predominantly reside as biofilms rather than in the planktonic state (Do *et al.*, 2013) and therefore the MBEC of triclosan was assessed in order to get an estimate of the concentration required to eradicate these bacteria in a biofilm. It was observed that the MBEC was almost 10-fold higher than the MIC for single species biofilms of both bacteria (50 µg/mL), which demonstrates the additional challenges faced in erradicating bacteria in this form.

The observation of zones of inhibition on bacterial lawn plates is a commonly used method for testing antimicrobial efficacy of materials. This method was therefore tested with triclosan solutions against *E. faecalis* and *S. anginosus* in order to observe whether this method would be suitable for testing triclosan liposomes and liposome-loaded hydrogels, which are discussed in subsequent chapters. Zones of inhibition were clearly observed on *E. faecalis* lawn plates at all concentrations that

had previously shown growth inhibition of planktonic bacteria. This was also true with *S. anginosus* however the zones of inhibition were not as distinguishable from the background bacterial growth. This may be due to the smaller colony size of *S. anginosus* and therefore the growth on the agar surface appears less opaque than that of *E. faecalis*. This may be improved by selecting a different culture medium or by different imaging methods, such as scanning and the use of image analysis software (e.g. ImageJ). The zones of lower growth ('halos') observed may show areas where triclosan is present at concentrations that slow the growth, identified by a longer lag phase, lower rate of growth and lower maximum absorbance in the previously shown growth curves.

These results suggest that this method may be suitable for testing the materials, however care must be taken when observing plates of *S. anginosus*.

2.5 Conclusions

From these data, it is concluded that triclosan is an effective antimicrobial against two strains of oral bacteria known to be implicated in pulpitis and secondary endodontic infections. These results serve as a basis for the further antimicrobial testing of liposomes containing triclosan and liposome-loaded hydrogels, for their suitability to treat endodontic infection.

Chapter 3

Preparation and Characterisation of Liposomes for Antimicrobial Drug Delivery

3.1 Introduction

The use of broad-spectrum antimicrobials in oral health care can help prevent the attachment, proliferation and migration of pathogenic oral bacteria, as has been seen in the case of triclosan in Chapter 2. Major challenges lie in the delivery of these antimicrobials to the correct area, at a clinically relevant concentration and for a suitable period of time. Drugs with poor water solubility are particularly difficult to adminster, as they require dissolution in organic solvents, which may have undesirable cytotoxic effects if used for prolonged periods of time. Liposomal delivery systems offer a solution to poor drug solubility, as the amphiphilic nature of liposomes allows for the loading of both hydrophilic and hydrophobic drugs at clinically significant concentrations.

Liposomes are nanometre-sized, artificially-produced, spherical vesicles comprising of one or more phospholipid bilayer membranes and an aqueous core (Sessa and Weissmann, 1968). Their ability to encapsulate a variety of molecules and their structural resemblance to the cell membranes makes them ideal candidates for drug

delivery systems. Liposomes are composed of natural lipids and are biodegradable, offering good biocompatibility. Additionally, the liposomal membrane may be modified to facilitate controlled release of therapeutics over time, as well as targeted delivery.

Drug structure, concentration and hydrophobicity can affect the formation and conformation of the liposomes. Larger, multilamellar vesicles (MLVs) may offer a higher drug-loading efficiency, however small unilamellar vesicles (SUVs) are less likely to be identified by the body's immune system and eradicated, therefore allowing for more effective drug delivery. Both MLVs and SUVs were prepared for this work, in order to compare the drug loading and overall efficacy of the two vesicle types.

Phosphatidylcholine (PC), shown in Figure 3.1, is a commonly used liposomal phospholipid. It is a major component of biological membranes and is therefore readily extracted and highly biocompatible. The head group of PC is cationic, however the overall charge is neutralised by the phosphate molecule at the phosphatidyl moiety.

Liposomes containing the antimicrobial drug triclosan have previously been studied for antimicrobial delivery. Various formulations were observed to have an antimicrobial effect *in vitro* against *Staphylococcus epidermidis* biofilms, which are prevalent in catheter and implant infections (Jones *et al.*, 1994), as well as biofilms of *Streptococcus sanguis*, which is found in dental plaque and can also colonise heart valves, causing endocarditis (Robinson *et al.*, 2001a). El-Zawawy *et al.* (2015) found that triclosan liposomes had efficacy against systemic *Toxoplasmosis gondii* infection in an *in vivo* murine model and that the triclosan liposomes were superior to triclosan in solutions. Liposomal encapsulation of triclosan has not, however, been considered for control of endodontic infections and there is a lack of systematic studies looking at the effect of drug loading concentration on liposome characteristics and efficacy.

This chapter describes the development of a liposomal delivery system for the hydrophobic antimicrobial triclosan, including the optimisation of drug loading concentration and preparation methodology, and how this relates to antimicrobial efficacy against common endodontic pathogens.

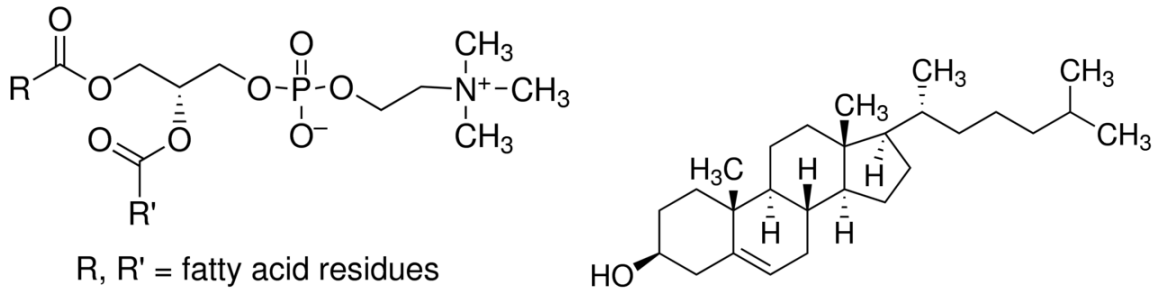

Figure 3.1: **Lipids used for liposome preparation.** The structure of phosphatidylcholine (left) and cholesterol (right), used for liposome preparation.

3.2 Materials and methods

3.2.1 Liposome preparation

Liposomes were prepared with egg yolk phosphatidylcholine (PC) and cholesterol (C), shown in Figure 3.1. PC and C were weighed and combined in a weight ratio of 7:1 respectively and placed in a 50 mL round-bottomed flask. Triclosan (0-1 mg/mL) was dissolved in chloroform and 5 mL of this solution was added to the flask with the lipids. The suspension was then vortexed until the lipids had dissolved. Chloroform was removed using rotary evaporation to leave a lipid film on the base of the flask. Distilled H_2O was added and the flask was vortexed to form a liposome suspension with lipid concentration of 1 mg/mL and triclosan concentrations of 0-500 µg/mL. At this stage, liposomes were assumed to be, and referred to as, multilameller vesicles (MLVs). Half of the suspension was retained for analysis and half was extruded 5 times under nitrogen pressure (8 bar maximum) using a Lipex extruder (Northern Lipids Inc., British Columbia, Canada) vertically through a 200 nm polycarbonate membrane (Whatman, UK) followed by further extrusion 10 times through a 100 nm polycarbonate membrane. These samples were assumed to be, and referred to as, small unilamellar vesicles (SUVs). All suspensions were stored at 4 °C prior to analysis. Table 3.1 shows a summary of the liposome formulations produced.

Table 3.1: **Summary of liposome formulations prepared for characterisation.**

Formulation Name	Lipid conc. added (mg/mL)	Triclosan conc. added (µg/mL)	Extruded? Y/N
T0 MLV	1	0	N
T0 SUV	1	0	Y
T50 MLV	1	50	N
T50 SUV	1	50	Y
T100 MLV	1	100	N
T100 SUV	1	100	Y
T300 MLV	1	300	N
T300 SUV	1	300	Y
T500 MLV	1	500	N
T500 SUV	1	500	Y

3.2.2 Size and polydispersity

The hydrodynamic diameter and polydispersity index of the liposome formulations was measured using dynamic light-scattering (DLS) in a Brookhaven Zeta Plus particle analyser (Brookhaven Instruments Corporation Holtsville, NY). Liposomes were diluted approximately 1:9 in H_2O and placed in a quarz cuvette (2 mL). A minimum of 3 measurements (2 min each) was taken for each sample and the mean hydrodynamic diameter and polydispersity index (PDI) were obtained.

3.2.2.1 Heat stability of liposomes

To ensure that the liposomes were able to withstand the high temperatures required for incorporation into a methylcellulose hydrogel (see Chapter 4), samples were placed in a waterbath set to 80 °C for 10 min, removed, and allowed to cool before the size was measured, as previously described.

3.2.2.2 Data analysis

Least-squares regression analysis was used to determine the coeffficient of determination (R^2) of the liposome size and PDI. A difference in the mean hydrodynamic diameter was tested for using ANOVA with post-hoc Tukey's test. A P value of 0.05 or less was considered statistically significant ("ns"=$P > 0.05$, *=$P < 0.05$,

**=$P < 0.01$, ***=$P < 0.001$).

3.2.3 Zeta potential

The zeta potential of liposomes was measured using a Malvern Nano-Zs Zeta Sizer (Malvern Instruments, Malvern, UK). Liposomes were diluted approximately 1:9 in H_2O and placed in a folded capillary zeta cell (1 mL). The zeta potential for each sample was taken as the mean of 3 measurements.

3.2.4 Phospholipid concentration

The phospholipid concentration of liposome suspensions was measured in order to ascertain whether there was a loss of materials throughout the preparation process. A phospholipid assay kit (Sigma Aldrich, Gillingham, UK) was used to quantify phospholipids. This assay enzymatically releases choline from samples, which is then quantified colourimetrically using choline oxidase and a H_2O_2 specific dye.

PC standard solution was diluted in Triton^{TM} X-100 (0.5 % v/v) to obtain concentrations of 0, 25, 50, 100 and 200 µmol/L. The liposome suspensions were diluted 1:7 in Triton^{TM} X-100 (0.5 % v/v). Standards or liposome samples were then pipetted in duplicate into a 96 well plate (20 µL/well) and 80 µL of the assay reaction mix, prepared according to the manufacturer's protocol (Appendix C), was added to each well. The plate was incubated in darkness at ambient temperature for 30 min before the absorbance was measured at 570 nm on a plate reader (FLUOstar Omega, BMG Labtech, Ortenberg, Germany). The sample phospholipid concentration was determined from comparison of the sample absorbance values to the standard curve produced from standard PC solution absorbance values. The concentration in µmol/L was converted to mg/mL, assuming that the PC used for liposome preparation had a molecular weight of 768 g/mol.

3.2.5 Triclosan concentration

3.2.5.1 HPLC apparatus

The triclosan concentration of liposome suspensions was measured using high-performance liquid chromatography (HPLC). The HPLC system comprised of an Agilent 1200 G1379B degasser, HP Agilent 1100 HPLC G1310A Isocratic Pump, HP Agilent 1100 G1313A Autosampler, and HP Agilent G1314A variable wavelength detector (VWD).

HPLC was performed using Agilent Eclipse Plus C18 column (4.6 mm × 100 mm, 3.5 µm). A 10 µL injection of sample or calibration standard was analysed by isocratic elution using mixed acetonitrile and H_2O (7:3) as HPLC mobile phase (flow rate 1 mL/min). The analytical wavelength was set at 285 nm. Data collection and analysis were performed using Agilent Chemstation.

3.2.5.2 Determination of optimum analytical wavelength for triclosan

Triclosan was dissolved in methanol at a concentration of 1 mg/mL. This was pipetted into a 96-well plate (90 µL/well) and the absorbance was measured at wavelengths 220-500 nm (1 nm intervals) in a FLUOStar Optima plate reader (BMG labtech, Ortenberg, Germany). The absorbance values were blank corrected by subtracting the measurement obtained from an empty well at each wavelength. An optimum analytical wavelength was chosen based on the presence of a peak in absorbance at that particular wavelength.

3.2.5.3 HPLC calibration standard solutions of triclosan

Calibration standard solutions of triclosan were prepared in methanol at concentrations of 0, 1, 2, 5, 10, 20, 30, 40, 50, 75 and 100 µg/mL. HPLC was performed as described above and the resulting peak areas for triclosan (y) were plotted against the respective triclosan concentration (x). Least-squares regression analysis was used to determine the slope and coeffficient of determination (R^2) of the data. The regression line equation was used to determine the triclosan concentration of liposome samples with unknown triclosan concentration.

3.2.5.4 Liposome samples

Liposome samples were diluted in methanol at a v/v ratio of 1:4 prior to HPLC analysis, as described above. The peak area of the triclosan was compared to those of the calibration standards in order to determine the triclosan concentration of the samples.

3.2.6 Triclosan:phospholipid ratio of liposome formulations

The drug:lipid ratio of liposome formulations was calculated from the triclosan concentration and phospholipid concentration values obtained from Sections 3.2.4 and 3.2.5. The ratio was determined by the formula:

$$\text{Triclosan:phospholipid ratio (w/w)} = \frac{\text{Triclosan concentration (µg/mL)}}{\text{Phospholipid concentration (µg/mL)}}.$$

3.2.7 Bacterial growth with triclosan liposomes

The antimicrobial efficacy of the liposomes was assessed using a growth inhibition experiment, as previously described in Chapter 2, Section 2.2.3.

Liposome suspensions were pipetted into a 96-well plate (20 µL/well). Overnight broth cultures of *E. faecalis* or *S. anginosus*, prepared as previously described (Section 2.2.1), were diluted in BHI to obtain an optical density of 0.08-0.1 at 600 nm. Two further 10-fold dilutions in BHI were then prepared and the resulting bacterial suspension pipetted onto the wells containing liposomes (180 µL/well). The plate was incubated in a plate reader (FLUOstar Omega, BMG Labtech, Ortenberg, Germany) at 37 °C in 5 % CO_2 for 20 h. The absorbance at 600 nm was measured every 1 h and the plate was shaken at 40 RPM for 30 s before each measurement.

The resulting bacterial growth curves were analysed as previously described in Chapter 2, Section 2.2.3.3.

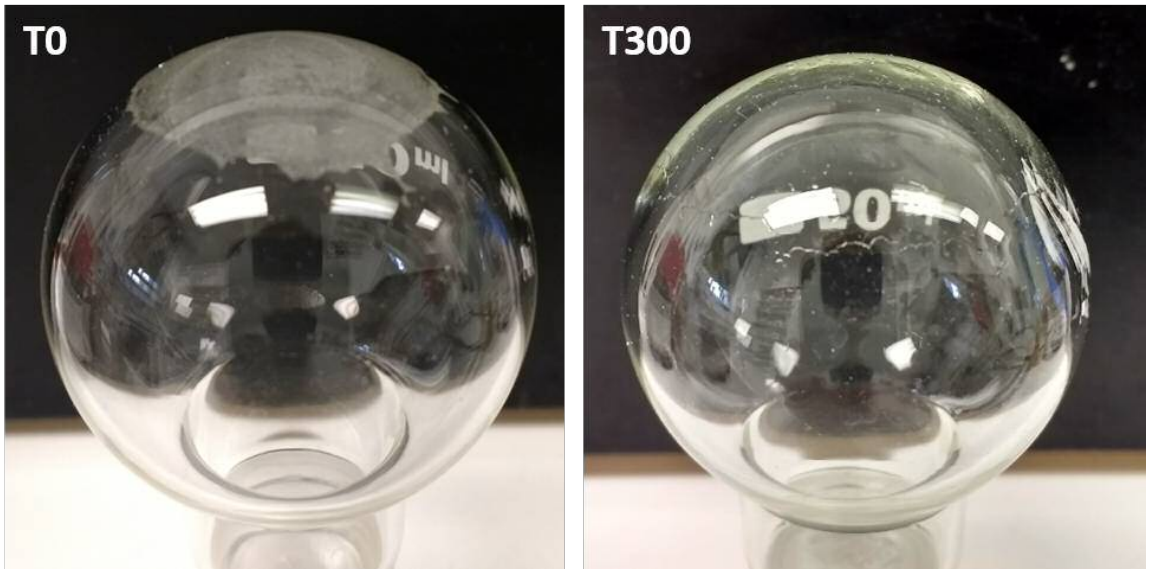

Figure 3.2: **Lipid films formed during liposome preparation.** Phospholipids with or without triclosan were dissolved in chloroform, which was then removed using rotary evaporation to form a lipid film on the bottom of the 50 mL round bottomed flasks. The formulation containing triclosan (T300, right) is more transparent than the control with no triclosan (T0, left).

3.3 Results

3.3.1 Liposome preparation

Liposomes were prepared with and without triclosan and qualitative differences were observed between the different formulations during the preparation process. Upon the removal of chloroform using rotary evaporation, the remaining lipid film was checked for any inconsistencies before it was resuspended in H_2O. Here it was observed that the lipid films with triclosan showed greater transparency than those that did not contain triclosan (an example is shown in Figure 3.2). In addition, the lipid film containing triclosan showed higher adhesion to the glass surface of the flask and it was not possible to remove all visible lipid residue from the side of the flask upon resuspension in H_2O. It was for this reason that the phospholipid and triclosan concentration of the different formulations was quantified, in order to ascertain how much of the original material was being lost at this stage in the production process.

3.3.2 Liposome size and polydispersity

The size of the liposomes was measured without extrusion (MLVs) and after extrusion through a 100 nm membrane (SUVs). It was also measured as a function of the triclosan concentration added to each formulation (0-500 µg/mL). The size of the liposomes is shown in Figure 3.3 and the PDI is shown in Table 3.2.

Liposome MLVs varied in size, with the hydrodynamic diameter ranging from approximately 200 to 1000 nm. After the liposomes had been extruded to SUVs, all samples had a hydrodynamic diameter of around 100 nm, with a narrow standard error (<10 nm).

There was a negative correlation observed between the concentration of triclosan added to the formulation and the hydrodynamic diameter of the MLVs up to 300 µg/mL triclosan(R^2=0.99). There was no significant difference between the size of T300 and T500 liposomes. There was also a weak negative correlation between the added triclosan concentration and the PDI of the liposome samples (R^2=0.71). This suggested that MLVs prepared with triclosan were smaller and less polydisperse than those without triclosan.

There was no change in the size of SUVs regardless of triclosan concentration, however there was a positive correlation between the added triclosan concentration and the PDI (R^2=0.72). There was also a convergence of PDI values seen between MLVs and SUVs, with a large difference observed in liposomes with no triclosan, and no difference seen between the MLVs and SUVs of samples with 500 µg/mL of triclosan added (T500). Therefore, liposomes prepared with 300 or 500 µg/mL of triclosan have a similar size and PDI, regardless of whether or not they are extruded after preparation, compared to control liposomes containing no triclosan.

3.3.2.1 Heat stability of liposomes

The stability of the liposomes was tested in order to ensure that the preparation methods of methylcellulose solutions would not have an adverse affect on the liposomes. Liposomes showed no significant change in size after heating to 80 °C for 10

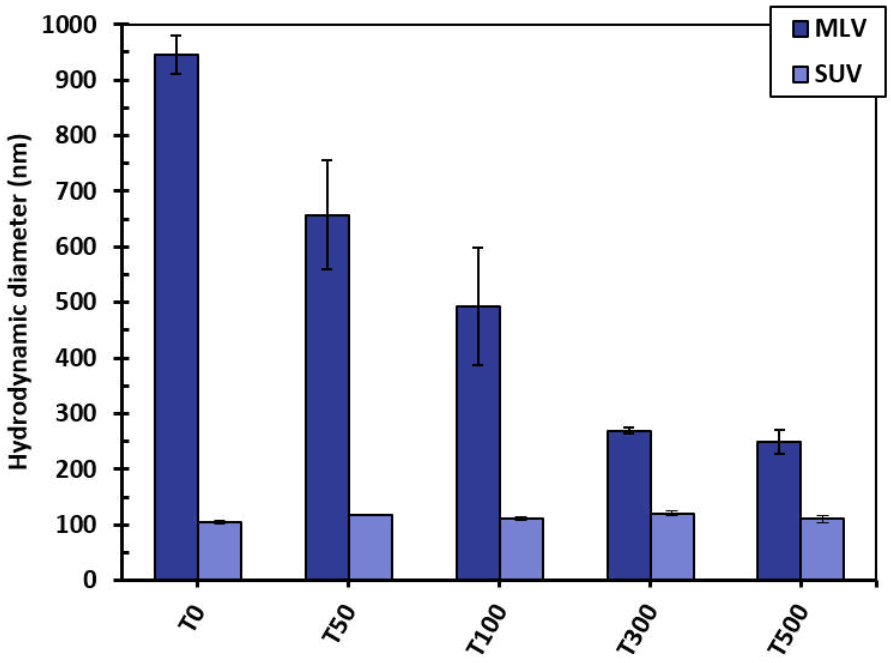

Figure 3.3: **Hydrodynamic diameter of PC:C liposomes prepared with triclosan.** Liposome MLVs and SUVs were prepared with various concentrations of triclosan (0-500 µg/mL). The graph shows the hydrodynamic diameter of each formulation, measured using DLS. Bars with error bars show mean with standard error of 3 independently prepared samples. Where error bars are not visible, they are contained within the bar.

Table 3.2: **Polydispersity index of liposome MLVs and SUVs prepared with triclosan.**

Liposome Formulation	Polydispersity index	
	MLV	SUV
T0	0.34 ± 0.02	0.11 ± 0.02
T50	0.30 ± 0.01	0.06 ± 0.02
T100	0.28 ± 0.03	0.10 ± 0.02
T300	0.23 ± 0.01	0.18 ± 0.03
T500	0.26 ± 0.03	0.26 ± 0.02

Values are mean value of 3 independently prepared samples ± standard error.

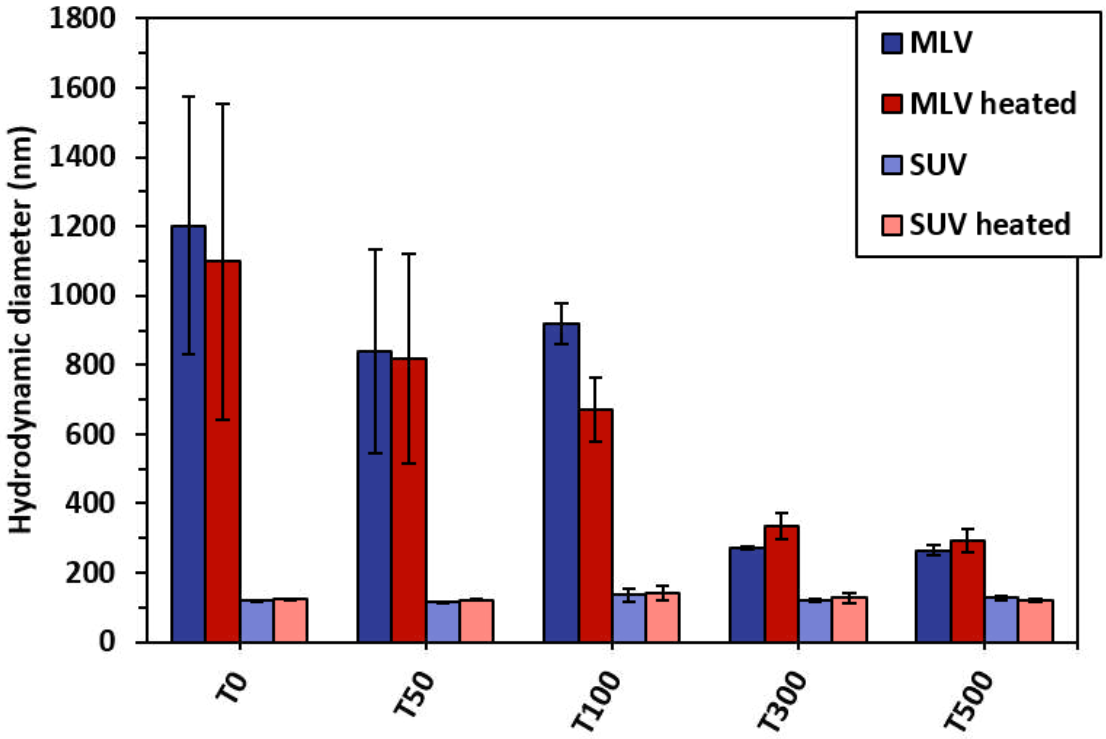

Figure 3.4: **Hydrodynamic diameter of liposomes before and after heating.** Liposome MLVs and SUVs, containing various concentrations of triclosan, were heated to 80 °C for 10 minutes. The graph shows hydrodynamic diameter of each formulation before and after heating, measured using DLS. Error bars show standard error of 3 independently prepared samples.

minutes, as shown in Figure 3.4.

3.3.3 Liposome zeta potential

Table 3.3 shows the zeta potential of liposome formulations. The zeta potential was negative, but absolute values are low, suggesting only a weakly negative charge is present. This may suggest that particles are more likely to aggregate over time. There was no significant difference between samples loaded with different triclosan concentrations, suggesting that the changes in hydrodynamic diameter were due to a difference in particle size and not particle charge.

Table 3.3: **Zeta potential of liposomes prepared with triclosan**

Liposome Formulation	Zeta potential (mV)	
	MLV	SUV
T0	-18.3 ± 1.5	-17.1 ± 2.1
T50	-22.4 ± 3.2	-15.2 ± 1.4
T100	-24.0 ± 0.8	-17.0 ± 1.0
T300	-19.2 ± 0.5	-17.0 ± 1.9
T500	-21.7 ± 2.5	-23.0 ± 2.7

Values are mean value of 3 independently prepared samples ± standard error.

3.3.4 Phospholipid concentration of liposome formulations

Figure 3.5 shows the phospholipid concentration of the liposome formulations, compared to the expected concentration, assuming that 100 % of the starting material was incorporated into the final product. The expected phospholipid concentration was 0.875 mg/mL, since this was the concentration of PC that is present in the initial formulation. Some phospholipid was lost in all cases, however this varied depending on the formulation. The mean phospholipid concentration decreased after extrusion to form SUVs for all formulations apart from T50, however this was within the experimental error for all cases apart from T500 MLVs and SUVs . There was a small decrease in T50 and T100 phospholipid concentration compared to T0, however this was again within the experimental error. The phospholipid concentration of formulations T300 and T500 were the lowest, with a loss of 83-94 % of the total phospholipid. Therefore, the phospholipid concentration of the final product was affected negatively by including a triclosan concentration of 300 µg or higher in the liposome formulation.

3.3.5 Determination of triclosan concentration

3.3.5.1 Analytical wavelength

The analytical wavelength was selected based on the UV absorbance spectrum of triclosan at wavelengths 220-500 nm, which is shown in Figure 3.6. A maximum absorbance was observed at 285 nm and therefore the selected optimum detection wavelength was 285 nm.

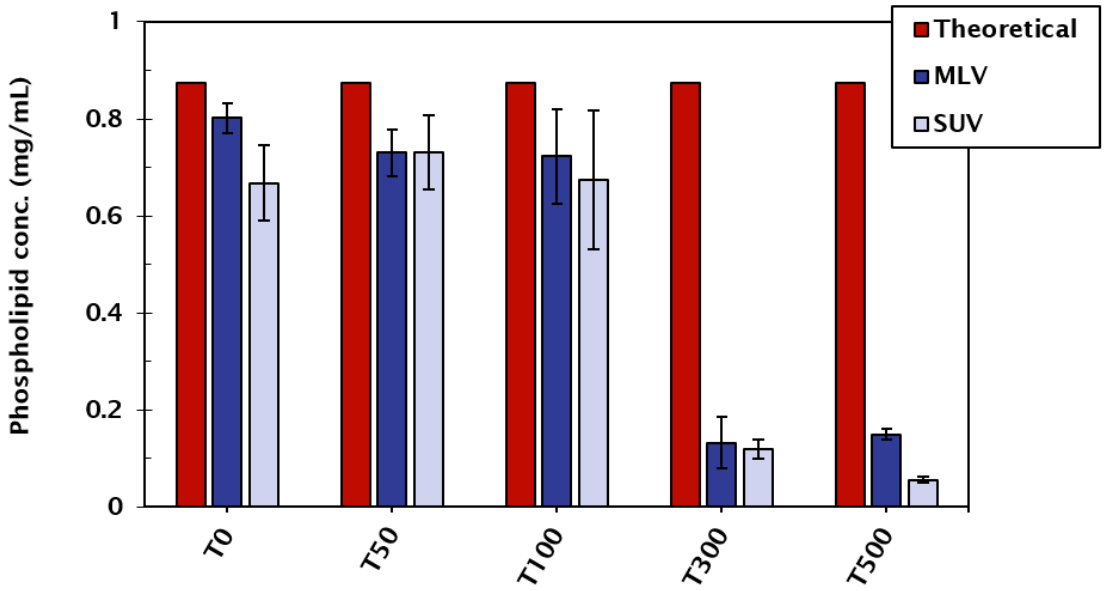

Figure 3.5: **Phospholipid concentration of liposome suspensions.** Liposome MLVs and SUVs containing various concentrations of triclosan (0, 50, 100, 300 and 500 µg/mL) were prepared and the concentration of phospholipids was measured using a phospholipid assay kit. The graph shows the mean phospholipid concentration, compared to the concentration that would be expected (red bars), assuming 100 % incorporation. Error bars show the standard error of 3 independently prepared samples.

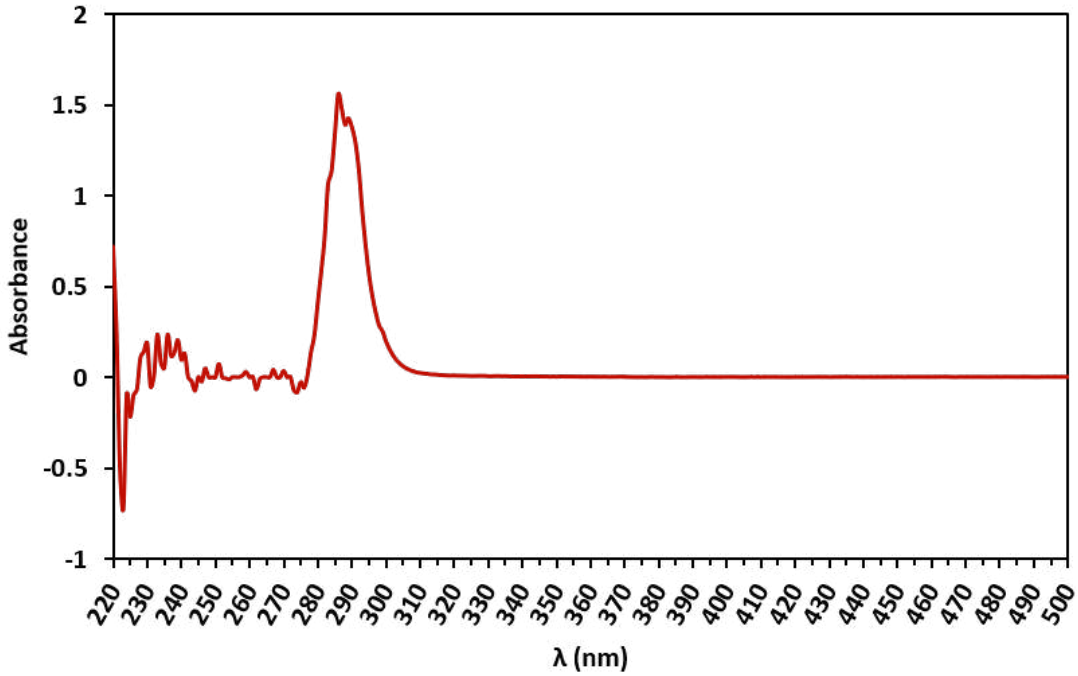

Figure 3.6: **UV absorbance spectrum of triclosan solution.**

3.3.5.2 Calibration curve

Triclosan solutions were analysed using HPLC and a peak was observed on the chromatorgram at retention time (RT) 6 min, with no other peaks observed. A calibration curve for the integrated area under this peak was produced for 10 concentrations of standard triclosan solutions (1, 2, 5, 10 20, 30, 40, 50, 75 and 100 µg/mL) and is shown in Figure 3.7. This shows good linearity within the concentration range and the correlation coefficient R^2=0.9974 was considered acceptable.

3.3.5.3 Triclosan concentration of liposome formulations

Liposome formulations were analysed in the same way as the triclosan standard solutions and a peak was again observed at RT 6 min. Chromatograms of liposomes containing no triclosan (T0) did not have a peak at this RT. As a control measure, liposome samples containing triclosan were spiked with standard triclosan solution, and a single peak at RT 6 min was still observed, suggesting that the peak seen in liposome samples was representative of the triclosan included in the formulation.

Figure 3.8 shows the triclosan concentration of liposome formulations, compared

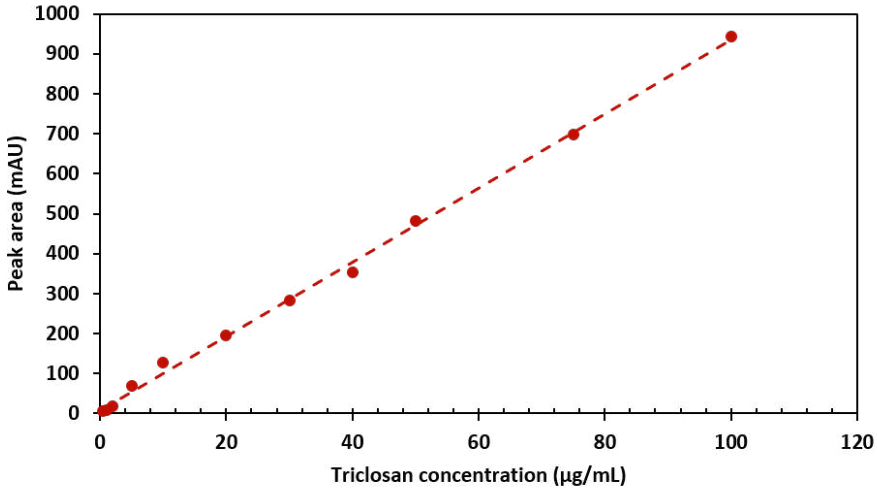

Figure 3.7: **Calibration curve of triclosan concentration against integrated HPLC peak values.** Standard solutions of triclosan were prepared and analysed using HPLC. The graph shows the integrated values of peaks observed at retention time 6 min for each concentration. Dashed line shows linear regression plot ($y = 9.3987x, R^2 = 0.9974$).

with the theoretical maximum. T50 and T100 liposomes were within experimental error of the theoretical 100 % encapsulation value, suggesting that no triclosan was lost in these formulations. A small decrease was seen between MLVs and SUVs of T50 and T100 liposomes, however these were within the experimental error. T300 and T500 liposomes had a lower than expected triclosan concentration, with T500 SUVs having the lowest (21.6 ± 2.3 µg/mL). T500 MLVs had a comparable triclosan concentration to T100 MLVs, however this was a much lower proportion of the overall triclosan added (23 % compared to 117 % for T100 MLVs). Additionally, the T100 formulation retained most of the triclosan once extruded to SUVs, whereas a decrease was seen in T500 SUV compared to T500 MLVs.

The HPLC results suggested that the maximum concentration of triclosan that could be incorporated into this system was around 100 µg/mL, even if more triclosan is added to the initial formulation. This is twice the value of the MBEC of triclosan against the bacteria of interest (Chapter 2, Section 2.3.2.3) and more than 10 times the MIC (Chapter 2, Section 2.3.2.1), suggesting that a clinically relevant concentration of triclosan could be incorporated into these liposomes.

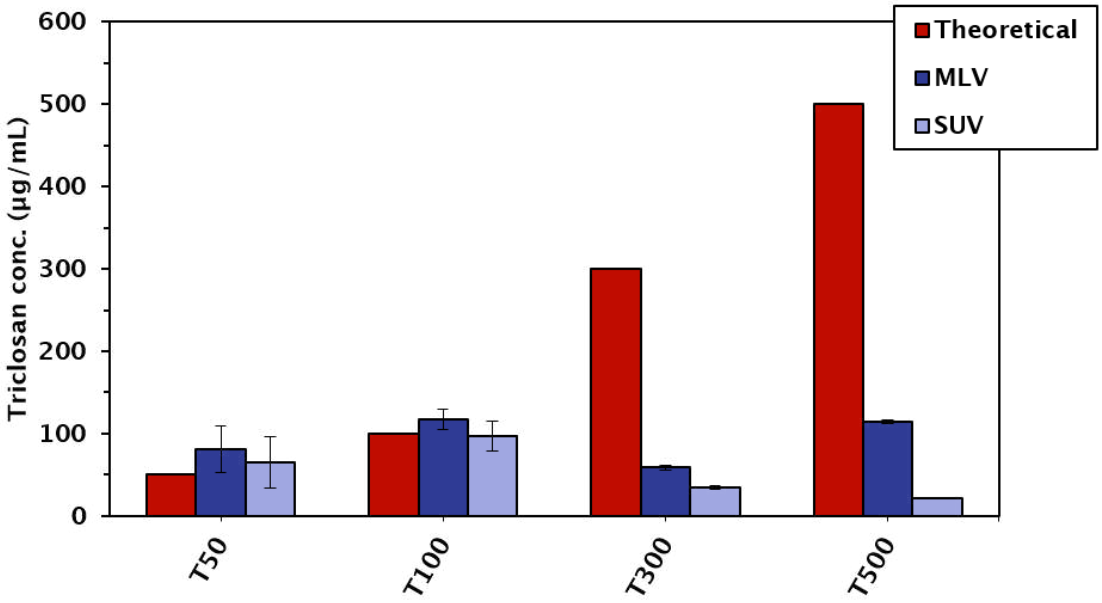

Figure 3.8: **Triclosan concentration of liposome suspensions.** Liposome MLVs and SUVs containing various concentrations of triclosan (0, 50, 100, 300 and 500 µg/mL) were prepared and the triclosan concentration was measured using HPLC. The graph shows the triclosan concentration, compared to the concentration that would be expected (red bars), assuming 100 % incorporation. Error bars show the standard error of 3 independently prepared samples.

Table 3.4: **Triclosan:phospholipid ratio of liposome formulations.**

Liposome formulation	Triclosan conc. (µg/mL)		Phospholipid conc. (mg/mL)		Triclosan:phospholipid ratio	
	MLV	SUV	**MLV**	SUV	**MLV**	SUV
T0	**0**	0	**0.80 ± 0.03**	0.67 ± 0.08	**NA**	NA
T50	**80.9 ± 14.0**	65.0 ± 15.8	**0.63 ± 0.07**	0.65 ± 0.11	**0.13 ± 0.03**	0.10 ± 0.03
T100	**117.2 ± 12.3**	97.3 ± 18.4	**0.71 ± 0.10**	0.72 ± 0.10	**0.17 ± 0.01**	0.13 ± 0.01
T300	**59.0 ± 8.4**	35.1 ± 6.1	**0.15 ± 0.05**	0.13 ± 0.01	**0.60 ± 0.32**	0.28 ± 0.06
T500	**114.6 ± 8.8**	21.6 ± 2.3	**0.15 ± 0.01**	0.06 ± 0.00	**0.78 ± 0.11**	0.37 ± 0.02

Values are mean value of 3 independently prepared samples ± standard error.

3.3.6 Triclosan:phospholipid ratio

The results of the HPLC analysis and phospholipid assay were compiled to obtain a ratio of triclosan:phospholipid found in the different liposome formulations. This is summarised in Table 3.4. The ratio was similar for T50 and T100 liposomes, with the MLVs having a ratio of 0.13-0.17 and SUVs having a ratio of 0.10-0.13. T300 and T500 liposomes had a higher ratio of triclosan:phospholipid, with MLVs having the highest ratio (0.60-0.78). This was halved when MLVs were extruded to SUVs.

These analyses suggest that although a higher triclosan loading concentration will not result in a higher triclosan concentration overall (see Section 3.3.5.3), it does result in a higher ratio of triclosan:phospholipid, owing to the reduction in phospholipid concentration seen in Section 3.3.4. This may have implications for the overall membrane structure and therapeutic efficacy of the liposomes.

3.3.7 Antimicrobial efficacy of liposomes

Bacteria were incubated with triclosan loaded lipsomes and the antimicrobial efficacy of the different liposomal formulations was assessed. Table 3.5 shows the parameters derived from growth curves of *E. faecalis* and *S. anginosus* with the liposome formulations.

Liposomes containing no triclosan did not change any of the growth parameters,

Table 3.5: **Growth parameters of *Enterococcus faecalis* (top) and *Streptococcus anginosus* (bottom) with triclosan-loaded liposomes.**

Liposome formulation	λ (h)			μ			A (OD_{600})		
	Mean	SEM	*sig.*	**Mean**	SEM	*sig.*	**Mean**	SEM	*sig.*
E. faecalis only	**2.37**	0.29	-	**0.20**	0.01	-	**1.03**	0.03	-
TO MLV	**1.94**	0.28	*ns*	**0.20**	0.01	*ns*	**1.09**	0.03	*ns*
TO SUV	**2.25**	0.32	*ns*	**0.21**	0.01	*ns*	***1.07***	0.05	*ns*
T50 MLV	**2.39**	0.70	*ns*	**0.15**	0.01	*ns*	**0.98**	0.06	*ns*
T50 SUV	**2.77**	0.74	*ns*	**0.14**	0.00	*ns*	**0.92**	0.06	*ns*
T100 MLV	**3.58**	0.66	*ns*	**0.09**	0.02	**	**0.77**	0.11	*ns*
T100 SUV	**NA**	NA	-	**NA**	NA	-	**0.46**	0.16	*ns*
T300 MLV	**NA**	NA	-	**NA**	NA	-	**0.30**	0.11	***
T300 SUV	**NA**	NA	-	**NA**	NA	-	**0.46**	0.16	**
T500 MLV	**NA**	NA	-	**NA**	NA	-	**0.35**	0.18	**
T500 SUV	**3.98**	0.93	*ns*	**0.10**	0.03		**0.63**	0.12	*ns*
BHI only	**NA**	NA	-	**NA**	NA	-	**0.15**	0.02	***

Liposome formulation	λ (h)			μ			A (OD_{600})		
	Mean	SEM	*sig.*	**Mean**	SEM	*sig.*	**Mean**	SEM	*sig.*
S. anginosus only	**3.50**	0.68	-	**0.12**	0.01	-	**0.72**	0.05	-
T0 MLV	**2.96**	0.54	*ns*	**0.12**	0.01	*ns*	***0.75***	0.03	*ns*
TO SUV	**3.25**	0.52	*ns*	**0.12**	0.01	*ns*	**0.70**	0.02	*ns*
T50 MLV	**3.87**	0.96	*ns*	**0.10**	0.01	*ns*	**0.70**	0.01	*ns*
T50 SUV	**4.26**	0.89	*ns*	**0.12**	0.01	*ns*	**0.71**	0.02	*ns*
T100 MLV	**4.69**	0.61	*ns*	**0.08**	0.01	*ns*	**0.67**	0.05	*ns*
T100 SUV	**5.10**	0.66	*ns*	**0.11**	0.02	*ns*	**0.67**	0.04	*ns*
T300 MLV	**NA**	NA	-	**NA**	NA	-	**0.33**	0.13	*
T300 SUV	**NA**	NA	-	**NA**	NA	-	**0.44**	0.16	*ns*
T500 MLV	**NA**	NA	-	**NA**	NA	-	**0.30**	0.13	*
T500 SUV	**NA**	NA	-	**NA**	NA	-	**0.44**	0.15	*ns*
BHI only	**NA**	NA	-	**NA**	NA	-	**0.16**	0.03	***

Bacteria were grown in BHI with liposomes in a 96-well plate for 20 h. Length of lag phase (λ), maximum growth rate (μ) and maximum absorbance value (A) of growth curves are shown. (*"SEM"= standard error of the mean of 3 independent experiments, "sig."= significance of difference in means compared to bacteria in BHI:"ns"=* $P > 0.05$, **=* $P < 0.05$, *** =*$P < 0.01$, ****=*$P < 0.001$)

neither did those loaded with 50 µg/mL triclosan. *E. faecalis* incubated with liposomes loaded with 100 µg/mL triclosan showed some changes in growth: a significant reduction in μ was seen with MLVs and A was reduced with SUVs, although not significantly so. These effects were not seen in *S. anginosus* with the same liposomal formulations. For liposomal formulations with a loading dose of 300 and 500 µg/mL, some differences in the growth parameters were seen. *E. faecalis* had a significant decrease in A with all but T500 SUVs, and these formulations also had no measurable λ or μ, suggesting that growth was inhibited in these conditions. For *S. anginosus* growth, only the MLVs of T300 and T500 caused a significant decrease in A, however no measurable λ or μ was derived from any of these 4 formulations.

These results indicate that liposomes formulated with a loading dose of 300 or 500 µg/mL of triclosan (T300 and T500) and not extruded (MLVs) showed the greatest inhibitory effect against both bacterial species *in vitro* over the time period tested.

3.4 Discussion

Liposomes composed of PC and C were prepared with the antimicrobial drug triclosan and assessed for their suitability for delivery of the drug.

Triclosan is a hydrophobic molecule with logP=4.76 (National Center for Biotechnology Information, 2005) so it was assumed that triclosan would integrate into the lipid bilayer of the liposome. It had been observed previously that liposomes containing hydrophobic molecules, anthracene, adamantane and anthraquinone form larger vesicles compared to control liposomes with no compound (Barlow-Myers 2017, MChem dissertation). The position of the drug in the membrane may affect the phospholipid packing, resulting in a change in bilayer curvature and therefore liposome size. This study observes a reduction in liposome MLV size with increased drug loading, suggesting that triclosan may cause an increased curvature of the bilayer. A study by Guillén *et al.* (2004) indicated that triclosan incorporated into a PC bilayer membrane is positioned in the upper region of the phospholipid membrane, with the hydroxyl group residing in the vicinity of the C=O/C2 carbon atoms of the

acyl chain of the phospholoipid. Knyght *et al.* (2016) observed other hydrophobic antimicrobial agents that reside near the headgroups of phospholipids and cause an increase in the thickness of the headgroup region of phospholipid monolayers. This, alongside the data from this chapter, may indicate that the decrease observed in liposome size is associated with a higher proportion of triclosan incorporated near the phospholipid headgroup in the membrane, resulting in a larger headgroup region and a higher degree of curvature in the vesicle-forming bilayer. This is supported by the correlation of a smaller hydrodynamic diameter in T300 and T500 MLVs to a higher triclosan:phospholipid ratio.

Liposome MLVs prepared with a higher concentration of triclosan had a hydrodynamic diameter and PDI more similar to their extruded counterparts than those of control liposomes with no triclosan. A difference of 138 nm in mean size between T500 MLVs and SUVs, however, may have an effect on the clinical efficacy of these liposomes and so for the methodology used, liposome extrusion may still be a crucial step in the formulation process. Generally, liposomes between 70-150 nm are employed in systemic therapeutic delivery (Allen and Cullis, 2004), as they are large enough to encapsulate clinically relevant concentration of drugs but small enough to circulate without becoming trapped in tissue microvasculature, and penetrate through pores and gaps in the vascular endothelium associated with areas of inflammation (Hobbs *et al.*, 1998; Klimuk *et al.*, 1999). Local delivery eliminates some of the challenges associated with systemic delivery and the physical barriers for antimicrobial delivery within the decellularised root canal include dentine tubules of diameter 2-4 µm (Schilke *et al.*, 2000) and penetration of the bacterial biofilm. Biofilms contain channels for the transport of water and nutrients, and work by Drury *et al.* (1993) showed that silicone beads with diameter 1000 nm could diffuse readily through these channels: a mechanism that has been subsequently studied for assessing the flow rate within biofilms (Evans, 2003). It is probable, therefore, that the liposomes produced in this work are physically small enough to migrate into dentinal tubules and penetrate a bacterial biofilm for local delivery of antimicrobials.

The results of the bacterial growth curves with liposomes in this study shows

that both MLVs and SUVs of T300 and T500 liposomes have a bacteriostatic effect on planktonically grown *E. faecalis* and *S. anginosus*, with MLVs having slightly greater efficacy. This suggests that the slightly larger hydrodynamic diameter does not have a negative impact on antimicrobial drug delivery in this setting, although there are other factors, such as phospholipid concentration, triclosan concentration and triclosan:phospholipid ratio to consider in the assessment of antimicrobial efficacy. Additionally, liposome size may have more of a bearing on biofilm penetration, which was not assessed in this instance.

A phospholipid quantification assay was used to confirm observations that some of the phospholipid membrane is unable to be resuspended from the glassware during liposome preparation. This confirmed that up to 86 % of the phospholipids were lost in MLV preparation (T300) and 93 % in SUV preparation (T500). This suggests a change in the membrane properties when triclosan is added that inhibits the hydration of the lipid film, however the mechanism for this is not clear. Lasic and Barenholz (1996) suggest that difficulty in hydrating lipid films could indicate the formation of nonbilayered phases. This may be driven by the hypothesised increase in headgroup size of PC due to triclosan binding, that could induce a polymorphic phase transition of the lipid membrane. Further analysis of the lipid film and the lipid particles produced would be required to assess this, using techniques such as Phosphorus-31 nuclear magnetic resonance (Seelig, 1978).

The method used to assess phospholipid concentration only detects choline from phospholipids and does not give any information on the cholesterol composition of the liposomes and whether this is different between formulations. Other studies have shown a slight increase in liposome size when cholesterol is added to PC liposomes (De Kruijff *et al.*, 1975; Lee *et al.*, 2005b), and so a change in cholesterol concentration could contribute to the different sizes observed in the different liposomes formulations. Previous changes in size due to cholesterol incorporation, however, were not as great as observed in this work, and it is likely that the triclosan concentration plays a greater role, as previously discussed.

Triclosan concentration of liposomes showed a similar overall trend to phospholipid concentration, in that adding 300 or 500 µg/mL of triclosan into the initial formulation resulted in a much lower yield in the final product. This suggests that triclosan is incorporated into the lipid film that cannot be resuspended using the current methodology, however the amount of triclosan lost was not proportional to the amount of phospholipid lost. This can be seen when calculating the triclosan:phospholipid ratio, which is higher for T300 and T500 liposomes than for T50 and T100 liposomes. This suggests that a higher drug:lipid ratio may be achieved by incorporating a higher drug concentration, but this may also cause changes to occur in the lipid film, leading to a loss of materials. Further work should look at liposomes with starting triclosan concentrations between 100 and 300 µg/mL to try to identify an optimal loading concentration for maximum drug:lipid ratio and minimum material loss.

The importance of the drug:lipid ratio is apparent when considering the antimicrobial efficacy. For the growth experiments, the liposomes were diluted 1:9 in bacterial suspension, resulting in a mean total triclosan concentration of approximately 8, 12, 6 and 11 µg/mL for T50, T100, T300 and T500 MLVs respectively and 7, 10, 4 and 2 µg/mL for T50, T100, T300 and T500 SUVs respectively, according to the triclosan concentration measurements. It would therefore be expected that all liposome MLV formulations and both T50 and T100 SUVs have antimicrobial potential, given that the minimum inhibitory concentration (MIC) of triclosan is 6.25 µg/mL (Chapter 2, Section 2.3.2.1). This was not the case, and only T300 and T500 liposomes had a significant effect on the growth of the bacteria, with the MLVs of these formulations being the most effective and the T300 SUVs showing inhibition of *E. faecalis* growth, despite having a triclosan concentration below the MIC.

The apparent lack of correlation between drug concentration in liposomes and antimicrobial efficacy may be accounted for by the triclosan:phospholipid ratio of the liposomes. The bioavailability of drugs is reduced when they are loaded into liposomes, and will only be active when it released from the lipid bilayer (Bozzuto and Molinari, 2015). It is therefore possible that a higher local concentration of

triclosan within the liposomal membrane leads to better bioavailability of the drug, and can even lower the MIC required in the system. For liposomes with a lower triclosan:phospholipid ratio but a higher total triclosan concentration, it is possible that a concentration of triclosan below the MIC is released over the 20 h incubation period and so no antimicrobial effect is observed. Although a slow release of drug over time may be desirable for a dental filling material, an initial release above the MIC is necessary to inhibit growth and prevent re-colonisation of the treated dental cavity. It has been suggested that the drug:lipid ratio will have an impact on the release profile of the liposomes, with a higher ratio being associated with more sustained release and higher drug retention, possibly mediated by the presence of drug precipitates in the liposomes, as was seen in the case of vincristine-loaded liposomes by Johnston *et al.* (2006). Further work is needed to assess the release profile of the liposomes prepared in this chapter, however this initial work suggests that a triclosan:phospholipid ratio higher than 0.3 is needed to achieve an antimicrobial effect in the first 20 h of treatement. A higher drug:lipid ratio is preferable in systemic drug delivery in order to minimise the amount of lipid that is required to deliver clinically relavent drug doses (Straubinger and Balasubramanian, 2005; Cern *et al.*, 2014), however this may not be as crucial for local delivery in this instance.

Liposomes were prepared as MLVs or SUVs for this work. The production of SUVs through extrusion is a limiting step in liposome production in terms of time and financial cost, and so it would be advantageous to use MLVs in future drug delivery formulations. Comparison of MLVs and SUVs in this study showed that there was no reduction in antimicrobial efficacy of MLVs, and in fact MLVs of T300 and T500 liposomes were more effective than SUVs against both species of bacteria. It is therefore worth considering the use of MLVs instead of SUVs for antimicrobial delivery in endodontic therapy. It would, however, be necessary to consider other factors, such as the delivery of MLVs to bacterial biofilms (potentially residing within narrow dentine tubules), MLV stability compared to SUVs as well as their efficacy once incorporated into a suitable dental filling material.

3.5 Conclusions

It has been shown that triclosan can be incorporated into PC:C liposomes, the assembled size of which are dependent upon the initial loading dose of the drug. Quantification of the encapsulated triclosan suggested that there is a limit to the amount that may be encapsulated, however this limit is above the concentration required to eradicate two oral pathogens, according to data from the previous chapter. Incubation of the liposomes with the bacteria confirmed that the liposomes had an antimicrobial effect, and this was seen predominantly in T300 and T500 liposomes that had not been extruded (MLVs). These formulations had a high drug:lipid ratio, which indicates that the membrane composition of the liposomes is important as well as the overall concentration of the drug within the system. The high loss of materials observed in these formulations is not desirable, but these results may inform more precise methods such as microfluidic preparation of liposomes in the optimum ratio of drug:lipid that should be used. Further work will assess the suitability of T300 and T500 liposomes to be incorporated into a hydrogel for endodontic drug delivery.

Chapter 4

Characterisation of a Hydrogel for the Delivery of Antimicrobial Liposomes

4.1 Introduction

Hydrogels are cross-linked networks of hydrophilic polymers that have solid-like properties but may contain high amounts of water or biological fluids (Peppas *et al.*, 2000). They are considered for local drug delivery in a number of biomedical applications, as their physical properties are tunable and they have potential to carry and deliver aqueous drug solutions. Hydrophobic drugs may not be suitable for incorporation into a hydrogel, however the previous chapter has shown that a hydrophobic antimicrobial, triclosan, can be incorporated into an aqueous dispersal of liposomes and retain its antimicrobial properties against oral pathogenic bacteria. A hydrogel may therefore be a suitable carrier of triclosan liposomes for use as a local dental medicament.

Methyl cellulose (MC) is a water-soluble, naturally derived "biopolymer" that is biocompatible and biodegradable, making it favourable for biomedical applications (Grijalvo *et al.*, 2016). It is produced from the modification of cellulose and its structure is shown in Figure 4.1. Natural, unmodified cellulose is hydrophilic in chemical

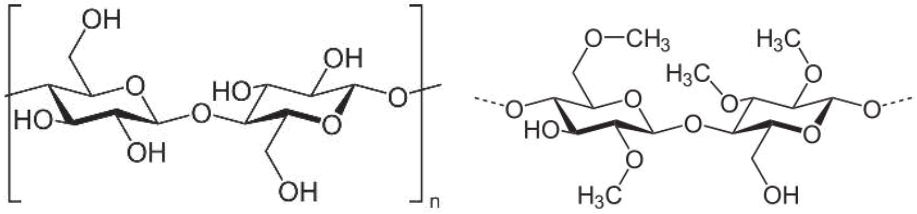

Figure 4.1: Structure of cellulose (left) and methyl cellulose (right)

structure but is water-insoluble due to strong intermolecular hydrogen bonding. Solubility can be achieved by substituting a certain proportion of the hydroxyl groups with hydrophobic groups: in MC these are methyl groups. To achieve water solubility, the degree of substitution (DS) must be high enough to prevent extensive intramolecular hydrogen bonding but low enough such that enough hydrophilic hydroxyl groups remain to hydrogen bond with water to confer solubility. The DS of cellulose that has undergone 100 % substitution is 3, as there are 3 reactive hydroxyl groups per anhydroglucose unit and all 3 have been substituted. The optimum DS for water solubility of hydrophobically modified cellulose is typically 1.7-2.0 (Li *et al.*, 2001). MC has reverse thermal gelling properties in aqueous solution. When the temperature of the solution rises above a critical temperature, the polymer forms a physical hydrogel due to hydrophobic interactions between the methyl groups (Li *et al.*, 2001). Increasing temperature is believed to cause distortion in the enclosed structures formed by water molecules that surround the hydrophobic methyl groups. This causes increased phase separation between hydrophobic and hydrophilic groups and results in the formation of hydrophobic aggregates. This effect is reversed when the temperature is decreased again. The gelation temperature of MC is dependent upon the polymer concentration, with a higher concentration resulting in a lower gelation temperature. At maximum soluble concentration (10 % w/w), methyl cellulose is reported to gel at around 30 °C (Sigma, 1997; Takahashi *et al.*, 2001). Gelation can also be modified by the addition of anions into the system, either by salt addition or an anionic polymer (Li *et al.*, 2001; Xu *et al.*, 2004).

This chapter will examine the suitability of a MC hydrogel to carry and deliver antimicrobial liposomes. The rheological properties of this system will be determined,

Table 4.1: **Summary of liposome formulations prepared for methyl cellulose incorporation.**

Formulation Name	Lipid conc. added (mg/mL)	Triclosan conc. added (µg/mL)	Extruded? Y/N
T0 MLV	1	0	N
T0 SUV	1	0	Y
T300 MLV	1	300	N
T300 SUV	1	300	Y
T500 MLV	1	500	N
T500 SUV	1	500	Y

including the effect of liposome incorporation, and the antimicrobial properties of the liposomes in the hydrogel also assessed.

4.2 Materials and methods

4.2.1 Preparation of methyl cellulose solutions containing liposomes

4.2.1.1 Liposome preparation

Multilamellar vesicle (MLV) and small unilamellar vesicle (SUV) liposomes were prepared as described in Chapter 3, Section 3.2.1. Liposomes containing no triclosan (T0 MLV and T0 SUV) and those prepared with 300 µg/mL and 500 µg/mL triclosan (T300/T500 MLV and T300/T500 SUV) were used in this chapter: a summary is shown in Table 4.1.

4.2.1.2 Incorporation of liposomes into methyl cellulose solution

Liposome dispersions were placed in a waterbath at 80 °C for 10 min before methyl cellulose (MC, 15 cP) was added (10 % w/w). The suspension was gently agitated until the MC powder appeared evenly dispersed. The suspension was then placed at 4 °C for 24 h under gentle agitation to allow for dissolution of the MC. Control solutions were prepared as above, but with H_2O used in place of the liposome dispersions.

4.2.2 Rheological analyses of methyl cellulose with liposomes

4.2.2.1 Rheometry apparatus

Rheological properties of MC solutions were measured using a Bohlin C-VOR 200 rheometer attached to a Bohlin KTB 30 waterbath for temperature control of the lower plate. A 40 mm parallel plate geometry was used for sample measurement and data were collected using Bohlin R6.51.0.3 software and then exported to Microsoft Excel for analysis.

4.2.2.2 Sample loading

MC solutions were equilibrated at ambient temperature before loading onto the rheometer. Using a 1 mL syringe, 0.8 mL of solution was applied to the lower plate of the rheometer, which had been equilibrated at the chosen measurement temperature. The upper plate was then lowered onto the sample (speed set to maximum) to a gap width of 0.5 mm, and any excess sample was removed where necessary. A new sample was loaded for each rheological test performed.

4.2.2.3 Viscosity

The viscosity of MC solutions containing T0 MLVs, T0 SUVs and H_2O only was measured. Shear viscosity (Pa.s) was measured at increasing shear rates of 0.15-2000 s^{-1}, with 30 readings taken at logarithmic intervals. The initial delay time for sample measurement was 100 s, set to decrease at each sample reading. All viscosity measurements were performed at 25 °C. The exact parameters set on the instrument are shown in Table 4.2A. Ambient temperature was 24-26 °C for these measurements.

4.2.2.4 Amplitude-dependent viscoelasticity

An amplitude sweep was performed in order to ascertain the linear viscoelastic (LVE) range at 25 °C of MC solutions containg T0 MLVs, T0 SUVs, and H_2O only. The oscillatory frequency was set to 1 Hz and the strain was increased from 0.01-100. The elastic modulus (G') and viscous modulus (G") were plotted against strain, and a

strain value within the LVE range was selected for further viscoelasticity measurements. The parameters for the amplitude sweep are shown in Table 4.2B. Ambient temperature was 24-26 °C for these measurements.

4.2.2.5 Temperature-dependent viscoelasticity

A temperature sweep was performed in order to estimate the gelation temperature of the MC solutions containing T0 MLVs, T0 SUVs and H_2O only. The rheometer was set to a constant oscillatory frequency (1 Hz) and amplitude (strain=0.5) and the temperature was increased from 25-55 °C at a rate of 2 °C/min. G' and G" were plotted against temperature in order to assess the temperature-dependent viscoelastic properties of the MC samples. The parameters for the temeperature sweep are shown in Table 4.2C. Ambient temperature was 24-26 °C for these measurements.

4.2.2.6 Time-dependent viscoelasticity at 3 constant temperatures

Viscoelasticity was also measured as a function of time at a constant temperature, oscillatory frequency (1 Hz) and amplitude (strain=0.5). This measurement was performed on T300 MLVs and T300 SUVs at 30, 35 and 40 °C for 20 min at each temperature. The lower plate of the rheometer was allowed to equilibrate to the set temperature before the sample was placed on the plate, as described in Section 4.2.2.2. The upper plate was then lowered onto the sample, taking approximately 50 s, and the measurement was started. G' and G" were plotted against measurement time in order to assess the viscoelastic properties of the MC samples over time at specific temperatures. The parameters for these measurements are shown in Table 4.2D. Ambient temperature was 31-33 °C for these measurements.

4.2.3 Release of components from hydrogel

Measurement of liposome release from MC was done under non-sink conditions. MC solutions were prepared (10 % w/w) containing liposome formulations T300 MLV/SUV, as described in Section 4.2.1. MC solutions containing triclosan only

Table 4.2: **Rheometer parameters.**

A: Viscometry –table of shears – controlled rate	
Geometry	PP40
Gap (mm)	0.5
Temperature (°C)	25
Shear rate min. (1/s)	0.15
Shear rate max. (1/s)	2000
Samples	30
Progression	Logarithmic
Delay Time (s)	100
Decreasing?	Y
Integration time (s)	5
Direction	up
Total test time (s)	354.2

B: Oscillation – amplitude sweep – strain control	
Geometry	PP40
Gap (mm)	0.5
Temperature (°C)	25
Frequency (Hz)	1
Strain min.	0.01
Strain max.	100
Direction	Up
Sequence	Logarithmic
Steady shear rate (1/s)	0
Delay time (s)	2
Integration time (s)	10
Periods	10
Points	4096
Number of samples	30
Time per point (s)	12
Total test time (s)	360

C: Oscillation – temperature sweep (up)	
Geometry	PP40
Gap (mm)	0.5
Auto-tension	Y
Thermal equilibrium time (s)	30
Start temperature (°C)	25
End temperature (°C)	55
Rate (°C/min)	2
Ramp time (min)	15
Frequency (Hz)	1
Strain	0.5
Integration time (s)	4
Periods	4
Points	2048
Delay time (s)	2
Number of samples	100
Wait time (s)	0
Continuous oscillation	Y
Total test time (s)	900

D: Oscillation – single frequency – strain control	
Geometry	PP40
Gap (mm)	0.5
Temperature (°C)	30/35/40
Frequency (Hz)	1
Strain	0.5
Steady shear rate (1/s)	0
Integration time (s)	4
Periods	4
Points	2048
Delay time (s)	2
Number of samples	200
Wait time (s)	0
Continuous oscillation	Y
Total test time (s)	1200

Instrument parameters for rheological analysis of (A) viscosity, (B) amplitude-dependent viscoelasticity, (C) temperature dependent viscoelasticity and (D) time-dependent viscoelasticity.

(100 µg/mL) and H_2O only were also prepared. The solutions were placed in a 24-well plate (0.2 g/well) and then the plate was placed in an incubator at 37 °C for 1 h until the solution had gelled. H_2O (1 mL, heated to 37 °C) was then added to each well. A different well was prepared for each time point. For the time point 0 h, the aqueous phase was immediately removed from the wells, leaving the gel behind, and the plate was returned to the incubator for subsequent time points. At times 2, 8, 24, 96 and 168 h, the aqueous phase was removed from the wells, leaving the gel behind. The removed aqueous phase was then analysed for triclosan concentration and phospholipid concentration.

4.2.3.1 Triclosan quantification using HPLC

An aliquot of the aqueous phase from the release assay was added to methanol (1:1) and then an HPLC assay was performed as detailed in Chapter 3, Section 3.2.5.

4.2.3.2 Phospholipid quantification using phospholipid assay

An aliquot of the aqueous phase from the release assay was added to 0.1 % Triton X-100 (1:1) and then the phospholipid assay was performed as detailed in Chapter 3, Section 3.2.4.

4.2.4 Antimicrobial efficacy of methyl cellulose loaded with triclosan liposomes

The antimicrobial efficacy of liposome-loaded MC was assessed by analysing the growth of *E. faecalis* and *S. anginosus* in the presence of the hydrogel. MC solutions containing liposomes were prepared as described in Section 4.2.1. Solutions containing T0 MLV/SUVs, T300 MLV/SUVs and T500 MLV/SUVs were prepared as well as control solutions containing 500 µg/mL triclosan in 1 % IPA and 1 % IPA only.

MC solutions at 4 °C were pipetted into a 96-well plate (20 µL/well) and then the plate was incubated at 37 °C for 20 min until the solutions had gelled. Overnight

broth cultures of *E. faecalis* or *S. anginosus*, prepared as previously described, were diluted in BHI to obtain an optical density of 0.08-0.1 at 600 nm. Two further 10-fold dilutions were then prepared and the resulting bacterial suspension was pipetted onto the wells containing MC hydrogels (180 µL/well). The plate was incubated in a plate reader (FLUOstar Omega, BMG Labtech, Ortenberg, Germany) at 37 °C in 5 % CO_2 for 20 h. The absorbance at 600 nm was measured every 1 h and the plate was shaken at 40 RPM for 30 s before each measurement.

The resulting bacterial growth curves were analysed as previously described in Chapter 2, Section 2.2.3.3.

4.3 Results

4.3.1 Rheological properties of methyl cellulose with liposomes

The rheological properties of MC solutions were measured as well as the effect of liposome MLV and SUV incorporation into the polymer solution.

4.3.1.1 Shear viscosity

Shear viscosity of MC solutions was measured at 25 °C (Figure 4.2). Control MC solutions (H_2O only) had a viscosity of 10±1 Pa.s at 0.15 s^{-1}, decreasing to 0.6±0.1 Pa.s at 2000 s^{-1}. Measurements of solutions containing MLVs or SUVs were within the experimental error of the control solutions, suggesting that the viscosity of MC solution was unaffected by the incorporation of liposomes, and that there was no difference seen between solutions containing MLVs or SUVs.

These results indicate that MC is shear-thinning when in solution at 25 °C, and the shear viscosity is unaffected by the addition of liposome MLVs or SUVs.

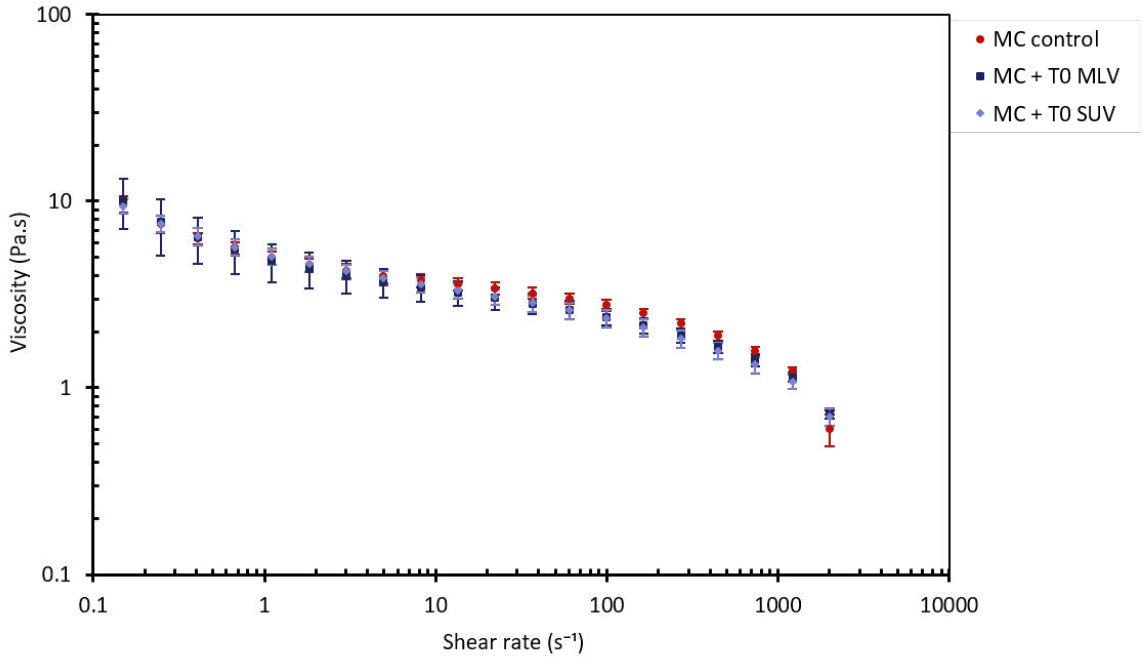

Figure 4.2: **Shear viscosity of methyl cellulose with Liposomes.** Liposome MLVs and SUVs were prepared and incorporated into a 10 % w/w MC solution. The viscosity of these solutions was measured as a function of increasing shear rate on a rotational rheometer. Graph shows mean shear viscosity with standard error of 3 independently prepared samples.

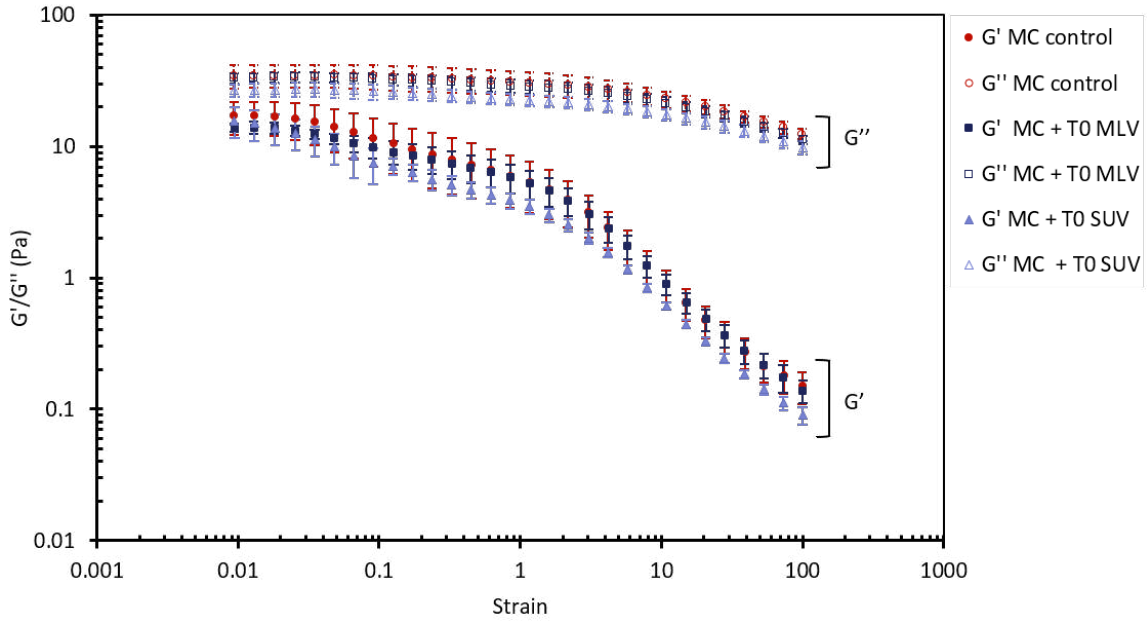

Figure 4.3: **Amplitude-dependent viscoelasticity of methyl cellulose with Liposomes.** Liposome MLVs and SUVs were prepared and incorporated into a 10 % w/w MC solution. The viscoelasticity was measured as a function of strain on a rotational rheometer. Graph shows the mean G' (elastic modulus) and G" (viscous modulus) with standard error of 3 independently prepared samples.

4.3.1.2 Amplitude-dependent viscoelasticity

The viscoelasticity at 25 °C of MC solutions containing liposomes was measured as a function of strain (Figure 4.3). In all measurements, the elastic modulus (G') was lower than the viscous modulus (G") at 25 °C, confirming that MC was a viscoelastic liquid at this temperature. The G' of all samples decreased with increasing strain, however the rate of decrease appeared greater after the strain increased above 0.8. The LVE range of the solution was therefore estimated to be under a strain value of 0.8. The measurements for MC containing MLVs and SUVs were within the experimental error of the control solutions, suggesting that liposomal incorporation did not affect the amplitude-dependent viscoelasticity of MC solution at 25 °C.

These data suggest that the amplitude-dependent viscoelasticity of MC was unaffected by liposome incorporation at strain values of 0.1-100, and that the LVE range was below 0.8. A strain value of 0.5 was therefore selected for further viscoelasticity measurements.

4.3.1.3 Temperature-dependent viscoelasticity

The viscoelasticity of MC was measured as the temperature was increased from 25-55 °C in order to assess the effect of liposomes on the gelation of MC solution (Figure 4.4). At 25 °C, G" was greater than G', indicating that MC was a liquid. As temperature increased, G' was constant until temperature reached 32 °C, where G' began to increase. At 37.7 °C, G' became greater than G", indicating that the solution had gelled at this temperature. MC containing MLVs and SUVs showed similar results, with G' exceeding G" at 38.5 °C.

These measurements suggested that liposome incorporation did not inhibit the thermo-responsive gelation mechanism of MC, however the gelation temperature with liposomes was higher than that of MC alone. It was considered that this difference may have been a function of time rather than temperature, as the temperature was steadily increased over the duration of the measurement. It was therefore decided to measure the viscoelasticity of the liposome-loaded MC over time whilst maintaining a constant temperature, in order to investigate this hypothesis.

4.3.1.4 Time-dependent viscoelasticity at 3 constant temperatures

Viscoelasticity was measured as a function of time at 30, 35 and 40 °C. Figure 4.5 shows the results of these measurements. The time shown does not include the approximate 50 s it took to lower the top plate before a measurement was taken.

At 30 °C, MC behaved as a solution, with G' lower than G". G' increased over the 20 min measurement period, becoming equal to, but not greater than, G" by the end of the measurement.

At 35 °C, G' had increased to within the experimental error of the G" in the 50 s pre-measurement. This continued to increase and became greater than G" at around 250 s of measurement time. This suggests that MC gels at 35 °C, and takes around 300 s to do so.

At 40 °C, G' was equal to G" by the time the measurement has started and continued to increase above G". This suggests that MC forms a gel faster at 40 °C,

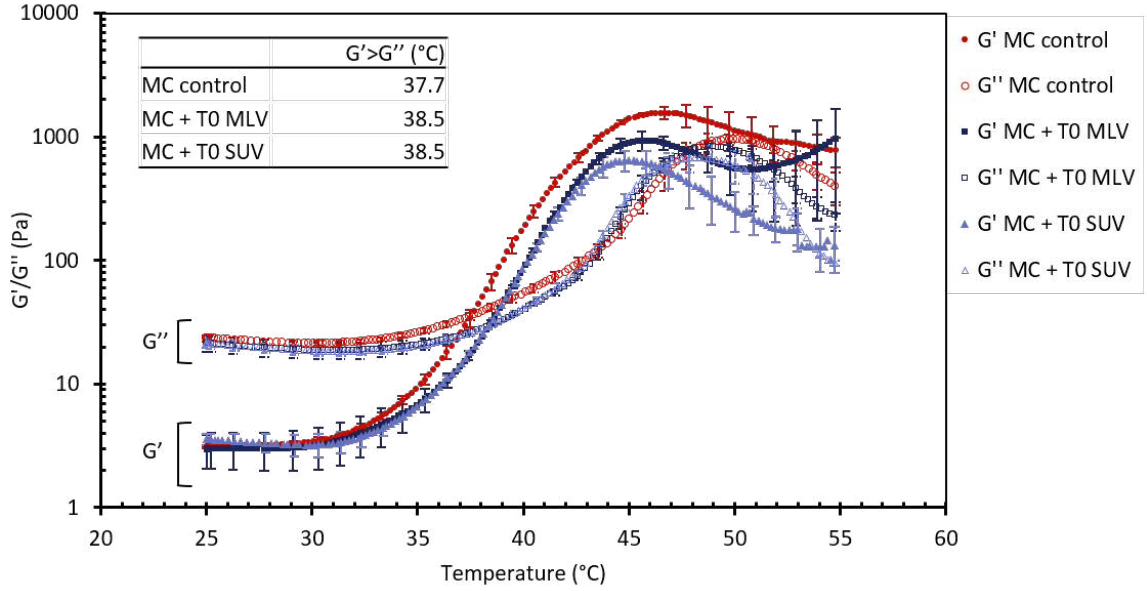

Figure 4.4: **Temperature-dependent viscoelasticity of methyl cellulose with liposomes.** Liposome MLVs and SUVs were prepared and incorporated into a 10 % w/w MC solution. The viscoelasticity was measured as a function of temperature on a rotational rheometer. Graph shows the mean G' (elastic modulus) and G" (viscous modulus) of 3 independently prepared samples. For clarity, error bars are shown for every 5^{th} measurement point. Table insert indicates the first temperature point at which mean G' is greater than mean G" for each formulation.

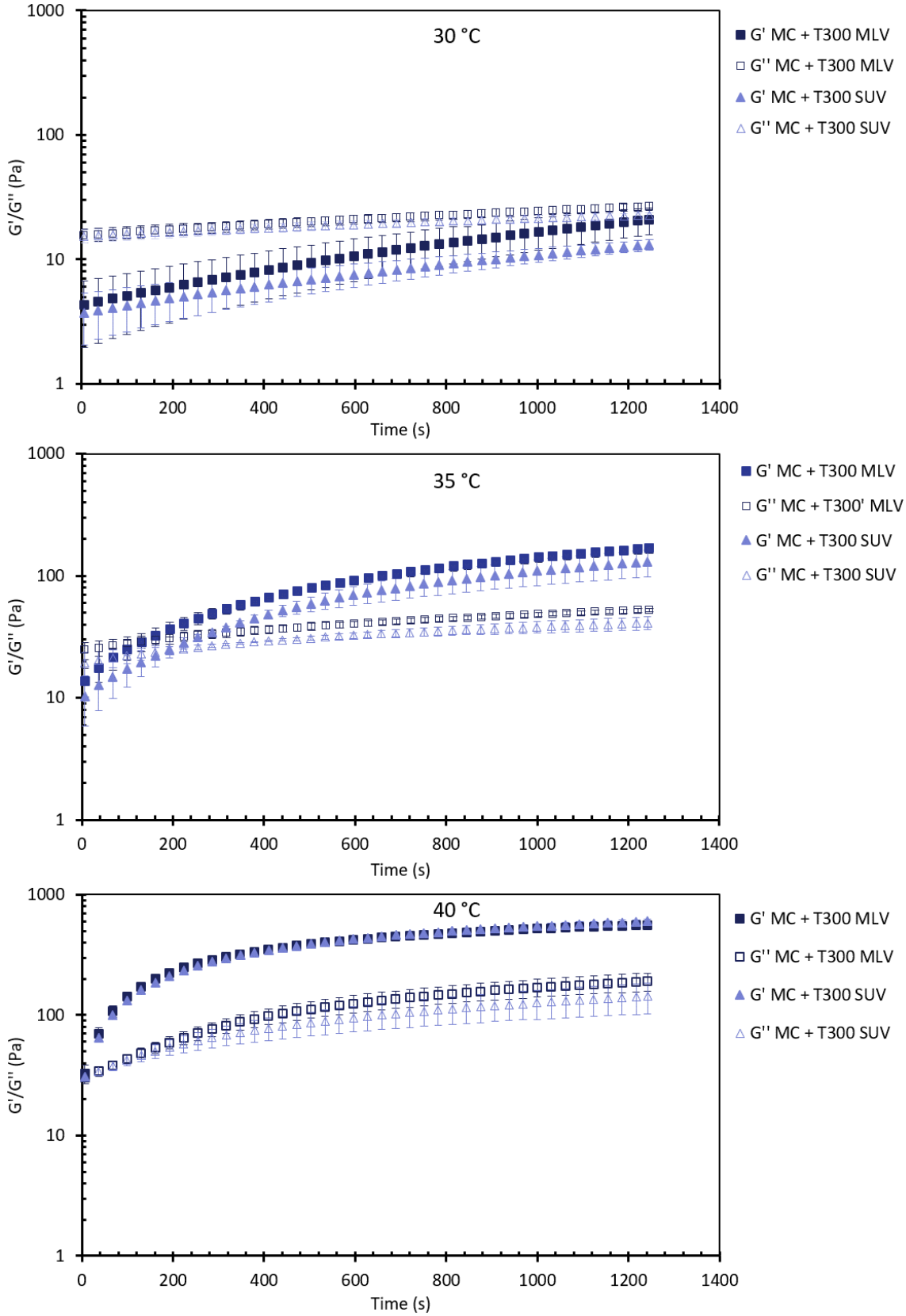

Figure 4.5: **Time-dependent viscoelasticity of methylcellulose with liposomes.** Liposomes were incorporated into a 10 % w/w methyl cellulose solution and the viscoelasticity was measured for 20 minutes at 30, 35 and 40 °C on a rotational rheometer. Graphs show G' and G" of methyl cellulose with T300 MLVs and SUVs. For clarity, every 5th measurement is shown only. Error bars show standard error of 3 independently produced samples.

taking around 50 s, and that the gel formed has a greater G' than that of the gel formed at 35 °C, within the 20 min measurement time.

These data suggest that MC containing T300 liposomes will gel at 30-35 °C, however the time-to-gel and the overall physical properties of the gel are temperature-dependent, within the temperature range tested.

4.3.2 Release of components from methyl cellulose

The release of phospholipids and triclosan from MC hydrogels was measured in order to estimate liposome release from the system. Phospholipid release could not be measured as the majority of samples were below the detection limit of the assay (2 µmol/L). The triclosan concentration was measured using HPLC and is shown in Figure 4.6. Hydrogel containing only triclosan did not release a detectable concentration of triclosan over 168 h, however MC containing triclosan MLVs and SUVs did release around 20 % of the original triclosan added over 168 h. A time-dependent increase in released triclosan is seen from 0-24 h, but the concentration remains the same from 24-168 h. Hydrogels containing MLVs released more triclosan than those containing SUVs, however there was high variability on these measurements and the values for MLVs and SUVs were within the experimental error of one another. These data suggest that triclosan is released from MC, but only when loaded into liposomes and there is no difference in the release profiles of MLV or SUV liposomes.

4.3.3 Antimicrobial properties of methyl cellulose with liposomes

Bacteria were incubated with MC hydrogels containing triclosan liposomes and the bacterial growth was assessed. T300 and T500 liposomes were selected for analysis as they showed the greatest antimicrobial activity when tested as liposomal suspensions (Chapter 3, Section 3.3.7). Figures 4.7 and 4.8 show the growth curves obtained from these analyses and Table 4.3 summarises the parameters derived from these growth curves.

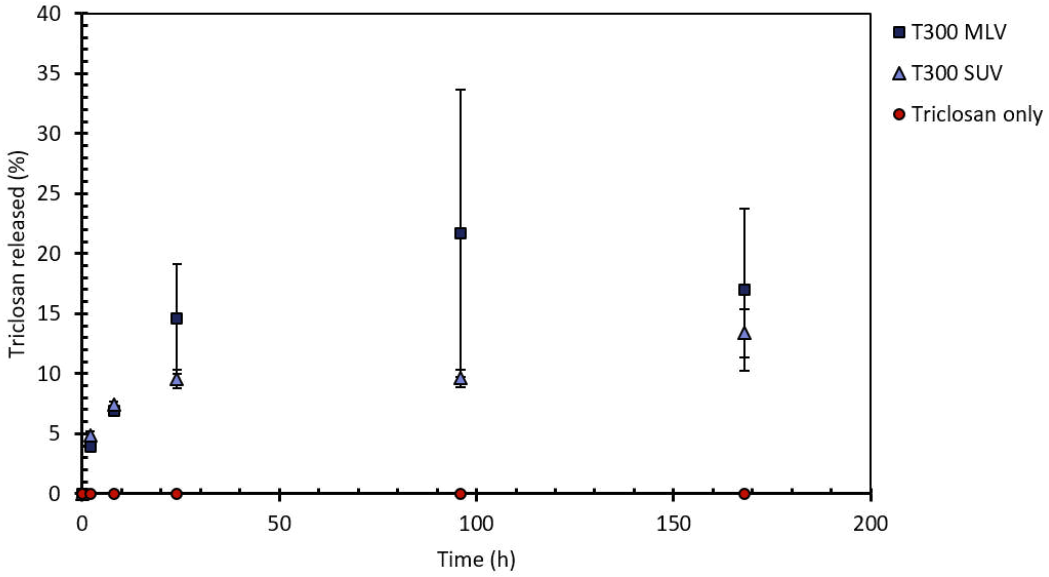

Figure 4.6: **Release of triclosan from methyl cellulose hydrogel.** Triclosan liposomes were incorporated into 10 % (w/w) MC solution and this was incubated at 37 °C for 168 h in H_2O. The H_2O was removed at 6 timepoints and analysed for the presence of triclosan. Graph shows the mean % of triclosan released from gels containing MLVs, SUVs or triclosan only. Error bars show standard error of 3 independently prepared samples. Where error bars are not visible, error lies within the point height.

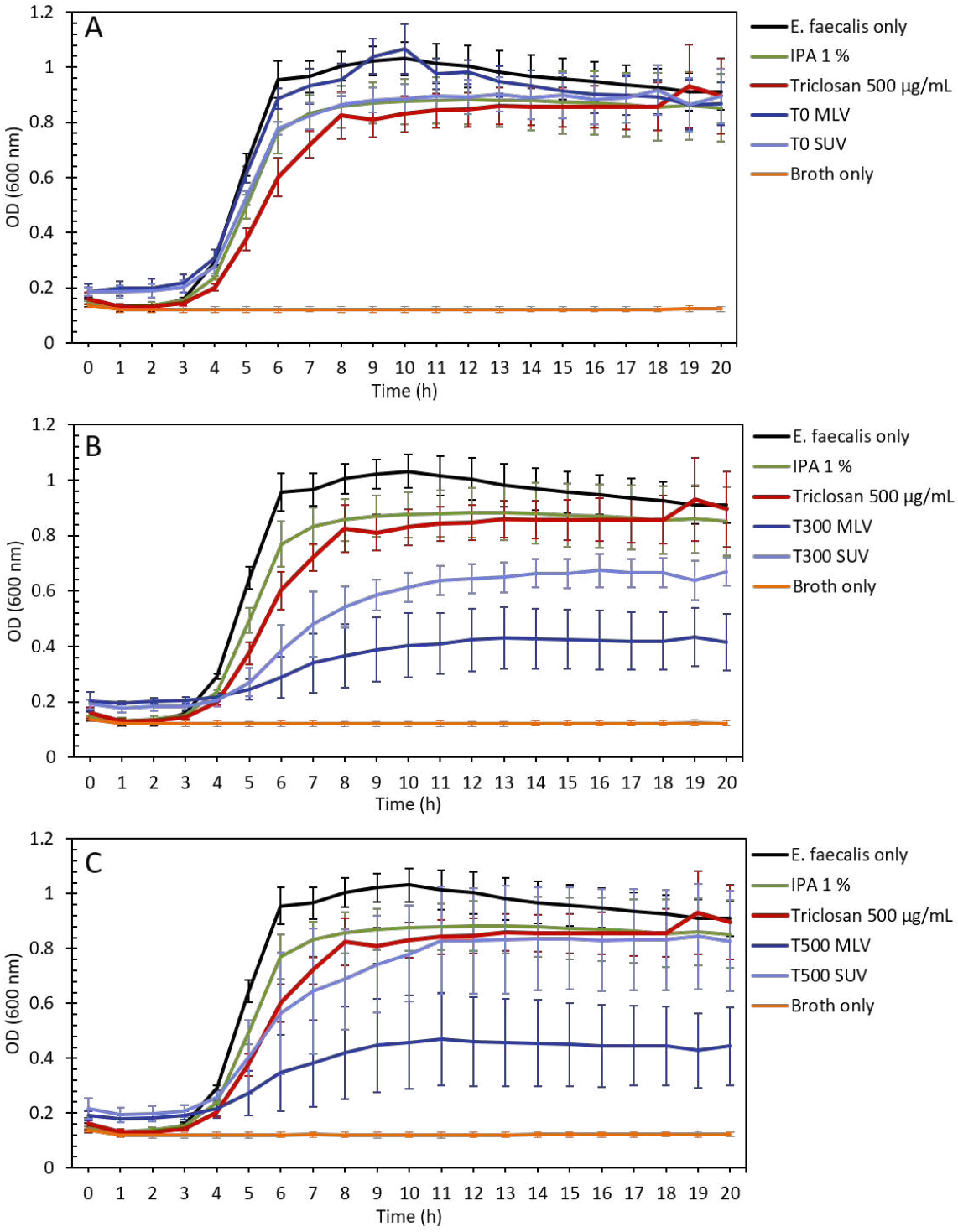

Figure 4.7: **Growth of *Enterococcus faecalis* with liposomes in MC hydrogel.** Liposomes prepared with 0 μg/mL (A), 300 μg/mL (B) and 500 μg/mL (C) of triclosan were incorporated into a 10 % w/w methyl cellulose solution and incubated with a broth culture of *E. faecalis*. Graphs show mean optical density (OD, measured at 600 nm) of the suspensions over 20 h, compared to controls of bacterial culture alone, MC containing triclosan only, and MC containg 1 % IPA. Error bars show standard error of 3 independent experiments.

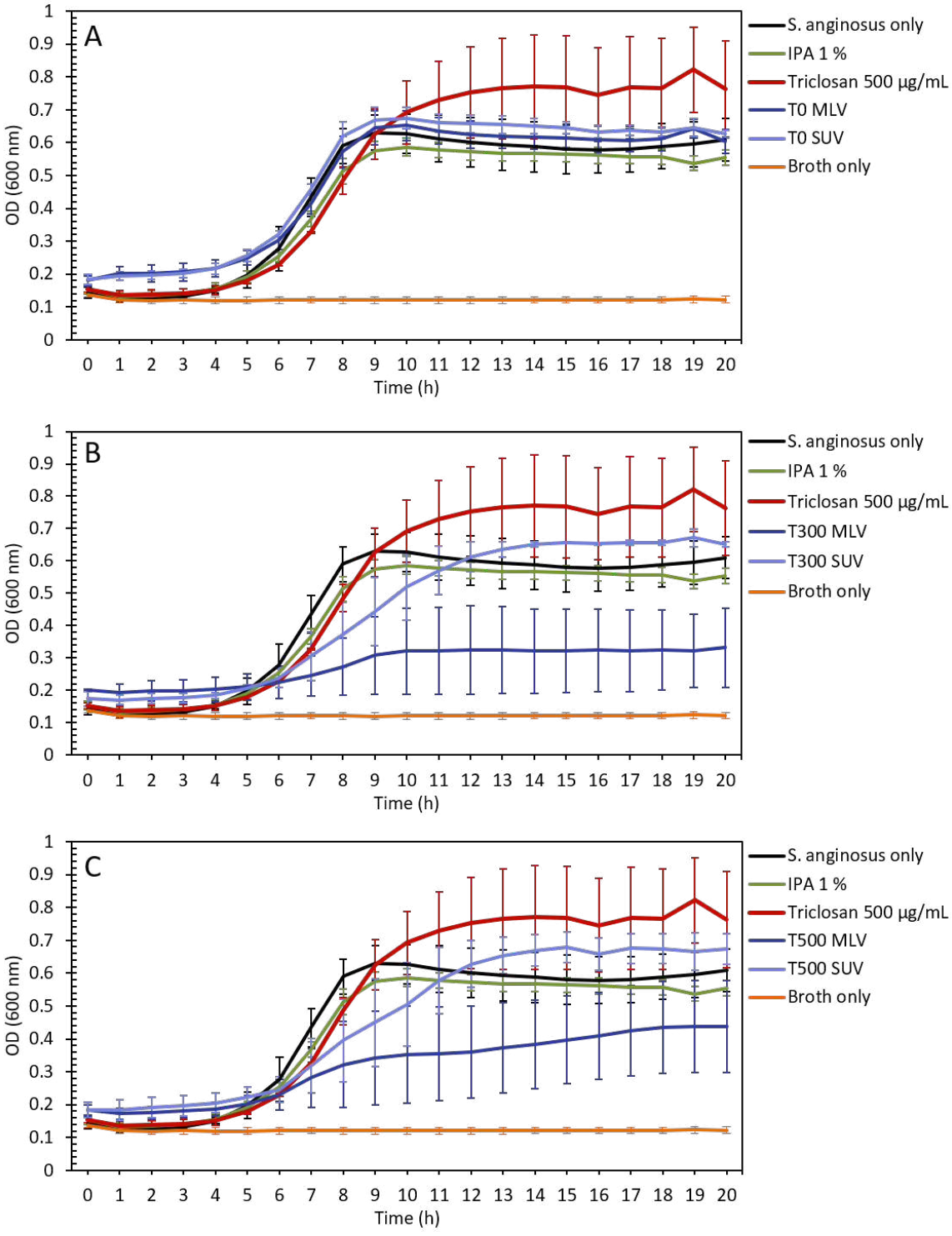

Figure 4.8: **Growth of *Streptococcus anginosus* with liposomes in MC hydrogel.** Liposomes prepared with 0 μg/mL (A), 300 μg/mL (B) and 500 μg/mL (C) of triclosan were incorporated into a 10 % w/w methyl cellulose solution and incubated with a broth culture of *S. anginosus*. Graphs show mean optical density (OD, measured at 600 nm) of the suspensions over 20 h, compared to controls of bacterial culture alone, MC containing triclosan only, and MC containg 1 % IPA. Error bars show standard error of 3 independent experiments.

Table 4.3: Growth parameters of *Enterococcus faecalis* (top) and *Streptococcus anginosus* (bottom) with liposomes in methyl cellulose.

	λ (h)			μ			A (OD_{600})		
	Mean	SEM	*sig.*	**Mean**	SEM	*sig.*	**Mean**	SEM	*sig.*
E. faecalis only	**2.0**	0.1	-	**0.20**	0.02	-	**1.04**	0.06	-
Broth only	**NA**	NA	*NA*	**NA**	NA	*NA*	**0.14**	0.00	***
In methyl cellulose:									
T0 MLV	**1.7**	0.2	*ns*	**0.18**	0.01	*ns*	**1.04**	0.05	*ns*
T0 SUV	**1.5**	0.3	*ns*	**0.15**	0.01	*ns*	**0.94**	0.08	*ns*
T300 MLV	**NA**	NA	*NA*	**NA**	NA	*NA*	**0.44**	0.11	*
T300 SUV	**1.8**	0.8	*ns*	**0.09**	0.01	*	**0.67**	0.06	*ns*
T500 MLV	**NA**	NA	*NA*	**NA**	NA	*NA*	**0.49**	0.16	*
T500 SUV	**1.5**	0.5	*ns*	**0.12**	0.05	*ns*	**0.88**	0.22	*ns*
IPA 1 %	**1.9**	0.1	*ns*	**0.17**	0.02	*ns*	**0.93**	0.11	*ns*
Triclosan 500 µg/mL	**2.2**	0.1	*ns*	**0.15**	0.01	*ns*	**0.96**	0.12	*ns*

	λ (h)			μ			A (OD_{600})		
	Mean	SEM	*sig.*	**Mean**	SEM	*sig.*	**Mean**	SEM	*sig.*
S. anginosus only	**2.9**	0.3	-	**0.11**	0.01	-	**0.65**	0.06	-
Broth only	**NA**	NA	*NA*	**NA**	NA	*NA*	**0.14**	0.00	**
In methyl cellulose:									
T0 MLV	**2.4**	0.1	*ns*	**0.09**	0.01	*ns*	**0.65**	0.04	*ns*
T0 SUV	**2.1**	0.4	*ns*	**0.10**	0.01	*ns*	**0.68**	0.03	*ns*
T300 MLV	**NA**	NA	*NA*	**NA**	NA	*NA*	**0.36**	0.12	*ns*
T300 SUV	**4.1**	0.8	*ns*	**0.09**	0.01	*ns*	**0.68**	0.01	*ns*
T500 MLV	**NA**	NA	*NA*	**NA**	NA	*NA*	**0.46**	0.14	*ns*
T500 SUV	**3.7**	1.1	*ns*	**0.09**	0.02	*ns*	**0.70**	0.06	*ns*
IPA 1 %	**2.8**	0.4	*ns*	**0.09**	0.01	*ns*	**0.59**	0.03	*ns*
Triclosan 500 µg/mL	**3.6**	0.4	*ns*	**0.12**	0.02	*ns*	**0.81**	0.14	*ns*

Bacteria were grown in BHI in a 96-well plate with methyl cellulose hydrogel formulations for 20 h. Length of lag phase (λ), maximum growth rate (μ) and maximum absorbance value (A) of growth curves are shown. (*"SEM"= standard error of the mean of 3 independent experiments, "sig."= significance of difference in means compared to bacteria in BHI:"ns"=* $P > 0.05$, **=* $P < 0.05$, *** =*$P < 0.01$, ****=*$P < 0.001$).

Bacterial growth was unaffected by MC containing T0 liposomes (Figures 4.7A and 4.8A). *E. faecalis* growth rate (μ) with T300 SUVs was significantly decreased ($P = 0.04$), however the maximum absorbance value (A) was not significantly lower than controls. No inhibition of growth was observed with T300 SUVs against *S. anginosus* or with T500 SUVs against either species. T300 and T500 MLVs caused a reduction in maximum absorbance (A), which was significant against *E. faecalis* ($P = 0.02$ and $P = 0.04$ respectively). These formulations did not significantly lower the maximum absorbance of *S. anginosus*, however no definitive lag phase or growth rate was identified, suggesting that growth was inhibited to some extent. MC containing triclosan only had no effect on bacterial growth of either species. These findings suggest that triclosan is not effective when loaded into MC alone, but liposomal triclosan shows antimicrobial efficacy, particularly against *E. faecalis*.

4.4 Discussion

MLVs and SUVs were loaded into a MC hydrogel to assess the suitability of this material to carry and deliver antimicrobial liposomes to root canals. This novel composite gel system has not previously been developed or tested for this use.

Rheological analyses confirmed that MC is a shear-thinning, viscoelastic liquid at 25 °C. This shear-thinning behaviour is typical in polymer solutions (Morris *et al.*, 1981) and has previously been observed in lower concentrations (2 % w/v) of MC (Haque and Morris, 1993). The results obtained here suggest that a 10 % w/w MC solution may be suitable for root canal injection, as it will decrease in viscosity as it pushed through a syringe, however further study would be required to investigate how the rheological data relate to practical use. Typically, the minimum diameter of a prepared root is around 200 µm, based on the tip diameter of conventional endodontic files (size 20 K-file and ProTaper F2), and so it would be advantageous to observe if the solution could be extruded through a 27-gauge endodontic irrigation needle, which has an internal diameter of 200 µm. In addition, it has not been investigated what happens to the viscosity once the shear stress is removed, and whether the

solution would flow freely into the root canal. No previous studies are available in the literature that indicate the ideal physical properties an intracanal dressing should achieve, however the maximum viscosity of MC was 10 Pa.s, and the viscosity of $Ca(OH)_2$ paste (the most commonly used intracanal medicament) is around 3.5 Pa.s (Estrela *et al.*, 2001), suggesting that the viscosity of the solutions prepared in this study may not be low enough for intracanal injection, depending on whether the solution will return to its maximum viscosity after shear-thinning has occurred.

A 10 % MC solution was used, as this is the maximum soluble concentration of MC in H_2O, resulting in the lowest gelation temperature without further modification. If a lower concentration of MC was required in order to lower the viscosity of MC solution upon injection, the addition of saline to the system would allow for the maintenance of a low gelation temperature whilst also lowering the MC concentration. Zuidema *et al.* (2014) used 6 % MC in saline solution and obtained a gel with a G' at 37 °C that was comparable to the G' of 10 % MC at 40 °C observed in this chapter. The addition of chitosan also influences the gelation temperature of MC, when combined with various salt solutions (Tang *et al.*, 2010).

Addition of liposomes had no significant effect on the viscosity of MC solution. No other studies were found on the effect of liposomes on MC rheology, however Mourtas *et al.* (2009) investigated the effect of PC:C liposomes on the viscosity of hydroxyethylcellulose, which is another ether of cellulose, and observed a concentration-dependent increase in viscosity when 5 mg/mL or 20 mg/mL liposomes were added to the polymer solution. Another study by the same group concluded that liposome size was not a contributing factor to these rheological differences (Mourtas *et al.*, 2008). The concentration added in this chapter was 1 mg/mL and so it is possible that higher liposome concentrations would affect the viscosity. This should be investigated if it became apparent that a higher concentration of liposomes were required for greater therapeutic efficacy. The lack of liposome size-dependent differences in rheology agree with those of the 2008 study.

Temperature-dependent measurements suggested that MC formed a gel as the

temperature increased above 37 °C and that liposomal MLVs and SUVs did not affect the ability of MC to form a gel. A slight increase in gelation temperature was observed in these samples when a temperature sweep was performed, however further rheological tests suggested that the liposome/MC solutions gelled at 35 °C, taking approximately 300 s to do so. This would suggest that the gelation temperature of 38.5 °C obtained from the temperature sweep was a result of increasing the temperature at a rate of 2 °C/min and therefore not allowing the sample sufficient time to equilibrate at each temperature. Generally, root canal medicaments do not need to set in the same way as a restorative material (such as a sealant) because they have no structural role, however the material must be able to fill the root canal whilst avoiding extrusion through the root apex into the periapical tissue (Carrotte, 2004).

The "working time" is considered the time during which the medicament is physically malleable enough to be placed in the root canal before the the consistency changes, and for currently used materials, is defined by the time it takes to observe a 10 % shrinkage in material volume due to dehydration (International Organisation of of Standardization, 2012). A study by Basrani *et al.* (2004) compared the working time of MC (4000 cP, 1 %) containing calcium hydroxide, chlorhexidine, or a combination of both, according to the ISO standards, and found a mean working time of 92-128 min for the materials tested. The liposomal MC prepared in this chapter did not use the same assessment criteria, but suggested that the working time was much shorter, if this were to be defined as the time taken for the MC solution to form a gel. Allan *et al.* (2001) showed that the working time for root canal sealants increased greatly when they were placed in high humidity, similar to that found in the oral cavity, suggesting that further experiments would need to assess the gelation time of the hydrogel in high humididty, in order to assess the working time in a more clinically relevant setting.

Time-dependent viscoelasticity measurements showed that MC with liposomes gels at 35 °C and 40 °C, however the gel formed at 40 °C has a shorter gelation time (∼50 s) and a higher G', suggesting that a stronger gel is formed. Although physiological temperature is considered to be 37 °C, there may be some fluctuations

in intra-oral temperatures due to external stimuli. Barclay *et al.* (2005) measured fluctuations in intra-oral temperature from 0-70 °C when cold and hot beverages were consumed, however this variation was observed on front teeth, and the variation was lower on pre-molars and molars. It is not clear how these temperature fluctuations would translate to the intra-canal environment, however the temperature-sensitive nature of the hydrogel may cause variation in the rheology of the gel over time *in vivo*. It has not been studied how fluctuations in temperature and/or rheological properties may affect the release profile of the gel, but premature burst release of the liposomes due to an unstable rheology may diminish the long-term efficacy of the material.

Overall, these rheological data suggest that MC is a shear-thinning, potentially injectable solution at ambient temperature and will gel as the internal temperature increases. Additionally, it could be used to carry liposomes for therapeutic purposes as they do not significantly alter the rheological properties.

Release of triclosan from MC was measured over 168 h. These data suggested that triclosan is released gradually over 24 h, but remains at the same concentration from 24-168 h. This may indicate that a maximum release of 20 % has been reached at 24 h, or that a longer incubation time is needed to observe further triclosan release. This experiment measured release in non-sink conditions, where the aqueous phase was left on the gel until the desired timepoint had been reached. This method will be dependent on the partition coefficient of the drug between the gel and aqueous phase, thus a maximum concentration of released triclosan may have been reached due to the partition coefficient rather than the the release (Washington, 1989). Following endodontic preparation, the dentine tubules are proposed to contain residual endodontic irrigants (NaOCl, water) as well as dentine fluid (Allan *et al.*, 2001). Once a medicament is placed and the dental crown is sealed, the remaining fluid is in a contained area, where aqueous turnover around the material is limited, assuming no coronal leakage occurs and that the apical foramen is sealed. A non-sink experiment was therefore selected to be a closer representation of a clinical setting under these assumptions. There are a lack of studies, however, evaluating aqueous flow (or lack

thereof) within the filled root canal. Non-sink conditions have been used to measure drug release from other endodontic materials, such as polymer coated drug devices containing chlorhexidine tested by Lee *et al.* (2005a).

Phospholipid was not quantifiable in the assay used, suggesting that concentrations below the detection limit of the kit were present in the aqueous phase of the experiment. If the triclosan was released in the form of intact liposomes, it would have been expected that comparable percentage of lipid would be released as that of triclosan. This, however, was not the case, since this would have yielded high enough concentrations to be detected by the assay. It is evident that liposomal encapsulation is necessary for hydrogel release because triclosan that was loaded directly into the gel was not released at all over the time period measured. This suggests that the diffusion of triclosan within the system is modified by liposomal loading but it may not be released in liposomal form. Further analyses may clarify the release mechanism of triclosan from the gel. Park *et al.* (2013) used DLS to confirm the presence of liposome-sized particles released from a cellulose hydrogel containing quertecin and rutin-loaded liposomes: a method which could be employed for triclosan liposome release from MC. Others have used fluorescent probes to model liposomal drug release and determine whether the compounds are released in liposomal form. Ruel-Gariépy *et al.* (2002) loaded liposomes with a hydrophilic, fluorescent dye, carboxyfluoroscein, and incorporated these into a chitosan-based hydrogel. Release was measured using fluorescence spectroscopy and the addition of Triton to the released components resulted in an increase in fluorescence, suggesting that the dye had been released from the gel in liposomal form and that the addition of Triton had ruptured the liposomes, resulting in an increase in fluorescence. The study also showed that liposome encapsulation resulted in a slower release of the dye compared to free dye alone, which is the converse to the observations of the chapter. This suggests that hydrophilic drug release may be slower upon liposome incorporation, but hydrophobic drugs, such as triclosan, require liposome encaspulation in order to facilitate their release.

It was also demonstrated that drug-loaded liposomes incorporated into MC retained their antimicrobial properties over 20 h and that this effect was greater in

MLVs than SUVs. These results are similar to those obtained with liposomes in suspension (Chapter 3, Section 3.3.7), suggesting that hydrogel incorporation does not negatively impact the antimicrobial properties of the triclosan liposomes. The reduction in growth of both bacteria was not as great with liposomes in MC as it was with liposome suspensions. This may be because only a proportion of the drug is released into the bacterial suspension over 24 h (as demonstrated in the gel release experiment), whereas it is assumed that liposomes delivered in suspension will be immediately dispersed into the bacterial broth. MC itself showed no antimicrobial effect, neither did MC loaded with T0 (empty) liposomes. Additionally, triclosan alone had no antimicrobial effect when incorporated into MC, compared to liposomal triclosan. This may be explained by the previous experiment, showing that triclosan is not released from MC unless it is incorporated into liposomes. Further work could use the aqueous phase of the hydrogel release experiments to assess the antimicrobial properties and elucidate whether the bacteria must be cultured with the gel or if the released components alone can elicit an antimicrobial effect.

4.5 Conclusions

It has been shown that a MC hydrogel containing triclosan MLVs and SUVs has rheological properties that may be suitable as an endodontic, intracanal medicament. It is shear-thinning at ambient temperature, suggesting that it may be injectable, and it forms a gel at physiological temperature. Triclosan liposomes are released from the gel over time and MLVs loaded with 300 and 500 µg/mL triclosan had an antimicrobial effect against two common pathogenic endodontic bacteria, particularly *E. faecalis*, which is commonly associated with failed endodontic restorations. In the gel system, the liposomes are essential for triclosan release to occur.

Chapter 5

Antimicrobial Efficacy of a Triclosan Liposome-Loaded Hydrogel in Endodontically Prepared Human Root Canals

5.1 Introduction

Results from previous chapters have suggested that methyl cellulose (MC) hydrogel containg triclosan-loaded liposomes inhibit the growth of two oral pathogens *in vitro*, however this was assessed with planktonic bacterial growth in a well plate. Whilst *in vitro* assays allow for greater control of experimental conditions, growing and treating the bacteria in a clinically more relevant setting would give a better indication of the material's efficacy for its potential use as an intracanal medicament during endodontic therapy. An *ex vivo* model of endodontic infection will therefore be developed to help predict how well the material will perform *in vivo* as there may be some barriers to delivery that cannot be accounted for during *in vitro* experiments.

It is well known that bacteria existing as a biofilm on a surface have greater potential to withstand antimicrobial treatment than those grown planktonically (Stewart, 2002): a characteristic that has been observed previously in Chapter 2. Even when

grown as a biofilm *in vitro*, the substrate type must be considered, as bacteria cultured on root dentine may display differences in attachment and biofilm formation compared to those cultured on plastic. This is, in part, due to differences in the physical properties of the substrates. The polystyrene used to produce tissue culture plastics is smooth, with surface roughness (Ra) of around 0-0.007 µm, whereas root dentine roughness is 0.11-0.26 µm, depending on the endodontic treatments used (Hatano *et al.*, 1999; Ari *et al.*, 2004; Zeiger *et al.*, 2013). Dentine is also porous, possessing dentine tubules that extend perpendicular to the root surface, allowing for bacterial migration and colonisation and ultimately providing a larger surface area for biofilm formation (Section 1.3). This may result in a greater proportion of the biofilm that is inaccessible for antimicrobial treatment and therefore decrease treatment efficacy.

As well as the physical properties of the dentine, root morphology is a challenge to endodontic antimicrobial delivery. During endodontic preparation bacteria can evade mechanical debridement and antimicrobial irrigation, residing in dentine tubules, isthmuses and accessory canals (Carrotte, 2004). Root curvature and root calcification may also restrict the working length during endodontic preparation and therefore increase the areas where bacteria may reside undisturbed (Tang *et al.*, 2011). Even when preparation is relatively straightforward, typically prepared roots will have narrow diameters of 60-500 µm at the apex (based on the tip diameter of conventional K-files and ProTaper endodontic files), depending on the original root dimensions. It is therefore important to assess the efficacy of new treatments in a setting that reflects this morphological complexity.

Studies have shown that intracanal medicament, which is placed as a temporary filling before the root is permanently filled, significantly decreases the presence of intracanal bacteria and therefore may lead to better treatment outcomes (Siqueira *et al.*, 2007b,a). Calcium hydroxide ($Ca(OH)_2$) is primarily used as an intracanal medicament, however there are limitations in its use. Its mode of action is raising the pH of the root in order to kill bacteria, but this effect is buffered by dentine proteins and carbonate ions, lowering the effective pH to around 10 (Athanassiadis *et al.*, 2009). This can be withstood by some fungal species, and by the bacterium

E. faecalis, which is commonly isolated from secondary root infections (Ferguson *et al.*, 2002; Mohammadi and Dummer, 2011).

This chapter will consider the use of a triclosan/liposome loaded hydrogel as an intracanal medicament for endodontic infection, using extracted human teeth as a model system. It will assess the hydrogel's efficacy in preventing *E. faecalis* invasion of the root canal space, following pre-culture of the tooth with the bacteria.

5.2 Materials and methods

5.2.1 Preparation of liposomes and liposome-loaded methyl cellulose

Multilamellar vesicle (MLV) liposomes were prepared with 300 μg/mL triclosan and 1 mg/mL phosphatidylcholine:cholesterol (mass ratio 7:1), as described in Chapter 3, Section 3.2.1 and defined as T300 MLVs.

The T300 MLVs were incorporated into a 10 % (w/w) methyl cellulose (MC) solution, as detailed in Chapter 4, Section 4.2.1.2. Control MC solution was prepared containing H_2O only.

5.2.2 Sample collection of human incisors and premolars

Following ethical approval, human incisors and pre molars were collected from Cardiff University School of Dentistry Tooth Bank (REC reference 12/WA/0289, project reference TB-14-008, approved on 08/01/2015). Teeth had been extracted for non-orthodontic reasons and were stored at -80 °C prior to use. Ten teeth were collected in total.

5.2.3 Endodontic preparation of extracted teeth

Teeth were prepared by a clinically qualified dentist. All teeth were radiographically examined using horizontal parallax technique to visualise root canal anatomy and estimate working length prior to preparation. Access cavities were prepared through

the occlusal surface using a diamond bur (501 HiDi, Dentsply Limited, Surrey, UK) with water coolant. Refinement of pulp chamber outline and enlargement of root canal orifices was achieved using an ultrasonic instrument without water coolant (P5 Newtron XS, Acteon, UK). Subsequently, canals were prepared using size 10, 15 and 20 stainless steel K-files (Dentsply Maillefer, Ballaigues, Switzerland). Where deemed necessary to improve preparation, coronal flaring of canals was undertaken using a rotary, nickel-titanium ProTaper SX file (Dentsply Limited, Surrey, UK), followed by the S1, S2, F1, and F2 files according to the manufacturer's instructions. After each file was used, the canal was irrigated with 2 % (w/v) sodium hypochlorite solution and recapitulated using a size 10 K-file to ensure apical patency.

Following instrumentation with the S1 rotary file, teeth were placed in alginate impression material to simulate periapical tissues, and an electronic apex locator (Mini Apex Locator, Kerr UK Limited, Uxbridge, UK) used to confirm the working length. After preparation was completed, canals were irrigated using 17 % (w/v) ethylenediaminetetraacetic acid (EDTA) solution and final irrigation using 0.9 % (w/v) sodium chloride solution to remove debris and any residual antimicrobial agents from prior irrigation. Radiographic examination was repeated following preparation to confirm adequate preparation quality. [1]

5.2.4 Infection and treatment of root canals

After endodontic preparation, teeth were exposed to 9100 cGy gamma irradiation over 40 min (Gamacell 1000 Elite, Noridon International inc., Oxfordshire, UK) to sterilise and then incubated overnight in brain heart infusion (BHI) broth to confirm effective sterilisation. If the BHI became turbid, indicating bacterial growth, the tooth was excluded from the experiment.

Teeth were placed in a sterile 1.5 mL microcentrifuge tube with the bottom cut away. The tube was then positioned inside a bijou tube containig 2.5 mL BHI so that the root apex was submerged. This arrangement is illustrated in Figure 5.1. An overnight culture of *E. faecalis* was diluted in BHI to obtain an absorbance value of

[1] Section 5.2.3 provided by Joshua Twigg

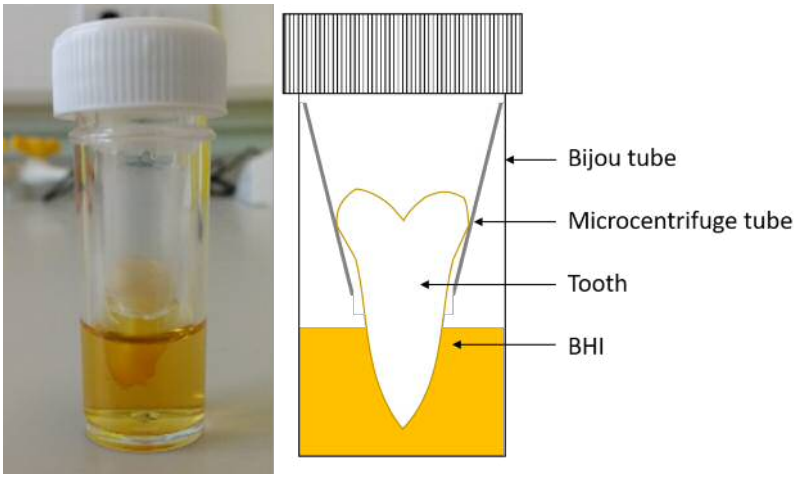

Figure 5.1: **Culture setup of tooth for infection model (Section 5.2.4).**

0.08-0.1 at 600 nm. Two further 10-fold dilutions were prepared and the resulting bacterial suspension was injected into the roots using a 21 gauge needle. The teeth were incubated for 24-48 h at 37 °C in 5 % CO_2. A control tooth was prepared with no bacterial inoculation.

The teeth were then washed in sterile phosphate-buffered saline (PBS), in order to remove any non-adherent bacteria, and placed into a fresh bijou containing BHI, as before. The roots were dried with sterile paper points, which were streaked onto a tryptone soya agar (TSA) plate to confirm that the roots were infected. Treatment was then applied to the roots using a 21 gauge needle as follows:

A BHI only (no initial bacterial inoculation),

B BHI only (with initial bacterial inoculation),*

C triclosan solution (200 μg/mL in 1 % IPA),*

D triclosan liposomes (T300 MLVs),

E triclosan liposomes in MC (T300 MLVs in 10 % w/w MC),

F MC in H_2O (10 % w/w).

*Conditions B and C were performed on a seperate occasion to others.

The teeth were then incubated with the treatment for a further 24 h at 37 °C in 5 % CO_2.

5.2.5 Histological prepartion of samples

5.2.5.1 Fixation and demineralisation

Teeth were removed from culture and placed in 10 % (v/v) neutral-buffered formalin solution for 48 h in order to fix the tissues. The teeth were then transferred to 15 % (v/v) formic acid for 14 days for tissue demineralisation to occur. During this time, the samples were removed and placed into fresh formic acid every 48 h. After demineralisation, the teeth were cut longitudinally with a scalpel and placed in a biopsy cassette.

5.2.5.2 Automated tissue processing and paraffin wax embedding

Samples were processed through graded chemicals on an automatic tissue processor, as follows:

1. 70 % ethanol, 1 h,
2. 90% ethanol, 1 h,
3. 100 % ethanol, 1.5 h,
4. 100 % ethanol, 1.5 h,
5. 100 % ethanol, 1.5 h,
6. 100 % ethanol, 1.5 h,
7. Xylene, 1.75 h,
8. Xylene, 1.75 h,
9. Xylene, 1.5 hr,
10. Molten wax, 2.5 h, 60-65 °C,

11. Molten wax, 2.5 h, 60-65 °C.

Following processing the tissues were embedded in paraffin wax using a processing machine (Shandon Pathcentre, Thermo Scientific, Surrey, UK) and aligned so that longitudinal sections of the teeth could be cut.

5.2.5.3 Sample sectioning

Sections of 6 µm thickness were cut from the wax blocks using a Leitz 1400 microtome (Leica, Buckingham shire, UK). The embedded sections were floated on H_2O (40 °C) and mounted on polylysine glass slides. Slides were placed at 60 °C for at least 1 h to allow for adhesion of the sample to the slide. The slides were then stained.

5.2.5.4 Haemotoxilyn and eosin staining

Slides were placed on an automated tissue stainer. The slides were taken through xylene, ethanol and water washes followed by haemotoxylin and eosin (H&E) stains. They were then taken through a further series of alcohol washes before finally being immersed in xylene. The slides were then removed and a coverslip was applied with DPX mountant.

5.2.5.5 Gram stain

Sections, mounted on slides, were sequentially submerged xylene, 99 % ethanol, and distilled H_2O for 5 min each. After flushing with crystal violet solution for 60 s, samples were rinsed with tap water and then flushed with Lugoli's iodine solution for 60 s. Acetone was used to rinse the slide until the acetone ran clear and then the slide was rinsed with tap water before Carbol fuchsin solution was applied for 60 s. The slide was then rinsed with tap water once more, left to air-dry, and then submerged in xylene for 5 min before a cover slip was applied with DPX mountant.

5.2.6 Imaging and analysis

Slides were scanned with an Aperio slide scanner and viewed using Aperio ImageScope software (Leica Biosystems, Buckinghamshire, UK). Representative images of each slide were taken at 20 X magnification. Images were taken of root interior, where the dentine tubules were observed to be perpendicular to the root surface.

Slides of Gram-stained sections were also viewed under oil immersion light microscopy at 100 X magnification (Nikon Eclipse 50i, Nikon Instruments, Amsterdam, Netherlands) and viewed using StCamSWare (Omron SenTech,Kanagawa, Japan) to view bacterial morphology.

5.3 Results

5.3.1 Tooth collection and preparation

Out of the 10 teeth collected, 4 were excluded from the experiment: one had a root fracture and was not suitable for endodontic preparation. The other 3 were not sterile following irradiation, indicated by the criteria set out in Section 5.2.4. Radiographs of the 6 teeth included in the experiment before and after endodontic preparation are shown in Figure 5.2. Each tooth was a premolar with single or double root canal. Some had an intact crown (2 and 6), one had no crown (3), and the others (1, 4 and 5) had evidence of caries and/or previous restoration that required removal.

5.3.2 Bacterial inoculation of teeth

Following incubation with *E. faecalis* and then washing with PBS, the root canals were dried and swabbed onto TSA. All swabs were positive for bacterial growth, apart from the sterile control that had not been inoculated with the bacterial suspension, confirming that the root canals had been successfully infected with *E. faecalis* prior to treatment (Table 5.1).

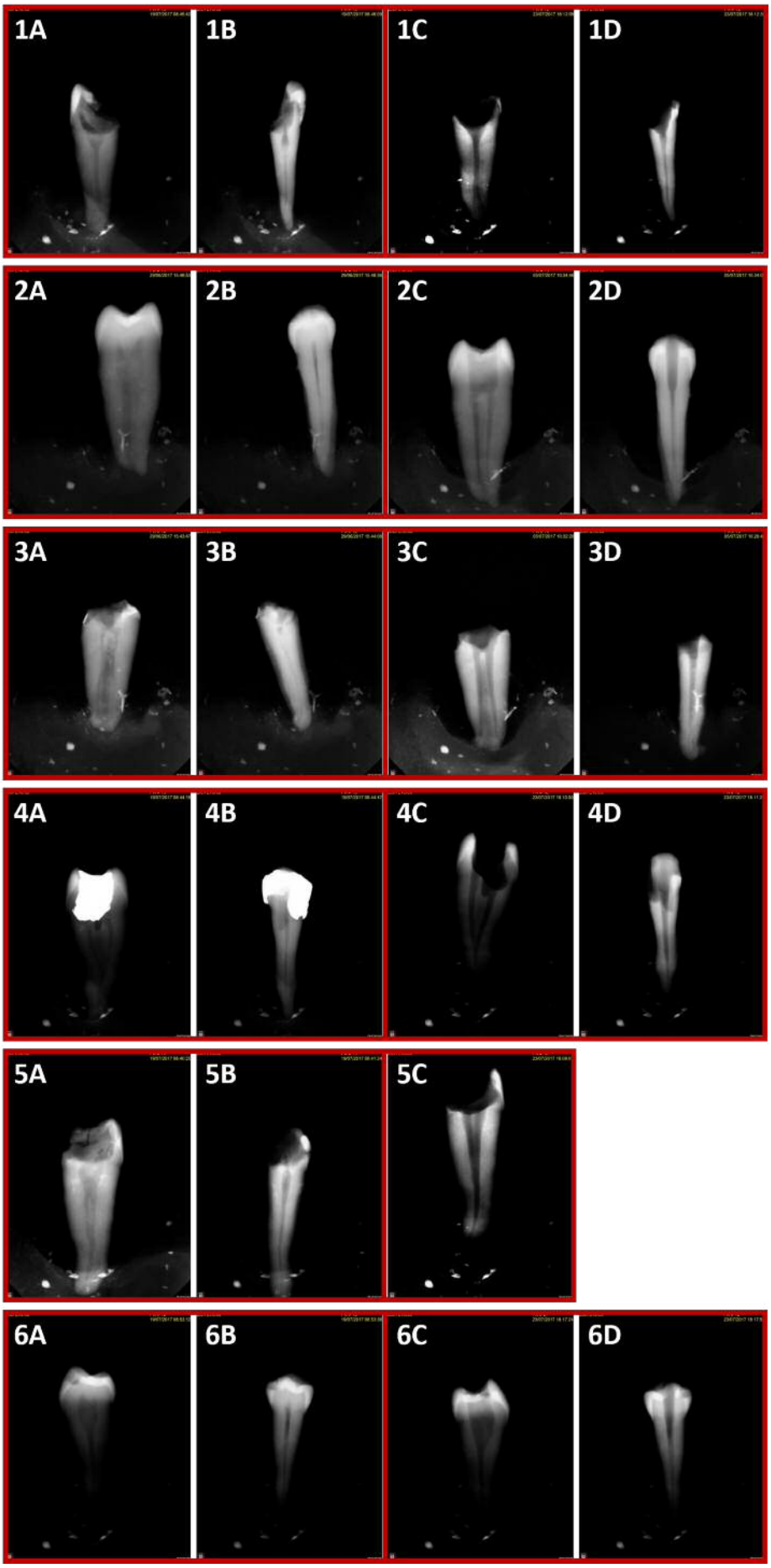

Figure 5.2: Radiographs taken of extracted teeth using horizontal parallax technique. Images show radiographs of 6 teeth (1-6) before (A+B) and after (C+D) endodontic preparation.

Table 5.1: **Growth of swabs taken from endodontically prepared teeth following 24-48 h bacterial inoculation.**

Tooth Sample	Bacterial growth (+/-)
A (no bacterial inoculation)	-
B	+
C	+
D	+
E	+
F	+

Extracted teeth were endodontically prepared, sterilised, and the root canals inoculated with E. faecalis *for 24-48 h. Root canals were then rinsed and dried before swabs were taken and streaked onto TSA plates. Table shows whether bacterial growth was positive or negative for each tooth swabbed (A-F).*

5.3.3 Histology sections: H&E staining

Histological sections of the infected and treated teeth were prepared and stained with H&E, which stains anionic structures blue and cationic structures pink, allowing clearer visualisation of tissues.

In all sections, the root dentine was identified as being stained pink, with the tubules being visible at a perpendicular angle to the intraroot surface. Some blue staining was observed along the tubules (Figure 5.3A-F).

In some sections, additional purple-stained structures were identified on the intraroot surfaces, which were believed to be evidence of a biofilm, due to the presence of dark, granular clusters that were consistent with bacterial cells and not present on the bacteria-free control (Figure 5.3A). This was particularly evident in samples B (no treatment, Figure 5.3B) and F (treated with MC in H_2O, Figure 5.3F).

These data suggest that a biofilm had formed on intraroot surfaces of teeth with no treatment or treated with the MC in H_2O control (Figure 5.3A and F). Teeth that were treated with triclosan solution, triclosan liposomes, and triclosan liposomes in MC, did not have evidence of biofilm formation (Figure 5.3B-E) and appeared more similar to the non-infected control (Figure 5.3A).

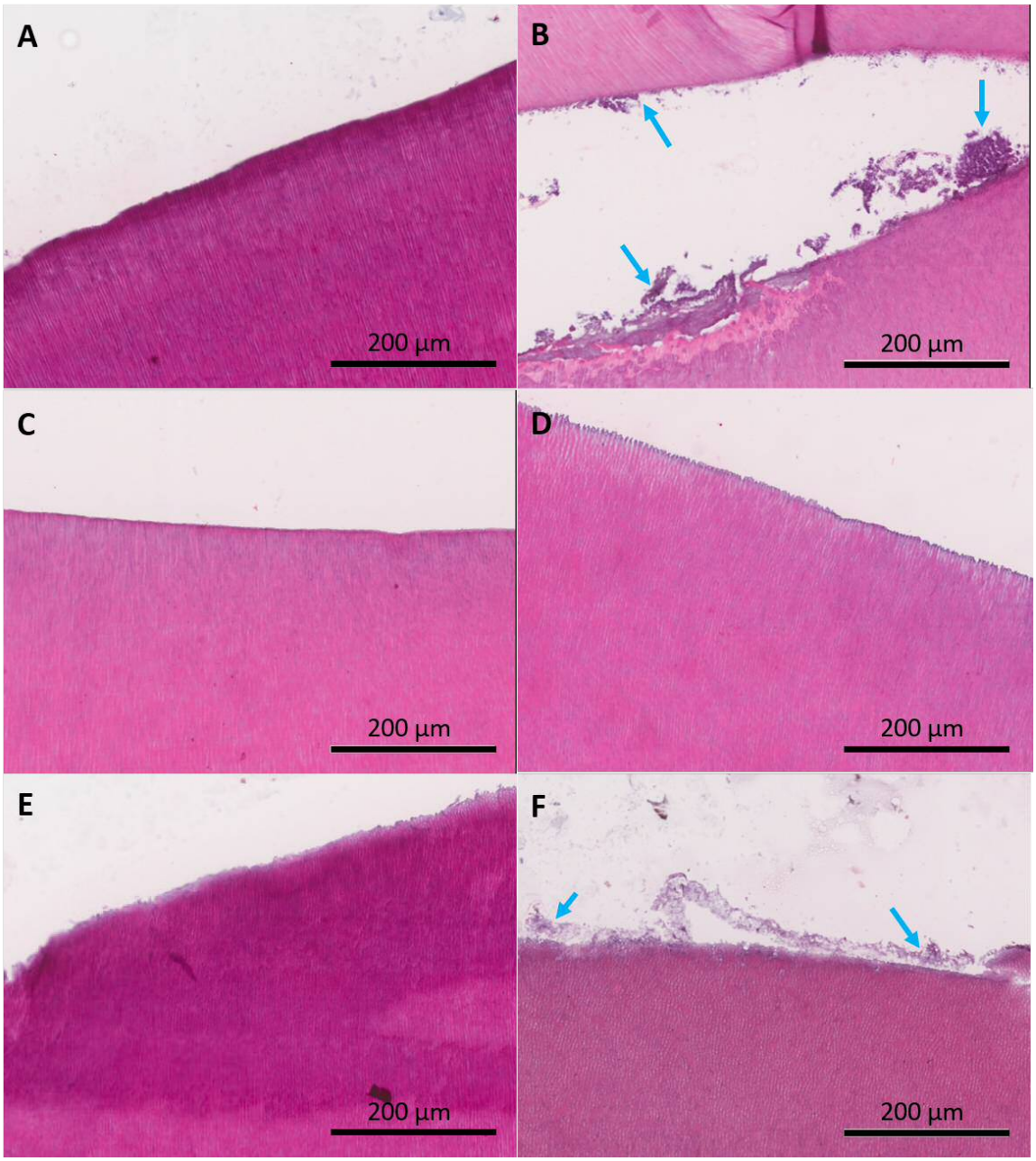

Figure 5.3: **H&E stained sections of human teeth treated with antimicrobial hydrogel.** Teeth were inoculated with *E. faecalis* suspension and then treated with: **A** BHI only (no initial bacterial inoculation); **B** BHI only (with initial bacterial inoculation); **C** triclosan solution (200 µg/mL in 1 % IPA); **D** triclosan liposomes (T300 MLVs); **E** triclosan liposomes in MC (T300 MLVs in 10 % w/w MC); **F** MC in H_2O. Teeth were fixed and sectioned and representative images are shown of root surface appearance after H&E staining (X20 magnification). Blue arrows indicate areas of possible biofilm formation (Section 5.3.3).

5.3.4 Histology sections: Gram-staining

Sections were treated with Gram stain, which stains Gram-positive bacteria purple (crystal violet), and Gram-negative bacteria and other structures pink (fuchsin). *E. faecalis* cells are Gram-positive cocci, as shown in Chapter 2, Figure 2.3.

Gram stains showed pink staining of dentine tissues, with dark purple staining suggesting the presence of Gram-positive bacteria along the dentine tubules (Figure 5.4A-F). All samples showed some positive staining from Gram-positive bacteria, including the tooth that was not inoculated with *E. faecalis* following sterilisation (Figure 5.4A). This suggests that the teeth contained residual bacterial infection prior to the experimental procedure. The tooth that was inoculated with *E. faecalis* and not treated showed material on the root surface containing Gram-positive staining that was consistent with the presence of a bacterial biofilm (Figure 5.4B). This was not as clearly present in other samples apart from the tooth treated with MC alone, which showed some evidence of biofilm presence on the root surface (Figure 5.4F).

Images of Gram-stained sections were taken at 100 X magnification in order to identify bacterial morphology in these sections (Figure 5.5). In the previously identified biofilms, evidence of Gram-positive cocci was seen: either as single cells, chains, or clusters. These are identified by blue arrows in Figure 5.5B and F. In all samples, some evidence of bacterial cocci, chains or clusters was observed in the dentine tubules (also denoted by blue arrows in Figure 5.5A-F), however these were not as clear.

Results of Gram stain imaging agreed with those of the H&E stain images and suggested the presence of a biofilm containing gram-positive cocci on the root surface of the tooth that was infected and left untreated as well as the tooth treated with MC in H_2O.

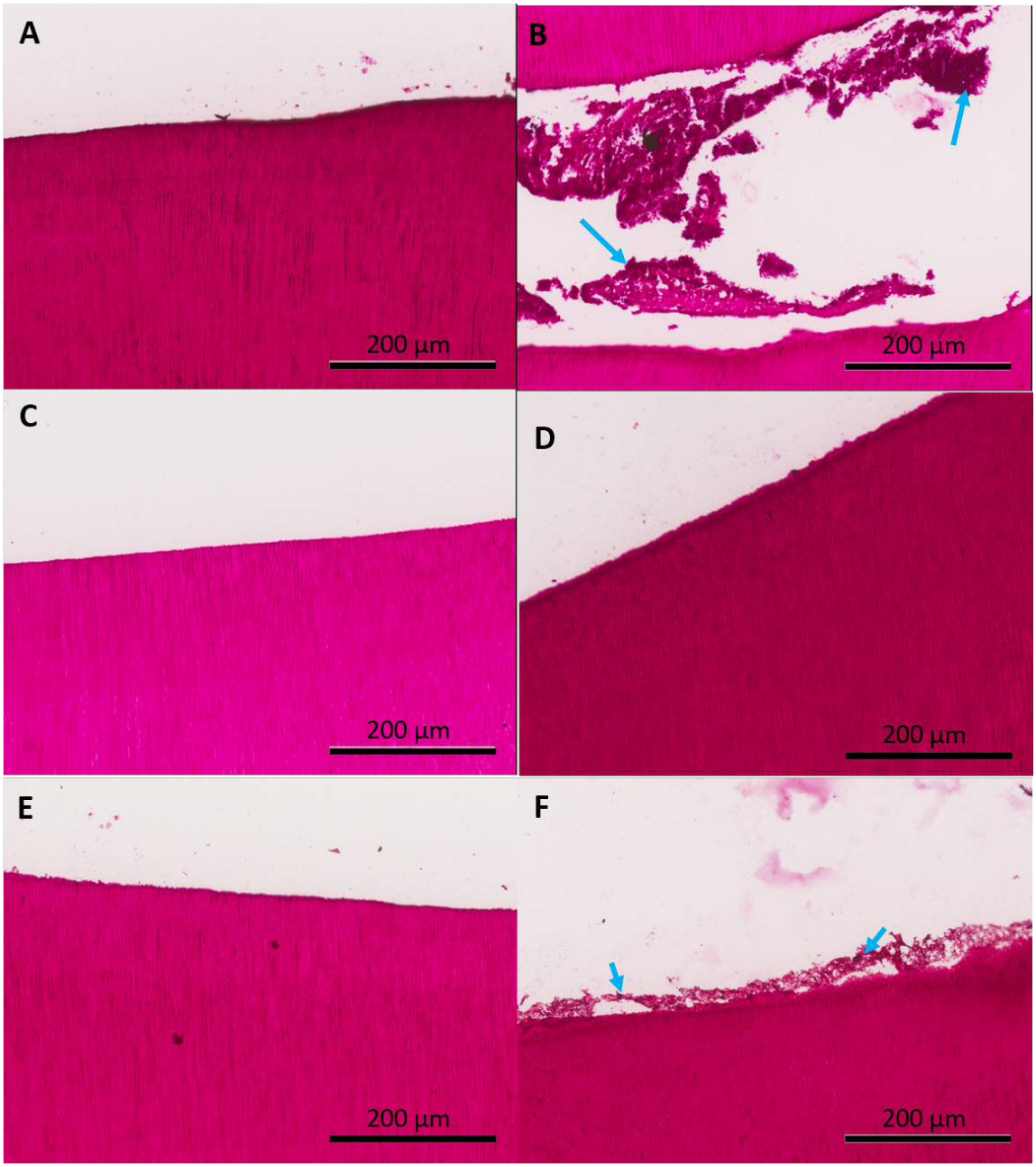

Figure 5.4: **Gram stained sections of human teeth treated with antimicrobial hydrogel.** Teeth were inoculated with *E. faecalis* suspension and then treated with: **A** BHI only (no initial bacterial inoculation); **B** BHI only (with initial bacterial inoculation); **C** triclosan solution (200 µg/mL in 1 % IPA); **D** triclosan liposomes (T300 MLVs); **E** triclosan liposomes in MC (T300 MLVs in 10 % w/w MC); **F** MC in H_2O. Teeth were fixed and sectioned and representative images are shown of root surface appearance after Gram-staining (X20 magnification). Black arrows indicate areas of possible biofilm formation (Section 5.3.4).

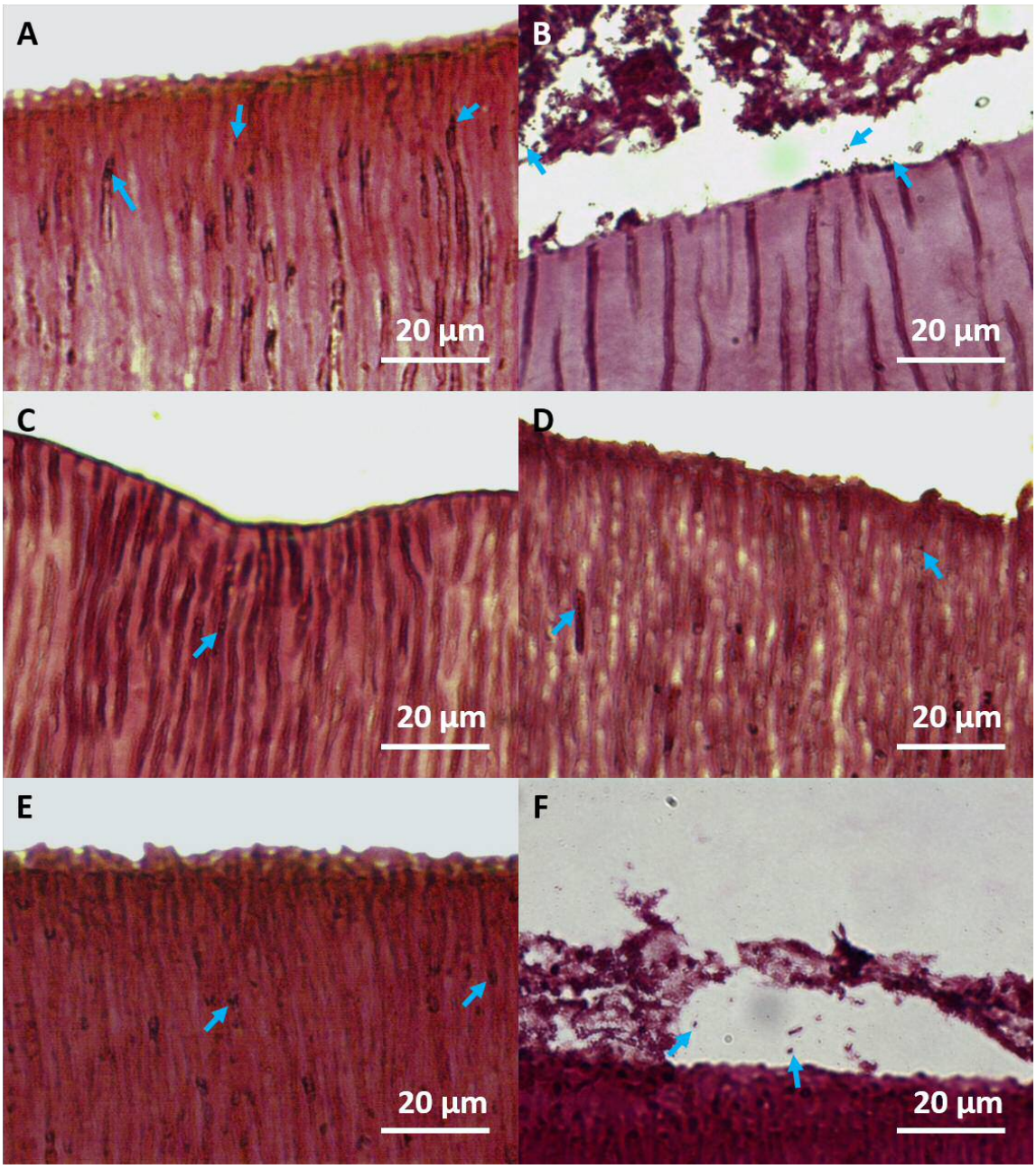

Figure 5.5: **Gram stained sections of human teeth treated with antimicrobial hydrogel.** Teeth were inoculated with *E. faecalis* suspension and then treated with: **A** BHI only (no initial bacterial inoculation); **B** BHI only (with initial bacterial inoculation); **C** triclosan solution (200 µg/mL in 1 % IPA); **D** triclosan liposomes (T300 MLVs); **E** triclosan liposomes in MC (T300 MLVs in 10 % w/w MC); **F** MC in H_2O. Teeth were fixed and sectioned and representative images are shown of root surface appearance after Gram-staining (X100 magnification). Blue arrows indicate possible single cells, chains or clusters of gram positive bacteria (Section 5.3.4).

5.4 Discussion

This preliminary experiment aimed to assess the efficacy of the previously developed MC hydrogel containing triclosan liposomes (T300 MLVs) in a clinically relevant setting. The data shown suggest that the hydrogel prevented the formation of a single-species *E. faecalis* biofilm on the intraroot surface of pre-infected human teeth. It is proposed that this is through the exposure of bacteria that has been introduced to the root canal to triclosan that has been released from the hydrogel, and has an inhibitory effect on further *E. faecalis* growth, as demonstrated in previous chapters. This prevention was also seen when triclosan solution and T300 MLV liposomal suspensions were used. Although triclosan solution and T300 MLV suspension showed prevention of *E. faecalis* growth, the use of a liquid would not be practical as a medicament as it would not be retained within the root canal due to potential leakage through the apical foramen (Bosch-Aranda *et al.*, 2012) and would be particularly difficult to apply to maxillary (upper) teeth as they would flow out through the coronal access due to gravity. Further investigation could be made, however, into their potential use as a root canal irrigant.

The efficacy of the T300 MLV in MC over 24 h is promising, however an intra-canal medicament would typically be placed for 14-28 days between appointments (Athanassiadis *et al.*, 2007). $Ca(OH)_2$ paste, which is the current gold standard, was shown by Bitter *et al.* (2017) to be bactericidal against *E. faecalis* after 7 days *ex vivo* culture in a canine root canal inoculated with the bacterium (i.e. no culturable bacteria were recovered from the root canal after this time). A similar study by Vivacqua-Gomes *et al.* (2005), however, showed that *E. faecalis* was recovered from 25 % of teeth that had been inoculated with the bacterium, endodontically prepared, and treated with $Ca(OH)_2$ for 14 days. It would therefore be advantageous to extend the incubation time with treatment to 7, 14 and 28 days to test the longer-term efficacy of the material.

The methodology used in this chapter allowed for the identification of Gram-positive bacteria in the dental root. If Gram-negative bacteria were to be investigated,

it would be preferable to reduce the level of background fuchsin staining by using a modified Gram stain such as the Brown and Brenn method, in order to counterstain the tissues against the bacteria (Dee Taylor, 1966). This method includes an additional picric acid/acetone wash, which results in a yellow counterstaining of tissues and a higher contrast against the pink or blue-stained bacteria.

One of the key disadvantages of many current endodontic disinfection methods and materials is the difficulty in accessing bacteria that reside in the dentine tubules (Wright and Walsh, 2017). In this study, bacteria appeared to be present in the dentine tubules of all samples, including the sterile control, suggesting a background level of contamination was present before the *in vitro* introduction of *E. faecalis* to the teeth. Although this contamination was eliminated by irradiation of the tooth before the experimental procedure, the analytical methodology used could not distinguish between live and dead bacteria. It was therefore not possible to differentiate between:

- background contamination, i.e. bacteria that was already present in the collected extracted tooth and then killed by irradiation prior to the experimental inoculation with *E. faecalis*,
- experimentally introduced *E. faecalis* that had colonised the dentine and remained alive even after treatment,
- experimentally introduced *E. faecalis* that had colonised the dentine and subsequently killed by the treatment.

It was not therefore possible to ascertain the material's efficacy in eliminating bacteria from dentine tubules using this methodology. Other methodology may preserve live bacteria, for example Azim *et al.* (2016) investigated the efficacy of root canal irrigation techniques by inoculating extracted tooth root canals with *E. faecalis* and, after administering the irrigation treatment, splitting the tooth in half longitudinally and then applying a live/dead fluorescent stain to be imaged using confocal microscopy. This technique distinguished between live and dead bacteria along the dentine tubules and allowed for an estimation of the penetration depth of

the administered antimicrobial irrigant. A similar methodology could be employed in the future to assess whether the gel not only prevents bacterial colonisation of the intraroot surface, but also kills bacteria residing in dentine tubules.

Although the rheological properties of the hydrogel have previously been characterised, it is unknown whether these properties are optimal for ensuring that the root canal is effectively filled upon injection, as discussed in Chapter 4, Section 4.4. The methodology used here did not keep the gel intact within the root in order to assess this: fixation and demineralisation processes were performed at ambient temperature, allowing for reversal of MC gelation and subsequent dilution out of the root canal. Future work aims to address this research question, which could be achieved by maintaining the tooth at 37 °C during the fixation process in order to preserve the hydrogel structure for histological analyses. Alternatively, a radio-opaque compound could be introduced to the gel in order to assess its filling efficacy by radiographic techniques. Simcock and Hicks (2006) obtained radiographic images of roots filled with $Ca(OH)_2$ using different filling techniques, which were assessed by independent examiners and scored (1-10) for filling quality. Additionally a comparison of the weight of $Ca(OH)_2$ in an "optimally filled" root compared to the weight in the experimentally filled roots gave quantitative data to assess filling efficacy, which correlated with the radiograph scores and confirmed that injection was the most effective delivery method. Jung *et al.* (2005) compared micro-computed tomography (micro-CT) 3D reconstructions to histological samples of root canals obturated with gutta-percha cones and concluded that there was a good correlation in results between the two techniques and that micro-CT could potentially be used to assess the filling efficacy of other materials.

Teeth were incubated at physiological temperature in 5 % CO_2 for this study and the root apex was submerged in BHI to allow bacteria access to a high-nutrient environment. *E. faecalis* forms biofilms with different properties, depending on whether conditions are aerobic or anaerobic, as well as the availability of nutrients to the bacteria (George *et al.*, 2005). It may be clinically more relevant to perform the experiment under anaerobic, low nutrient conditions, to mimic the biological setting

(Narayanan and Vaishnavi, 2010). This could be achieved by incubating the tooth in an anaerobic chamber and replacing the BHI with a lower-nutrient medium (e.g. by using buffered saline).

Experimental variation is introduced when using extracted teeth, as the individual root anatomy is inherently variable and an increase in anatomical complexity of the root canal system has been shown to correlate with the occurence of secondary endodontic infection, potentially due to the difficulty of root preparation (Vertucci, 2005). This was somewhat controlled for by the experimental design, as the teeth carried no residual infection after preparation, due to the irradiation of the samples prior to introducing *E. faecalis* culture. In addition, the use of extracted teeth allowed the clinician to adopt optimal working conditions for tooth preparation, and factors such as tooth position in the oral cavity and patient compliance were eliminated.

Dentine anatomy varies due to a number of factors including patient age and previous trauma, which will result in the presence of tertiary dentine that has anatomical differences to primary and secondary dentine (Chapter 1, Section 1.2.5.1). Tertiary, or sclerotic dentine with no tubules can physically impede bacterial colonisation of the dentine (Love, 2004). This may influence the degree of biofilm formation on the intraroot surface as well as the biomass of bacteria residing in dentine tubules following the initial inoculation and removal of non-adherent cells. These experiments would therefore need to be repeated before drawing firm conclusions from these data. The current results, however, provide promising evidence that the liposomal hydrogel has good efficacy against *E. faecalis* in an *ex vivo* model of endodontic infection.

5.5 Conclusions

These preliminary data suggest that MC hydrogel containg T300 MLV liposomes prevents the colonisation and biofilm formation of *E. faecalis* in pre-infected human root canals that have undergone endodontic preparation. Future work aims to assess the efficacy of the gel in the dentinal tubules as well as the filling efficacy of the gel in the intraroot space.

Chapter 6

General Summary and Future Direction

The aim of this project was to develop a material for antimicrobial drug delivery in the dental cavity. In particular, the target material was considered as an intracanal medicament for the prevention of secondary endodontic infection. Such materials are already used in the clinic, with $Ca(OH)_2$ being the most widely used intracanal medicament, however a proportion of endodontic treatments still fail due to secondary microbial infection. There was therefore a clinical need identified to improve upon the process of bacterial eradication from dental root canals. The proposed material comprised of three main components: triclosan, which is a hydrophobic, antimicrobial drug; liposomes composed of phosphatidylcholine and cholesterol, for the potential encapsualtion and delivery of the antimicrobial; and a methyl cellulose (MC) hydrogel to carry and deliver the drug-loaded liposomes in the dental root canal.

Triclosan was selected as a broad-spectrum antimicrobial that is already widely used in oral health products. Its efficacy against streptococci and *Enterecoccos* spp. has previously been reported by others, and was demonstrated in this work to have a concentration-dependent inhibitory and biocidal effect on clinical strains of *E. faecalis* and *S. anginosus* when grown planktonically or as a single-species biofilm. Liposomal drug encapsulation had been shown by others to mediate effective, prolonged drug delivery and enhanced drug potency in some cases (Lian and Ho, 2001; Samad *et al.*,

2007), so it was investigated whether it would be suitable to load the triclosan into an aqueous suspension of liposomes, and whether this showed any advantages over triclosan in solution. Triclosan retained its antimicrobial properties when incorporated into liposomes, and in some instances appeared effective at concentrations below the previously ascertained MIC (in the case of T300 SUVs). This suggests that liposomal encapsulation may increase drug potency of triclosan, which has also been reported by others: El-Zawawy *et al.* (2015) observed improved efficacy of triclosan liposomes *in vivo* against *Toxoplasma gondii* when compared to triclosan in solution.

Unlike triclosan in solution, liposomal triclosan efficacy was not solely dependent on the absolute triclosan concentration of the suspension. It was observed that the drug:lipid ratio of the liposomes may also play a role in the efficacy of the liposomes. This was achieved by increasing the initial amount of triclosan added to the liposome preparation, and it was found that a starting concentration of 300 µg/mL (T300) resulted in a high drug:lipid ratio compared to T50 and T100 liposomes, and that these T300 liposomes had the greatest antimicrobial effect. These data imply that liposomal triclosan delivery is not a passive process (i.e. with triclosan simply being released into the surrounding aqueous suspension) but an interactive process between the liposomes and bacterial cells. Two mechanisms of liposomal delivery to microbes have been proposed previously in the literature: either by fusion of liposomes to the bacterial cell wall/membrane and release of their contents directly to the bacterium; or by binding of the liposomes to the bacterium, serving as a "drug depot" that continuously releases the drug, resulting in a higher local concentration surrounding the bacterium compared to the absolute concentration of the system (Zhang *et al.*, 2010). Future work should aim to elucidate the mechanism by which triclosan liposomes deliver their cargo to the bacteria, potentially through electron microscopy, to assess co-localisation of the bacteria and the liposomes (Mugabe *et al.*, 2006), or through differential fluorescent labelling of the bacteria and liposomes in order to assess membrane fusion through fluorescence spectroscopy (Hoekstra *et al.*, 1984).

Incorporation of T300 and T500 triclosan liposomes into a MC hydrogel resulted in similar antimicrobial properties of the liposome suspensions, with slightly lower

efficacy. This could be related to the release properties of the MC hydrogel, which showed that only 20 % of triclosan was released from the gel over 24 h, meaning it is possible that the bacteria were exposed to a lower concentration of the drug during this time period. Gels containing triclosan alone did not result in any triclosan release. This was supported by the fact that triclosan in MC had no antimicrobial effect against *E. faecalis* and *S. anginosus*, despite the fact that the equivalent concentration was both bacteriostatic and bactericidal in solution. This suggests that liposome encapsulation is essential for allowing the release of triclosan from the gel. Triclosan solutions used for the initial antimicrobial assays (Chapter 2) contained 1 % IPA to facilitate triclosan dissolution. This was not included in the release assay, as it was preferable to have a direct comparison with liposomal triclosan, which is prepared only in water. The triclosan in MC prepared for the antimicrobial assays, however, did contain IPA, and an antimicrobial effect was still not observed, showing that solvent addition is not sufficient to obtain the same triclosan release and efficacy as liposomal encapsulation when considering delivery by a MC hydrogel.

Rheological analyses of MC solutions containing triclosan liposomes suggested that the physical properties may be desirable for injection in the root canal , however this was not directly assessed. Future work should demonstrate the depth of gel penetration into the root cavity and relate this to its rheological properties. Methods for such analyses include the incorporation of a dye into the gel so penetration can be viewed microscopically (Weis *et al.*, 2004) and microCT analysis (Swain and Xue, 2009). Qualitative analysis showed that incubation of human teeth following injection of the gel into the root canal resulted in a prevention of a biofilm growth of *E. faecalis*. This provides indirect evidence that the physical properties are sufficient to allow MC penetration into root canals and that the composite system has a potentially useful effect on bacterial activity on the intraroot surface. The capacity of the material to penetrate into dentine tubules was not assessed, nor was the antimicrobial activity against bacteria that may reside in these tubules. The same microscopy and contrast tomography methods would be applicable to assess this and this may contribute to an understanding of the optimal rheological properties required for effective root canal

medicament delivery, which are not currently available in the literature.

The two bacterial strains selected for antimicrobial testing in this work were chosen on the basis of applying the developed material to pulpal and endodontic infections, in which *S. anginosus* group bacteria and *E. faecalis* are widely implicated. *E. faecalis* was used in the human endodontic infection model as it is associated with cases of failed endodontic treatment and so the efficacy of this material against that particular species was considered important. Triclosan is a broad-spectrum antimicrobial, and so the hydrogel may be applicable to other oral clinical settings. Additionally, the gel was not tested on a vital pulp model of dental infection, and so this could be explored in order to assess the gel's potential application in vital pulp therapy and/or pulp capping. This could be done using previously developed pulpal infection models, which have already been used to determine the effect of free triclosan on *S. anginosus* infection of rat pulp cells (Roberts *et al.*, 2013c). Periodontitis is another plaque-related oral disease that results in the degradation of tissue surrounding the tooth exterior. Antimicrobial medicaments may be placed in periodontal "pockets", or voids between the tooth and the gingiva where periodontitis has occurred (Vyas *et al.*, 2000) and so the physical and antimicrobial properties of the gel could be assessed for this application with the potential to optimise the material properties for this alternative oral location.

In conclusion, a novel antimicrobial composite gel system was developed that showed promising results in the prevention of oral microbial infection, particularly in the case of *E. faecalis* infection in dental root canals. The further development and use of this material as an intracanal medicament may result in the reduction of secondary, progressive endodontic infections where *E. faecalis* is the main pathogen, thus reducing the need for additional and more complex treatment in some patients.

Bibliography

Adler-Moore, J. 1993. Ambisome targeting to fungal infections. *Bone Marrow Transplantation* 14, pp. S3–7.

Aguilar, P. and Linsuwanont, P. 2011. Vital pulp therapy in vital permanent teeth with cariously exposed pulp: a systematic review. *Journal of Endodontics* 37(5), pp. 581–587.

Allan, N. A., Walton, R. E. and Schaffer, M. 2001. Setting times for endodontic sealers under clinical usage and in vitro conditions. *Journal of Endodontics* 27(6), pp. 421–423.

Allen, P. and Whitworth, J. 2004. Endodontic considerations in the elderly. *Gerodontology* pp. 185–194.

Allen, T. M. and Cullis, P. R. 2004. Drug delivery systems: entering the mainstream. *Science* 303(5665), pp. 1818–1822.

Alves, F. R., Siqueira, J. F., Carmo, F. L., Santos, A. L., Peixoto, R. S., Rôças, I. N. and Rosado, A. S. 2009. Bacterial community profiling of cryogenically ground samples from the apical and coronal root segments of teeth with apical periodontitis. *Journal of Endodontics* 35(4), pp. 486–492.

Andreasen, J. O., Farik, B. and Munksgaard, E. C. 2002. Long-term calcium hydroxide as a root canal dressing may increase risk of root fracture. *Dental Traumatology* 18(3), pp. 134–137.

Angelova Volponi, A., Kawasaki, M. and Sharpe, P. 2013. Adult human gingival epithelial cells as a source for whole-tooth bioengineering. *Journal of Dental Research* 92(4), pp. 329–334.

Aramaki, K., Watanabe, Y., Takahashi, J., Tsuji, Y., Ogata, A. and Konno, Y. 2016. Charge boosting effect of cholesterol on cationic liposomes. *Colloids and Surfaces A: Physicochemical and Engineering Aspects* 506, pp. 732–738.

Ari, H., Erdemir, A. and Belli, S. 2004. Evaluation of the effect of endodontic irrigation solutions on the microhardness and the roughness of root canal dentin. *Journal of Endodontics* 30(11), pp. 792–795.

Asam, D. and Spellerberg, B. 2014. Molecular pathogenicity of streptococcus anginosus. *Molecular Oral Microbiology* 29(4), pp. 145–155.

Asgary, S., Eghbal, M. J., Ghoddusi, J. and Yazdani, S. 2013. One-year results of vital pulp therapy in permanent molars with irreversible pulpitis: an ongoing multicenter, randomized, non-inferiority clinical trial. *Clinical Oral Investigations* 17(2), pp. 431–439.

Athanassiadis, B., Abbott, P., George, N. and Walsh, L. 2009. An in vitro study of the antimicrobial activity of some endodontic medicaments and their bases using an agar well diffusion assay. *Australian Dental Journal* 54(2), pp. 141–146.

Athanassiadis, B., Abbott, P. and Walsh, L. J. 2007. The use of calcium hydroxide, antibiotics and biocides as antimicrobial medicaments in endodontics. *Australian Dental Journal* 52(s1).

Avilés-Reyes, A., Miller, J., Lemos, J. and Abranches, J. 2017. Collagen-binding proteins of streptococcus mutans and related streptococci. *Molecular Oral Microbiology* 32(2), pp. 89–106.

Azim, A. A., Aksel, H., Zhuang, T., Mashtare, T., Babu, J. P. and Huang, G. T.-J. 2016. Efficacy of 4 irrigation protocols in killing bacteria colonized in dentinal tubules examined by a novel confocal laser scanning microscope analysis. *Journal of Endodontics* 42(6), pp. 928–934.

Balakrishnan, B. and Jayakrishnan, A. 2005. Self-cross-linking biopolymers as injectable in situ forming biodegradable scaffolds. *Biomaterials* 26(18), pp. 3941–3951.

Bangham, A., Standish, M. and Watkins, J. 1965. Diffusion of univalent ions across the lamellae of swollen phospholipids. *Journal of Molecular Biology* 13(1), pp. 238–IN27.

Barclay, C., Spence, D. and Laird, W. 2005. Intra-oral temperatures during function. *Journal of Oral Rehabilitation* 32(12), pp. 886–894.

Barthel, C. R., Rosenkranz, B., Leuenberg, A. and Roulet, J.-F. 2000. Pulp capping of carious exposures: treatment outcome after 5 and 10 years: a retrospective study. *Journal of Endodontics* 26(9), pp. 525–528.

Basrani, B., Ghanem, A. and Tjäderhane, L. 2004. Physical and chemical properties of chlorhexidine and calcium hydroxide-containing medications. *Journal of Endodontics* 30(6), pp. 413–417.

Berger, N., Sachse, A., Bender, J., Schubert, R. and Brandl, M. 2001. Filter extrusion of liposomes using different devices: comparison of liposome size, encapsulation efficiency, and process characteristics. *International Journal of Pharmaceutics* 223(1), pp. 55–68.

Bernardo, M., Luis, H., Martin, M. D., Leroux, B. G., Rue, T., Leitão, J. and DeRouen, T. A. 2007. Survival and reasons for failure of amalgam versus composite posterior restorations placed in a randomized clinical trial. *The Journal of the American Dental Association* 138(6), pp. 775–783.

Bessa, P. C., Casal, M. and Reis, R. 2008. Bone morphogenetic proteins in tissue engineering: the road from laboratory to clinic, part ii (bmp delivery). *Journal of tissue engineering and regenerative medicine* 2(2-3), pp. 81–96.

Bitter, K., Vlassakidis, A., Niepel, M., Hoedke, D., Schulze, J., Neumann, K., Moter, A. and Noetzel, J. 2017. Effects of diode laser, gaseous ozone, and medical dressings on enterococcus faecalis biofilms in the root canal ex vivo. *BioMed Research International* 2017.

Bjørndal, L. 2001. Presence or absence of tertiary dentinogenesis in relation to caries progression. *Advances in Dental Research* 15, pp. 80–83.

Bosch-Aranda, M. L., Canalda-Sahli, C., Figueiredo, R. and Gay-Escoda, C. 2012. Complications following an accidental sodium hypochlorite extrusion: a report of two cases. *Journal of Clinical and Experimental Dentistry* 4(3), p. e194.

Boyar, R., Thylstrup, A., Holmen, L. and Bowden, G. 1989. The microflora associated with the development of initial enamel decalcification below orthodontic bands in vivo in children living in a fluoridated-water area. *Journal of Dental Research* 68(12), pp. 1734–1738.

Bozzuto, G. and Molinari, A. 2015. Liposomes as nanomedical devices. *International Journal of Nanomedicine* 10, pp. 975–99.

British Standards Institution. 2005. *BS EN 1040:2005: Chemical disinfectants and antiseptics Quantitative suspension test for the evaluation of basic bactericidal activity of chemical disinfectants and antiseptics Test method and requirements (phase 1)*. London: BSI.

Bulbake, U., Doppalapudi, S., Kommineni, N. and Khan, W. 2017. Liposomal formulations in clinical use: An updated review. *Pharmaceutics* 9(2), p. 12.

Burke, F. J. T. and Lucarotti, P. S. K. 2009. How long do direct restorations placed within the general dental services in England and Wales survive? *British Dental Journal* 206(1), p. E2.

Burke, F. J. T., Lucarotti, P. S. K. and Holder, R. L. 2005. Outcome of direct restorations placed within the general dental services in England and Wales (Part 2): variation by patients' characteristics. *Journal of Dentistry* 33(10), pp. 817–826.

Busscher, H., Cowan, M. and Van der Mei, H. 1992. On the relative importance of specific and non-specific approaches to oral microbial adhesion. *FEMS Microbiology Reviews* 8(3-4), pp. 199–209.

Camps, J. and Pashley, D. 2003. In vivo sensitivity of human root dentin to air blast and scratching. *Journal of Periodontology* 74(11), pp. 1589–1594.

Carrotte, P. 2004. Endodontics: Part 9 calcium hydroxide, root resorption, endo-perio lesions. *British Dental Journal* 197(12), pp. 735–743.

Cawson, R. A. and Odell, E. W. 2008. *Cawson's Essentials of Oral Pathology and Oral Medicine*. London: Elsevier Ltd, 8 ed.

Cern, A., Barenholz, Y., Tropsha, A. and Goldblum, A. 2014. Computer-aided design of liposomal drugs: in silico prediction and experimental validation of drug candidates for liposomal remote loading. *Journal of Controlled Release* 173, pp. 125–131.

Chávez de Paz, L. E. 2007. Redefining the persistent infection in root canals: possible role of biofilm communities. *Journal of Endodontics* 33(6), pp. 652–662.

Chávez de Paz, L. E. 2018. Aetiology of persistent endodontic infections in root-filled teeth. In: *Apical Periodontitis in Root-Filled Teeth*, Springer, pp. 21–32.

Chen, C., Han, D., Cai, C. and Tang, X. 2010. An overview of liposome lyophilization and its future potential. *Journal of Controlled Release* 142(3), pp. 299–311.

Chestnutt, I., Binnie, V. and Taylor, M. 2000. Reasons for tooth extraction in Scotland. *Journal of Dentistry* 28(4), pp. 295–297.

Chin, J., Thomas, M., Locke, M. and Dummer, P. 2016. A survey of dental practitioners in wales to evaluate the management of deep carious lesions with vital pulp therapy in permanent teeth. *British Dental Journal* 221(6), pp. 331–338.

Chugal, N., Wang, J.-K., Wang, R., He, X., Kang, M., Li, J., Zhou, X., Shi, W. and Lux, R. 2011. Molecular characterization of the microbial flora residing at the apical portion of infected root canals of human teeth. *Journal of Endodontics* 37(10), pp. 1359–1364.

Ciobanu, B. C., Cadinoiu, A. N., Popa, M., Desbrières, J. and Peptu, C. A. 2014. Modulated release from liposomes entrapped in chitosan/gelatin hydrogels. *Materials Science and Engineering: C* 43(0), pp. 383–391.

Cisar, J., Sandberg, A. and Mergenhagen, S. 1984. The function and distribution of different fimbriae on strains of actinomyces viscosus and actinomyces naeslundii. *Journal of Dental Research* 63(3), pp. 393–396.

Colombo, J. S., Moore, A. N., Hartgerink, J. D. and D'Souza, R. N. 2014. Scaffolds to control inflammation and facilitate dental pulp regeneration. *Journal of Endodontics* 40(4 Suppl), pp. S6–12.

Cooper, P. R., Takahashi, Y., Graham, L. W., Simon, S., Imazato, S. and Smith, A. J. 2010. Inflammation-regeneration interplay in the dentine-pulp complex. *Journal of Dentistry* 38(9), pp. 687–697.

Cope, A., Francis, N., Wood, F., Mann, M. K. and Chestnutt, I. G. 2014. Systemic antibiotics for symptomatic apical periodontitis and acute apical abscess in adults. *The Cochrane Database of Systematic Reviews* 26(6), p. CD010136.

Couve, E. 1986. Ultrastructural changes during the life cycle of human odontoblasts. *Archives of Oral Biology* 31(10), pp. 643–651.

Cullinan, M., Bird, P., Heng, N., West, M. and Seymour, G. 2014. No evidence of triclosan-resistant bacteria following long-term use of triclosan-containing toothpaste. *Journal of Periodontal Research* 49(2), pp. 220–225.

da Silva Ventura, T. M., Cassiano, L. d. P. S., de Souza e Silva, C. M., Taira, E. A., de Lima Leite, A., Rios, D. and Buzalaf, M. A. R. 2017. The proteomic profile of the acquired enamel pellicle according to its location in the dental arches. *Archives of Oral Biology* 79, pp. 20–29.

Davis, D., Fiske, J., Scott, B. and Radford, D. 2001. The emotional effects of tooth loss in a group of partially dentate people: a quantitative study. *The European Journal of Prosthodontics and Restorative Dentistry* 9(2), pp. 53–57.

De Kruijff, B., Cullis, P. and Radda, G. 1975. Differential scanning calorimetry and 31p nmr studies on sonicated and unsonicated phosphatidylcholine liposomes. *Biochimica et Biophysica Acta (BBA)-Biomembranes* 406(1), pp. 6–20.

Dee Taylor, R. 1966. Modification of the brown and brenn gram stain for the differential staining of gram-positive and gram-negative bacteria in tissue sections. *American Journal of Clinical Pathology* 46(4), pp. 472–474.

Delius, J., Trautmann, S., Médard, G., Kuster, B., Hannig, M. and Hofmann, T. 2017. Label-free quantitative proteome analysis of the surface-bound salivary pellicle. *Colloids and Surfaces B: Biointerfaces* 152, pp. 68–76.

Demarco, F. F., Collares, K., Coelho-de Souza, F. H., Correa, M. B., Cenci, M. S., Moraes, R. R. and Opdam, N. J. 2015. Anterior composite restorations: A systematic review on long-term survival and reasons for failure. *Dental Materials* 31(10), pp. 1214–1224.

Demel, R. A. and De Kruyff, B. 1976. The function of sterols in membranes. *Biochimica et Biophysica Acta (BBA)-Reviews on Biomembranes* 457(2), pp. 109–132.

Dibdin, G. and Shellis, R. 1988. Physical and biochemical studies of streptococcus mutans sediments suggest new factors linking the cariogenicity of plaque with its extracellular polysaccharide content. *Journal of Dental Research* 67(6), pp. 890–895.

Do, T., Devine, D. and Marsh, P. D. 2013. Oral biofilms: molecular analysis, challenges, and future prospects in dental diagnostics. *Clinical, Cosmetic and Investigational Dentistry* 5, p. 11.

Drury, W. J., Stewart, P. S. and Characklis, W. G. 1993. Transport of 1-μm latex particles in pseudomonas aeruginosa biofilms. *Biotechnology and Bioengineering* 42(1), pp. 111–117.

El-Zawawy, L. A., El-Said, D., Mossallam, S. F., Ramadan, H. S. and Younis, S. S. 2015. Triclosan and triclosan-loaded liposomal nanoparticles in the treatment of acute experimental toxoplasmosis. *Experimental Parasitology* 149, pp. 54–64.

Elliott Donaghue, I., Tator, C. H. and Shoichet, M. S. 2014. Sustained delivery of bioactive neurotrophin-3 to the injured spinal cord. *Biomater. Sci.* 3(1), pp. 65–72.

Er, K., Tasdemir, T., Siso, S. H., Celik, D. and Cora, S. 2011. Fracture resistance of retreated roots using different retreatment systems. *European Journal of Dentistry* 5(4), p. 387.

Essner, M. D., Javed, A. and Eleazer, P. D. 2011. Effect of sodium hypochlorite on human pulp cells: an in vitro study. *Oral Surgery, Oral Medicine, Oral Pathology, Oral Radiology, and Endodontology* 112(5), pp. 662–666.

Estrela, C., Bammann, L., Pimenta, F. and Pécora, J. 2001. Control of microorganisms in vitro by calcium hydroxide pastes. *International Endodontic Journal* 34(5), pp. 341–345.

Evans, L. V. 2003. *Biofilms: recent advances in their study and control*. CRC press.

Farac, R. V., Morgental, R. D., de Pontes Lima, R. K., Tiberio, D. and dos Santos, M. T. B. R. 2012. Pulp sensibility test in elderly patients. *Gerodontology* 29(2), pp. 135–139.

Featherstone, J. D. 2000. The science and practice of caries prevention. *Journal of the American Dental Association* 131(7), pp. 887–899.

Ferguson, J., Hatton, J. and Gillespie, M. J. 2002. Effectiveness of intracanal irrigants and medications against the yeast candida albicans. *Journal of Endodontics* 28(2), pp. 68–71.

Ferracane, J. L. 2013. Resin-based composite performance: are there some things we can't predict? *Dental Materials* 29(1), pp. 51–58.

Finkelman, R. D., Mohan, S., Jennings, J. C., Taylor, A. K., Jepsen, S. and Baylink, D. J. 1990. Quantitation of growth factors igf-i, sgf/igf-ii, and tgf-β in human dentin. *Journal of Bone and Mineral Research* 5(7), pp. 717–723.

Fisher, L. and Russell, R. 1993. The Isolation and Characterization of Milleri Group Streptococci from Dental Periapical Abscesses. *Journal of Dental Research* 72(8), pp. 1191–1193.

Fiske, J., Davis, D., Frances, C. and Gelbier, S. 1998. The emotional effects of tooth loss in edentulous people. *British Dental Journal* 184(2), pp. 90–93.

Fouad, A. and Acosta, A. 2001. Periapical lesion progression and cytokine expression in an lps hyporesponsive model. *International Endodontic Journal* 34(7), pp. 506–513.

Fox, L. T., Senia, E. S. and Zeagler, J. 1984. Another look at the odontoblast process. *Journal of Endodontics* 10(11), pp. 538–543.

Gallon, V., Chen, L., Yang, X. and Moradian-Oldak, J. 2013. Localization and quantitative co-localization of enamelin with amelogenin. *Journal of Structural Biology* 183(2), pp. 239–249.

Garcés-Ortíz, M., Ledesma-Montes, C. and Reyes-Gasga, J. 2015. Scanning electron microscopic study on the fibrillar structures within dentinal tubules of human dentin. *Journal of Endodontics* 41(9), pp. 1510–1514.

George, S., Kishen, A. and Song, P. 2005. The role of environmental changes on monospecies biofilm formation on root canal wall by enterococcus faecalis. *Journal of Endodontics* 31(12), pp. 867–872.

Goldberg, M. and Smith, A. J. 2004. Cells and extracellular matrices of dentin and pulp: a biological basis for repair and tissue engineering. *Critical Reviews in Oral Biology and Medicine* 15(1), pp. 13–27.

Gomes, B. P. F. A., Pinheiro, E. T., Gade-Neto, C. R., Sousa, E. L. R., Ferraz, C. C. R., Zaia, A. A., Teixeira, F. B. and Souza-Filho, F. J. 2004. Microbiological examination of infected dental root canals. *Oral Microbiology and Immunology* 19(2), pp. 71–76.

Grigoratos, D., Knowles, J., Ng, Y.-L. and Gulabivala, K. 2001. Effect of exposing dentine to sodium hypochlorite and calcium hydroxide on its flexural strength and elastic modulus. *International Endodontic Journal* 34(2), pp. 113–119.

Grijalvo, S., Mayr, J., Eritja, R. and Díaz, D. D. 2016. Biodegradable liposome-encapsulated hydrogels for biomedical applications: a marriage of convenience. *Biomaterials Science* 4(4), pp. 555–574.

Gronthos, S., Brahim, J., Li, W., Fisher, L., Cherman, N., Boyde, A., DenBesten, P., Robey, P. G. and Shi, S. 2002. Stem Cell Properties of Human Dental Pulp Stem Cells. *Journal of Dental Research* 81(8), pp. 531–535.

Gubernator, J. 2011. Active methods of drug loading into liposomes: recent strategies for stable drug entrapment and increased in vivo activity. *Expert opinion on drug delivery* 8(5), pp. 565–580.

Guillén, J., Bernabeu, A., Shapiro, S. and Villalaín, J. 2004. Location and orientation of Triclosan in phospholipid model membranes. *European Biophysics Journal* 33(5), pp. 448–453.

Gupta, D., Tator, C. H. and Shoichet, M. S. 2006. Fast-gelling injectable blend of hyaluronan and methylcellulose for intrathecal, localized delivery to the injured spinal cord. *Biomaterials* 27(11), pp. 2370–2379.

Gupta, P., Vermani, K. and Garg, S. 2002. Hydrogels: from controlled release to pH-responsive drug delivery. *Drug Discovery Today* 7(10), pp. 569–579.

Hahn, C.-L. and Liewehr, F. R. 2007. Innate immune responses of the dental pulp to caries. *Journal of Endodontics* 33(6), pp. 643–651.

Hallsworth, A., Robinson, C. and Weatherell, J. 1972. Mineral and magnesium distribution within the approximal carious lesion of dental enamel. *Caries Research* 6(2), pp. 156–168.

Han, G. Y., Park, S. H. and Yoon, T. C. 2001. Antimicrobial activity of $Ca(OH)_2$ containing pastes with Enterococcus faecalis in vitro. *Journal of endodontics* 27(5), pp. 328–32.

Hannig, M. and Joiner, A. 2006. The structure, function and properties of the acquired pellicle. In: *The Teeth and Their Environment*, Karger Publishers, vol. 19, pp. 29–64.

Haque, A. and Morris, E. R. 1993. Thermogelation of methylcellulose. part i: molecular structures and processes. *Carbohydrate Polymers* 22(3), pp. 161–173.

Hatano, K., Inoue, H., Kojo, T., Matsunaga, T., Tsujisawa, T., Uchiyama, C. and Uchida, Y. 1999. Effect of surface roughness on proliferation and alkaline phosphatase expression of rat calvarial cells cultured on polystyrene. *Bone* 25(4), pp. 439–445.

Heath, R., Rubin, J., Holland, D., Zhang, E., Snow, M. and Rock, C. 1999. Mechanism of triclosan inhibition of bacterial fatty acid synthesis. *The Journal of Biological Chemistry* 274(16), pp. 11110–11114.

Heath, R. J. and Rock, C. O. 2000. erratum: A triclosan-resistant bacterial enzyme. *Nature* 406(6798), p. 848.

Hernández-Caselles, T., Villalaín, J. and Gómez-Fernández, J. C. 1993. Influence of liposome charge and composition on their interaction with human blood serum proteins. *Molecular and Cellular Biochemistry* 120(2), pp. 119–126.

Hoare, T. R. and Kohane, D. S. 2008. Hydrogels in drug delivery: Progress and challenges. *Polymer* 49(8), pp. 1993–2007.

Hobbs, S. K., Monsky, W. L., Yuan, F., Roberts, W. G., Griffith, L., Torchilin, V. P. and Jain, R. K. 1998. Regulation of transport pathways in tumor vessels: role of tumor type and microenvironment. *Proceedings of the National Academy of Sciences* 95(8), pp. 4607–4612.

Hoekstra, D., De Boer, T., Klappe, K. and Wilschut, J. 1984. Fluorescence method for measuring the kinetics of fusion between biological membranes. *Biochemistry* 23(24), pp. 5675–5681.

Horiuchi, M., Washio, J., Mayanagi, H. and Takahashi, N. 2009. Transient acid-impairment of growth ability of oral Streptococcus, Actinomyces, and Lactobacillus: a possible ecological determinant in dental plaque. *Oral Microbiology and Immunology* 24(4), pp. 319–324.

Hoshino, E. 1985. Predominant obligate anaerobes in human carious dentin. *Journal of Dental Research* 64(10), pp. 1195–1198.

Hosseini, H., Li, Y., Kanellakis, P., Tay, C., Cao, A., Tipping, P., Bobik, A., Toh, B.-H. and Kyaw, T. 2015. Phosphatidylserine liposomes mimic apoptotic cells to attenuate atherosclerosis by expanding polyreactive igm producing b1a lymphocytes. *Cardiovascular Research* 106(3), pp. 443–452.

Iijima, M., Fan, D., Bromley, K. M., Sun, Z. and Moradian-Oldak, J. 2010. Tooth enamel proteins enamelin and amelogenin cooperate to regulate the growth morphology of octacalcium phosphate crystals. *Crystal Growth and Design* 10(11), pp. 4815–4822.

Ingebrigtsen, S. G., Didriksen, A., Johannessen, M., Škalko-Basnet, N. and Holsæter, A. M. 2017. Old drug, new wrapping- a possible comeback for chloramphenicol? *International Journal of Pharmaceutics* 526(1), pp. 538–546.

International Organisation of of Standardization. 2012. ISO 6876:2012(en) dentistry root canal sealing materials. Tech. rep., International Organization for Standardization, Geneva, Switzerland.

Iwu, C., MacFarlane, T. W., MacKenzie, D. and Stenhouse, D. 1990. The microbiology of periapical granulomas. *Oral Surgery, Oral Medicine, Oral Pathology* 69(4), pp. 502–505.

Jacobs, J. and Stobberingh, E. 1995. Hydrolytic enzymes of streptococcus anginosus, streptococcus constellatus and streptococcus intermedius in relation to infection. *European Journal of Clinical Microbiology and Infectious Diseases* 14(9), pp. 818–820.

James, A. W., LaChaud, G., Shen, J., Asatrian, G., Nguyen, V., Zhang, X., Ting, K. and Soo, C. 2016. A review of the clinical side effects of bone morphogenetic protein-2. *Tissue Engineering Part B: Reviews* 22(4), pp. 284–297.

Jatariu Cadinoiu, A. N., Popa, M., Curteanu, S. and Peptu, C. A. 2011. Covalent and ionic co-cross-linking: an original way to prepare chitosan-gelatin hydrogels for biomedical applications. *Journal of Biomedical Materials Research. Part A* 98(3), pp. 342–350.

Jenkinson, H., Terry, S., McNab, R. and Tannock, G. 1993. Inactivation of the gene encoding surface protein sspa in streptococcus gordonii dl1 affects cell interactions with human salivary agglutinin and oral actinomyces. *Infection and Immunity* 61(8), pp. 3199–3208.

Jenkinson, H. F. and Demuth, D. R. 1997. Structure, function and immunogenicity of streptococcal antigen i/ii polypeptides. *Molecular Microbiology* 23(2), pp. 183–190.

Johnston, M. J., Semple, S. C., Klimuk, S. K., Edwards, K., Eisenhardt, M. L., Leng, E. C., Karlsson, G., Yanko, D. and Cullis, P. R. 2006. Therapeutically optimized rates of drug release can be achieved by varying the drug-to-lipid ratio in liposomal vincristine formulations. *Biochimica et Biophysica Acta (BBA)-Biomembranes* 1758(1), pp. 55–64.

Jones, G. L., Muller, C., O'reilly, M. and Stickler, D. 2005. Effect of triclosan on the development of bacterial biofilms by urinary tract pathogens on urinary catheters. *Journal of antimicrobial chemotherapy* 57(2), pp. 266–272.

Jones, M. N., Kaszuba, M., Reboiras, M. D., Lyle, I. G., Hill, K. J., Song, Y.-H., Wilmot, S. W. and Creeth, J. E. 1994. The targeting of phospholipid liposomes to bacteria. *Biochimica et Biophysica Acta (BBA) - Biomembranes* 1196(1), pp. 57–64.

Jung, M., Lommel, D. and Klimek, J. 2005. The imaging of root canal obturation using micro-CT. *International Endodontic Journal* 38(9), pp. 617–626.

Kahm, M., Hasenbrink, G., Lichtenberg-Fraté, H., Ludwig, J. and Kschischo, M. 2010. Grofit : Fitting Biological Growth Curves with *R*. *Journal of Statistical Software* 33(7), pp. 1–21.

Keenan, J. V., Farman, A. G., Fedorowicz, Z. and Newton, J. T. 2006. A Cochrane systematic review finds no evidence to support the use of antibiotics for pain relief in irreversible pulpitis. *Journal of Endodontics* 32(2), pp. 87–92.

Kelly, P. and Smales, R. 2004. Long-term cost-effectiveness of single indirect restorations in selected dental practices. *British Dental Journal* 196(10), pp. 639–643.

Kent, L. W., Rahemtulla, F. and Michalek, S. M. 1999. Interleukin (il)-1 and porphyromonas gingivalis lipopolysaccharide stimulation of il-6 production by fibroblasts derived from healthy or periodontally diseased human gingival tissue. *Journal of Periodontology* 70(3), pp. 274–282.

Kidd, E. and Fejerskov, O. 2004. What Constitutes Dental Caries? Histopathology of Carious Enamel and Dentin Related to the Action of Cariogenic Biofilms. *Journal of Dental Research* 83(suppl 1), pp. C35–C38.

Kim, S. G. 2017. Biological molecules for the regeneration of the pulp-dentin complex. *Dental Clinics of North America* 61(1), pp. 127–141.

Klimuk, S. K., Semple, S. C., Scherrer, P. and Hope, M. J. 1999. Contact hypersensitivity: a simple model for the characterization of disease-site targeting by liposomes. *Biochimica et Biophysica Acta (BBA)-Biomembranes* 1417(2), pp. 191–201.

Knutsson, G., Jontell, M. and Bergenholtz, G. 1994. Determination of plasma proteins in dentinal fluid from cavities prepared in healthy young human teeth. *Archives of Oral Biology* 39(3), pp. 185–190.

Knyght, I., Clifton, L., Saaka, Y., Lawrence, M. J. and Barlow, D. J. 2016. Interaction of the Antimicrobial Peptides Rhesus θ-Defensin and Porcine Protegrin-1 with Anionic Phospholipid Monolayers. *Langmuir* 32(29), pp. 7403–7410.

Koburger, T., Hübner, N.-O., Braun, M., Siebert, J. and Kramer, A. 2010. Standardized comparison of antiseptic efficacy of triclosan, pvp–iodine, octenidine dihydrochloride, polyhexanide and chlorhexidine digluconate. *Journal of Antimicrobial Chemotherapy* 65(8), pp. 1712–1719.

Kolenbrander, P. E., Andersen, R. N., Blehert, D. S., Egland, P. G., Foster, J. S. and Palmer, R. J. 2002. Communication among Oral Bacteria. *Microbiology and Molecular Biology Reviews* 66(3), pp. 486–505.

Kolenbrander, P. E., Palmer, R. J., Rickard, A. H., Jakubovics, N. S., Chalmers, N. I. and Diaz, P. I. 2006. Bacterial interactions and successions during plaque development. *Periodontology 2000* 42(1), pp. 47–79.

Kopperud, S. E., Tveit, A. B., Gaarden, T., Sandvik, L. and Espelid, I. 2012. Longevity of posterior dental restorations and reasons for failure. *European Journal of Oral Sciences* 120(6), pp. 539–548.

Lacruz, R. S., Habelitz, S., Wright, J. T. and Paine, M. L. 2017. Dental enamel formation and implications for oral health and disease. *Physiological Reviews* 97(3), pp. 939–993.

Lamothe, M. 1990. Streptococcus milleri an important but unappreciated pathogen. *Infectious Diseases Newsletter* 9(7), pp. 52–55.

Lasic, D. D. and Barenholz, Y. 1996. *Handbook of nonmedical applications of liposomes: Theory and basic sciences*, vol. 1. CRC Press.

Ledder, R., Gilbert, P., Willis, C. and McBain, A. 2006. Effects of chronic triclosan exposure upon the antimicrobial susceptibility of 40 ex-situ environmental and human isolates. *Journal of Applied Microbiology* 100(5), pp. 1132–1140.

Lee, D.-Y., Spångberg, L. S., Bok, Y.-B., Lee, C.-Y. and Kum, K.-Y. 2005a. The sustaining effect of three polymers on the release of chlorhexidine from a controlled release drug device for root canal disinfection. *Oral Surgery, Oral Medicine, Oral Pathology, Oral Radiology, and Endodontology* 100(1), pp. 105–111.

Lee, S.-C., Lee, K.-E., Kim, J.-J. and Lim, S.-H. 2005b. The effect of cholesterol in the liposome bilayer on the stabilization of incorporated retinol. *Journal of Liposome Research* 15(3-4), pp. 157–166.

Leme, A. P., Koo, H., Bellato, C., Bedi, G. and Cury, J. 2006. The role of sucrose in cariogenic dental biofilm formationnew insight. *Journal of dental research* 85(10), pp. 878–887.

Li, J., Helmerhorst, E. J., Leone, C. W., Troxler, R. F., Yaskell, T., Haffajee, A. D., Socransky, S. S. and Oppenheim, F. G. 2004. Identification of early microbial colonizers in human dental biofilm. *Journal of Applied Microbiology* 97(6), pp. 1311–1318.

Li, J. and Mooney, D. J. 2016. Designing hydrogels for controlled drug delivery. *Nature Reviews Materials* 1, p. 16071.

Li, L., Thangamathesvaran, P. M., Yue, C. Y., Tam, K. C., Hu, X. and Lam, Y. C. 2001. Gel Network Structure of Methylcellulose in Water. *Langmuir* 17(26), pp. 8062–8068.

Lian, T. and Ho, R. J. 2001. Trends and developments in liposome drug delivery systems. *Journal of Pharmaceutical Sciences* 90(6), pp. 667–680.

liana Eli, Bar-Tat, Y. and Kostovetzki, I. 2001. At First Glance: Social Meanings of Dental Appearance. *Journal of Public Health Dentistry* 61(3), pp. 150–154.

Liu, D.-Z., Chen, W.-Y., Tasi, L.-M. and Yang, S.-P. 2000. Microcalorimetric and shear studies on the effects of cholesterol on the physical stability of lipid vesicles. *Colloids and Surfaces A: Physicochemical and Engineering Aspects* 172(1), pp. 57–67.

Lodi, G., Figini, L., Sardella, A., Carrassi, A., Del Fabbro, M. and Furness, S. 2012. Antibiotics to prevent complications following tooth extractions. *The Cochrane Database of Systematic Reviews* 11, p. CD003811.

Love, R. M. 2004. Invasion of dentinal tubules by root canal bacteria. *Endodontic Topics* 9(1), pp. 52–65.

Lucarotti, P. S. K., Lessani, M., Lumley, P. J. and Burke, F. J. T. 2014. Influence of root canal fillings on longevity of direct and indirect restorations placed within the General Dental Services in England and Wales. *British Dental Journal* 216(6), p. E14.

Lynch, C. D. and Wilson, N. H. F. 2013. Managing the phase-down of amalgam: part II. Implications for practising arrangements and lessons from Norway. *British Dental Journal* 215(4), pp. 159–162.

Maestrelli, F., González-Rodríguez, M. L., Rabasco, A. M. and Mura, P. 2006. Effect of preparation technique on the properties of liposomes encapsulating ketoprofen–cyclodextrin complexes aimed for transdermal delivery. *International Journal of Pharmaceutics* 312(1), pp. 53–60.

Malam, Y., Loizidou, M. and Seifalian, A. M. 2009. Liposomes and nanoparticles: nanosized vehicles for drug delivery in cancer. *Trends in Pharmacological Sciences* 30(11), pp. 592–599.

Manhart, J., Chen, H., Hamm, G. and Hickel, R. 2004. Review of the clinical survival of direct and indirect restorations in posterior teeth of the permanent dentition. *Operative Dentistry-University of Washington* 29, pp. 481–508.

Mannocci, F. and Cowie, J. 2014. Restoration of endodontically treated teeth. *British Dental Journal* 216(6), p. 341.

Mao, Y., Li, X., Chen, G. and Wang, S. 2016. Thermosensitive hydrogel system with paclitaxel liposomes used in localized drug delivery system for in situ treatment of tumor: better antitumor efficacy and lower toxicity. *Journal of pharmaceutical sciences* 105(1), pp. 194–204.

Marcenes, W., Kassebaum, N., Bernab, E., Flaxman, A., Naghavi, M., Lopez, A. and Murray, C. 2013. Global burden of oral conditions in 1990-2010. *Journal of Dental Research* 92(7), pp. 592–597.

Marsh, P. and Bradshaw, D. 1995. Dental plaque as a biofilm. *Journal of Industrial Microbiology* 15(3), pp. 169–175.

Marsh, P. and Zaura, E. 2017. Dental biofilm: ecological interactions in health and disease. *Journal of Clinical Periodontology* 44(S18).

Marsh, P. D. 1994. Microbial ecology of dental plaque and its significance in health and disease. *Advances in Dental Research* 8(2), pp. 263–271.

Marsh, P. D. 2010. Controlling the oral biofilm with antimicrobials. *Journal of Dentistry* 38(Suppl 1), pp. S11–15.

Marshall, G. W., Marshall, S. J., Kinney, J. H. and Balooch, M. 1997. The dentin substrate: structure and properties related to bonding. *Journal of dentistry* 25(6), pp. 441–458.

Martin, F. E., Nadkarni, M. A., Jacques, N. A. and Hunter, N. 2002. Quantitative microbiological study of human carious dentine by culture and real-time pcr: Association of anaerobes with histopathological changes in chronic pulpitis. *Journal of Clinical Microbiology* 40(5), pp. 1698–1704.

McDonnell, G., Klein, D., Haines, K. and Pretzer, D. 1998. The importance of neutralization in the evaluation of triclosan-containing products. *Journal of Industrial Microbiology and Biotechnology* 21(4), pp. 184–186.

McKenzie, M., Betts, D., Suh, A., Bui, K., Kim, L. D. and Cho, H. 2015. Hydrogel-based drug delivery systems for poorly water-soluble drugs. *Molecules* 20(11), pp. 20397–20408.

Mejàre, I. A., Axelsson, S., Davidson, T., Frisk, F., Hakeberg, M., Kvist, T., Norlund, A., Petersson, A., Portenier, I., Sandberg, H., Tranaeus, S. and Bergenholtz, G. 2012. Diagnosis of the condition of the dental pulp: a systematic review. *International Endodontic Journal* 45(7), pp. 597–613.

Michaelson, P. and Holland, G. 2002. Is pulpitis painful? *International Endodontic Journal* 35(10), pp. 829–832.

Min, K.-S., Kwon, Y.-Y., Lee, H.-J., Lee, S.-K., Kang, K.-H., Lee, S.-K. and Kim, E.-C. 2006. Effects of proinflammatory cytokines on the expression of mineralization markers and heme oxygenase-1 in human pulp cells. *Journal of Endodontics* 32(1), pp. 39–43.

Mirucki, C. S., Abedi, M., Jiang, J., Zhu, Q., Wang, Y.-H., Safavi, K. E., Clark, R. B. and Nichols, F. C. 2014. Biologic activity of porphyromonas endodontalis complex lipids. *Journal of Endodontics* 40(9), pp. 1342–1348.

Mohammadi, Z. and Dummer, P. M. H. 2011. Properties and applications of calcium hydroxide in endodontics and dental traumatology. *International Endodontic Journal* 44(8), pp. 697–730.

Mohammadi, Z., Shalavi, S. and Yazdizadeh, M. 2012. Antimicrobial activity of calcium hydroxide in endodontics: A review. *Chonnam Medical Journal* 48(3), p. 133.

Mohammed, A., Weston, N., Coombes, A., Fitzgerald, M. and Perrie, Y. 2004. Liposome formulation of poorly water soluble drugs: optimisation of drug loading and esem analysis of stability. *International Journal of Pharmaceutics* 285(1), pp. 23–34.

Morris, E., Cutler, A., Ross-Murphy, S., Rees, D. and Price, J. 1981. Concentration and shear rate dependence of viscosity in random coil polysaccharide solutions. *Carbohydrate Polymers* 1(1), pp. 5–21.

Morrissey, I., Oggioni, M. R., Knight, D., Curiao, T., Coque, T., Kalkanci, A., Martinez, J. L., Consortium, B. *et al.* 2014. Evaluation of epidemiological cut-off values indicates that biocide resistant subpopulations are uncommon in natural isolates of clinically-relevant microorganisms. *PLoS One* 9(1), p. e86669.

Mourtas, S., Aggelopoulos, C. A., Klepetsanis, P., Tsakiroglou, C. D. and Antimisiaris, S. G. 2009. Complex hydrogel systems composed of polymers, liposomes, and cyclodextrins: implications of composition on rheological properties and aging. *Langmuir* 25(15), pp. 8480–8488.

Mourtas, S., Haikou, M., Theodoropoulou, M., Tsakiroglou, C. and Antimisiaris, S. G. 2008. The effect of added liposomes on the rheological properties of a hydrogel: A systematic study. *Journal of Colloid and Interface Science* 317(2), pp. 611–619.

Mugabe, C., Halwani, M., Azghani, A. O., Lafrenie, R. M. and Omri, A. 2006. Mechanism of enhanced activity of liposome-entrapped aminoglycosides against resistant strains of pseudomonas aeruginosa. *Antimicrobial Agents and Chemotherapy* 50(6), pp. 2016–2022.

Nagaoka, S., Tokuda, M., Sakuta, T., Taketoshi, Y., Tamura, M., Takada, H. and Kawagoe, M. 1996. Interleukin-8 gene expression by human dental pulp fibroblast in cultures stimulated with prevotella intermedia lipopolysaccharide. *Journal of Endodontics* 22(1), pp. 9–12.

Nair, P. R. 1987. Light and electron microscopic studies of root canal flora and periapical lesions. *Journal of Endodontics* 13(1), pp. 29–39.

Nanci, A. 2013. *Ten Cate's Oral Histology: Development, Structure and Function*. Elsevier Health Sciences, 8 ed.

Narayanan, L. L. and Vaishnavi, C. 2010. Endodontic microbiology. *Journal of Conservative Dentistry* 13(4), p. 233.

National Center for Biotechnology Information. 2005. *Triclosan*, [Online].

Nedeljkovic, I., Teughels, W., Munck, J. D., Meerbeek, B. V. and Landuyt, K. L. V. 2015. Is secondary caries with composites a material-based problem? *Dental Materials* 31(11), pp. e247–e277.

Nguyen, S., Hiorth, M., Rykke, M. and Smistad, G. 2011. The potential of liposomes as dental drug delivery systems. *European Journal of Pharmaceutics and Biopharmaceutics* 77(1), pp. 75–83.

Nudera, W. J., Fayad, M. I., Johnson, B. R., Zhu, M., Wenckus, C. S., BeGole, E. A. and Wu, C. D. 2007a. Antimicrobial Effect of Triclosan and Triclosan with Gantrez on Five Common Endodontic Pathogens. *Journal of Endodontics* 33(10), pp. 1239–1242.

Nudera, W. J., Fayad, M. I., Johnson, B. R., Zhu, M., Wenckus, C. S., BeGole, E. A. and Wu, C. D. 2007b. Antimicrobial effect of triclosan and triclosan with gantrez on five common endodontic pathogens. *Journal of Endodontics* 33(10), pp. 1239–1242.

Nyvad, B. and Kilian, M. 1987. Microbiology of the early colonization of human enamel and root surfaces in vivo. *Scandinavian Journal of Dental Research* 95(5), pp. 369–80.

Omidian, H. and Park, K. 2012. Hydrogels. In: Siepmann, J., Siegel, R. and Rathbone, M., eds., *Fundamentals and Applications of Controlled Release Drug Delivery*, New York: Springer, chap. 4, pp. 75–106.

Ota-Tsuzuki, C. and Mayer, M. P. A. 2010. Collagenase production and hemolytic activity related to 16s rrna variability among parvimonas micra oral isolates. *Anaerobe* 16(1), pp. 38–42.

Papahadjopoulos, D. and Watkins, J. 1967. Phospholipid model membranes. ii. permeability properties of hydrated liquid crystals. *BBA - Biomembranes* 135(4), pp. 639–652.

Park, S. N., Lee, M. H., Kim, S. J. and Yu, E. R. 2013. Preparation of quercetin and rutin-loaded ceramide liposomes and drug-releasing effect in liposome-in-hydrogel complex system. *Biochemical and Biophysical Research Communications* 435(3), pp. 361–366.

Pashley, D. H., Nelson, R. and Pashley, E. L. 1981. In vivo fluid movement across dentine in the dog. *Archives of Oral Biology* 26(9), pp. 707–710.

Patil, Y. P. and Jadhav, S. 2014. Novel methods for liposome preparation. *Chemistry and Physics of Lipids* 177, pp. 8–18.

Paula-Silva, F. W. G., Ghosh, A., Silva, L. A. B. and Kapila, Y. L. 2009. TNF-alpha promotes an odontoblastic phenotype in dental pulp cells. *Journal of Dental Research* 88(4), pp. 339–344.

Peppas, N., Bures, P., Leobandung, W. and Ichikawa, H. 2000. Hydrogels in pharmaceutical formulations. *European Journal of Pharmaceutics and Biopharmaceutics* 50(1), pp. 27–46.

Pinheiro, E., Gomes, B., Ferraz, C., Sousa, E., Teixeira, F., Souza-Filho, F. *et al.* 2003. Microorganisms from canals of root-filled teeth with periapical lesions. *International Endodontic Journal* 36(1), pp. 1–11.

Pladisai, P., Ampornaramveth, R. S. and Chivatxaranukul, P. 2016. Effectiveness of different disinfection protocols on the reduction of bacteria in enterococcus faecalis biofilm in teeth with large root canals. *Journal of Endodontics* 42(3), pp. 460–464.

Portenier, I., Waltimo, T. M. and Haapasalo, M. 2003. Enterococcus faecalis–the root canal survivor and starin post-treatment disease. *Endodontic Topics* 6(1), pp. 135–159.

Prasanth, M. and Capoor, A. K. 2013. Antimicrobial effect of mouthwashes: An in vitro study. *Research Journal of Pharmacy and Technology* 6(6), pp. 662–668.

Public Health England. 2014. UK standards for microbiology investigations: Identification of streptococcus species, enterococcus species and morphologically similar organisms. Tech. rep., Standards Unit, Microbiology Services, Public Health England.

R Core Team. 2013. *R: A Language and Environment for Statistical Computing*. R Foundation for Statistical Computing, Vienna, Austria.

Rasines Alcaraz, M. G., Veitz-Keenan, A., Sahrmann, P., Schmidlin, P. R., Davis, D. and Iheozor-Ejiofor, Z. 2014. Direct composite resin fillings versus amalgam fillings for permanent or adult posterior teeth. *The Cochrane Database of Systematic Reviews* 3, p. CD005620.

Richards, W., Ameen, J., Coll, A. M. and Higgs, G. 2005. Reasons for tooth extraction in four general dental practices in South Wales. *British Dental Journal* 198(5), pp. 275–8.

Ricucci, D., Loghin, S., Lin, L. M., Spångberg, L. S. and Tay, F. R. 2014. Is hard tissue formation in the dental pulp after the death of the primary odontoblasts a regenerative or a reparative process? *Journal of Dentistry* 42(9), pp. 1156–1170.

Riley, P. and Lamont, T. 2013. Triclosan/copolymer containing toothpastes for oral health. *Cochrane Database Syst Rev* 12.

Roberts, J., Lynch, C., Marsh, L., Denyer, S., Maillard, J. and Sloan, A. 2013a. Antimicrobial control of streptococcus anginosus infection in an ex vivo model. *Journal of Dental Research* 92(Special Issue A), p. 1349.

Roberts, J., Natarjan, M., Marsh, L., Denyer, S., Maillard, J., Lynch, C. and Sloan, A. 2013b. Triclosan activity against pulpal pathogens in an ex-vivo model. Presented at British Society for Oral and Dental Research 2013, Bath, United Kingdom: abstract number 0086.

Roberts, J. L., Maillard, J.-Y., Waddington, R. J., Denyer, S. P., Lynch, C. D. and Sloan, A. J. 2013c. Development of an ex vivo coculture system to model pulpal infection by streptococcus anginosus group bacteria. *Journal of Endodontics* 39(1), pp. 49–56.

Robertson, D. and Smith, A. J. 2009. The microbiology of the acute dental abscess. *Journal of Medical Microbiology* 58(2), pp. 155–162.

Robinson, A. M., Bannister, M., Creeth, J. E. and Jones, M. N. 2001a. The interaction of phospholipid liposomes with mixed bacterial biofilms and their use in the delivery of bactericide. *Colloids and Surfaces A: Physicochemical and Engineering Aspects* 1(186), pp. 43–53.

Robinson, A. M., Bannister, M., Creeth, J. E. and Jones, M. N. 2001b. The interaction of phospholipid liposomes with mixed bacterial biofilms and their use in the delivery of bactericide. *Colloids and Surfaces A: Physicochemical and Engineering Aspects* 186(1-2), pp. 43–53.

Rôças, I. N., Lima, K. C., Assunção, I. V., Gomes, P. N., Bracks, I. V. and Siqueira, J. F. 2015. Advanced caries microbiota in teeth with irreversible pulpitis. *Journal of Endodontics* 41(9), pp. 1450–1455.

Rôças, I. N. and Siqueira, J. F. 2011. In vivo antimicrobial effects of endodontic treatment procedures as assessed by molecular microbiologic techniques. *Journal of Endodontics* 37(3), pp. 304–310.

Rôças, I. N., Siqueira, J. F. and Santos, K. R. 2004. Association of enterococcus faecalis with different forms of periradicular diseases. *Journal of Endodontics* 30(5), pp. 315–320.

Ruel-Gariépy, E., Leclair, G., Hildgen, P., Gupta, A. and Leroux, J.-C. 2002. Thermosensitive chitosan-based hydrogel containing liposomes for the delivery of hydrophilic molecules. *Journal of Controlled Release* 82(2-3), pp. 373–383.

Russell, A. D. 2004. Whither triclosan? *Journal of Antimicrobial Chemotherapy* 53(5), pp. 693–695.

Rutherford, R. B. and Gu, K. 2000. Treatment of inflamed ferret dental pulps with recombinant bone morphogenetic protein-7. *European Journal of Oral Sciences* 108(3), pp. 202–206.

Saintrain, M. V. d. L. and de Souza, E. H. A. 2012. Impact of tooth loss on the quality of life. *Gerodontology* 29(2), pp. e632–e636.

Samad, A., Sultana, Y. and Aqil, M. 2007. Liposomal drug delivery systems: an update review. *Current Drug Delivery* 4(4), pp. 297–305.

Sasaki, H. and Stashenko, P. 2012. Interrelationship of the pulp and apical periodontitis. In: Hargreaves, K. M., Goodis, H. E., Tay, F. R. *et al.*, eds., *Seltzer and Benders Dental Pulp, Second Ed.*, Chicago, IL: Quintessence Publishing, pp. 277–299.

Schilke, R., Lisson, J. A., Bauß, O. and Geurtsen, W. 2000. Comparison of the number and diameter of dentinal tubules in human and bovine dentine by scanning electron microscopic investigation. *Archives of Oral Biology* 45(5), pp. 355–361.

Scientific Committee on Consumer Safety. 2010. Opinion on triclosan (antimicrobial resistance) european commission. Tech. rep., SCCS.

Sedgley, C., Buck, G. and Appelbe, O. 2006. Prevalence of enterococcus faecalis at multiple oral sites in endodontic patients using culture and pcr. *Journal of Endodontics* 32(2), pp. 104–109.

Seelig, J. 1978. 31p nuclear magnetic resonance and the head group structure of phospholipids in membranes. *Biochimica et Biophysica Acta (BBA)-Reviews on Biomembranes* 515(2), pp. 105–140.

Selwitz, R. H., Ismail, A. I. and Pitts, N. B. 2007. Dental caries. *The Lancet* 369(9555), pp. 51–59.

Sessa, G. and Weissmann, G. 1968. Phospholipid spherules (liposomes) as a model for biological membranes. *J. Lipid Res.* 9(3), pp. 310–318.

Shibata, S., Nagata, K., Nakamura, R., Tsunemitsu, A. and Misaki, A. 1980. Interaction of parotid saliva basic glycoprotein with streptococcus sanguis atcc 10557. *Journal of periodontology* 51(9), pp. 499–504.

Shweta, S. 2013. Dental abscess: A microbiological review. *Dental Research Journal* 10(5), p. 585.

Sigma. 1997. *Product Information Sheet: Methyl Cellulose*, [Online].

Simcock, R. M. and Hicks, M. L. 2006. Delivery of calcium hydroxide: comparison of four filling techniques. *Journal of Endodontics* 32(7), pp. 680–682.

Simon, S., Smith, A., Lumley, P., Berdal, A., Smith, G., Finney, S. and Cooper, P. 2009. Molecular characterization of young and mature odontoblasts. *Bone* 45(4), pp. 693–703.

Simon, S., Smith, A. J., Berdal, A., Lumley, P. J. and Cooper, P. R. 2010. The map kinase pathway is involved in odontoblast stimulation via p38 phosphorylation. *Journal of Endodontics* 36(2), pp. 256–259.

Simón-Soro, Á., Guillén-Navarro, M. and Mira, A. 2014. Metatranscriptomics reveals overall active bacterial composition in caries lesions. *Journal of Oral Microbiology* 6(1), p. 25443.

Siqueira, J. 2001. Aetiology of root canal treatment failure: why well-treated teeth can fail. *International Endodontic Journal* 34(1), pp. 1–10.

Siqueira, J., Machado, A., Silveira, R., Lopes, H. and Uzeda, M. d. 1997. Evaluation of the effectiveness of sodium hypochlorite used with three irrigation methods in the elimination of enterococcus faecalis from the root canal, in vitro. *International Endodontic Journal* 30(4), pp. 279–282.

Siqueira, J. and Rôças, I. 2005. Uncultivated phylotypes and newly named species associated with primary and persistent endodontic infections. *Journal of Clinical Microbiology* 43(7), pp. 3314–3319.

Siqueira, J. F. 2002. Endodontic infections: Concepts, paradigms, and perspectives. *Oral Surgery, Oral Medicine, Oral Pathology, Oral Radiology, and Endodontology* 94(3), pp. 281–293.

Siqueira, J. F., Guimarães-Pinto, T. and Rôças, I. N. 2007a. Effects of chemomechanical preparation with 2.5% sodium hypochlorite and intracanal medication with calcium hydroxide on cultivable bacteria in infected root canals. *Journal of Endodontics* 33(7), pp. 800–805.

Siqueira, J. F., Magalhães, K. M. and Rôças, I. N. 2007b. Bacterial reduction in infected root canals treated with 2.5% naocl as an irrigant and calcium hydroxide/camphorated paramonochlorophenol paste as an intracanal dressing. *Journal of Endodontics* 33(6), pp. 667–672.

Siqueira, J. F., Rôças, I. N., Favieri, A. and Lima, K. C. 2000. Chemomechanical reduction of the bacterial population in the root canal after instrumentation and irrigation with 1%, 2.5%, and 5.25% sodium hypochlorite. *Journal of Endodontics* 26(6), pp. 331–334.

Sitkiewicz, I. 2017. How to become a killer, or is it all accidental? virulence strategies in oral streptococci. *Molecular Oral Microbiology* .

Sloan, A., Perry, H., Matthews, J. and Smith, A. 2000. Transforming growth factor-β isoform expression in mature human healthy and carious molar teeth. *The Histochemical Journal* 32(4), pp. 247–252.

Sloan, A., Shelton, R., Hann, A., Moxham, B. and Smith, A. 1998. An in vitro approach for the study of dentinogenesis by organ culture of the dentine–pulp complex from rat incisor teeth. *Archives of Oral Biology* 43(6), pp. 421–430.

Sloan, A. J. and Waddington, R. J. 2009. Dental pulp stem cells: what, where, how? *International Journal of Paediatric Dentistry* 19(1), pp. 61–70.

Smith, A. and Lesot, H. 2001. Induction and regulation of crown dentinogenesis: embryonic events as a template for dental tissue repair? *Critical Reviews in Oral Biology & Medicine* 12(5), pp. 425–437.

Smith, A. J., Cassidy, N., Perry, H., Bègue-Kirn, C., Ruch, J. V. and Lesot, H. 1995. Reactionary dentinogenesis. *The International Journal of Developmental Biology* 39(1), pp. 273–280.

Smith, A. J., Cassidy, N., Perry, H., Begue-Kirn, C., Ruch, J.-V. and Lesot, H. 2003. Reactionary dentinogenesis. *International Journal of Developmental Biology* 39(1), pp. 273–280.

Smith, A. J., Patel, M., Graham, L., Sloan, A. J. and Cooper, P. R. 2005. Dentine regeneration: key roles for stem cells and molecular signalling. *Oral Biosci Med* 2(2/3), pp. 127–132.

Smithson, J., Newsome, P., Reaney, D. and Owen, S. 2011. Direct or indirect restorations? *Int Dent-African Ed* 1(1).

Stewart, P. S. 2002. Mechanisms of antibiotic resistance in bacterial biofilms. *International Journal of Medical Microbiology* 292(2), pp. 107–113.

Straubinger, R. M. and Balasubramanian, S. V. 2005. Preparation and characterization of taxane-containing liposomes. *Methods in Enzymology* 391, pp. 97–117.

Stuart, C. H., Schwartz, S. A., Beeson, T. J. and Owatz, C. B. 2006. Enterococcus faecalis: its role in root canal treatment failure and current concepts in retreatment. *Journal of Endodontics* 32(2), pp. 93–98.

Suller, M. and Russell, A. 1999. Antibiotic and biocide resistance in methicillin-resistant staphylococcus aureus and vancomycin-resistant enterococcus. *Journal of Hospital Infection* 43(4), pp. 281–291.

Sun, J. and Song, X. 2011. Assessment of antimicrobial susceptibility of *Enterococcus faecalis* isolated from chronic periodontitis in biofilm versus planktonic phase. *Journal of Periodontology* 82(4), pp. 626–631.

Sutherland, I. W. 2001. The biofilm matrix: an immobilized but dynamic microbial environment. *Trends in Microbiology* 9(5), pp. 222–227.

Swain, M. V. and Xue, J. 2009. State of the art of micro-ct applications in dental research. *International Journal of Oral Science* 1(4), pp. 177–188.

Szabo, J., Trombitas, K. and Szabo, I. 1984. The odontoblast process and its branches in human teeth observed by scanning electron microscopy. *Archives of oral biology* 29(4), pp. 331–333.

Tabassum, S. and Khan, F. R. 2016. Failure of endodontic treatment: The usual suspects. *European Journal of Dentistry* 10(1), p. 144.

Takahashi, M., Shimazaki, M. and Yamamoto, J. 2001. Thermoreversible gelation and phase separation in aqueous methyl cellulose solutions. *Journal of Polymer Science Part B: Polymer Physics* 39(1), pp. 91–100.

Takahashi, N. and Nyvad, B. 2011. The role of bacteria in the caries process: ecological perspectives. *Journal of Dental Research* 90(3), pp. 294–303.

Tang, L., Sun, T.-Q., Gao, X.-J., Zhou, X.-D. and Huang, D.-M. 2011. Tooth anatomy risk factors influencing root canal working length accessibility. *International Journal of Oral Science* 3(3), pp. 135–140.

Tang, Y., Wang, X., Li, Y., Lei, M., Du, Y., Kennedy, J. F. and Knill, C. J. 2010. Production and characterisation of novel injectable chitosan/methylcellulose/salt blend hydrogels with potential application as tissue engineering scaffolds. *Carbohydrate Polymers* 82(3), pp. 833–841.

Tziafas, D. and Papadimitriou, S. 1998. Role of exogenous tgf-β in induction of reparative dentinogenesis in vivo. *European Journal of Oral Sciences* 106(S1), pp. 192–196.

Van der Hoeven, J., Toorop, A. and Mikx, F. 1978. Symbiotic relationship of veillonella alcalescens and streptococcus mutans in dental plaque in gnotobiotic rats. *Caries Research* 12(3), pp. 142–147.

Veerayutthwilai, O., Byers, M., Pham, T.-T., Darveau, R. and Dale, B. 2007. Differential regulation of immune responses by odontoblasts. *Molecular Oral Microbiology* 22(1), pp. 5–13.

Vertucci, F. J. 2005. Root canal morphology and its relationship to endodontic procedures. *Endodontic Topics* 10(1), pp. 3–29.

Vianna, M., Horz, H.-P., Conrads, G., Zaia, A., Souza-Filho, F. and Gomes, B. 2007. Effect of root canal procedures on endotoxins and endodontic pathogens. *Molecular Oral Microbiology* 22(6), pp. 411–418.

Vidana, R. 2015. *Origin of intraradicular infection with Enterococcus faecalis in endodontically treated teeth*. Inst för odontologi/Dept of Dental Medicine.

Vidana, R., Sullivan, Å., Billström, H., Ahlquist, M. and Lund, B. 2011. Enterococcus faecalis infection in root canals: host-derived or exogenous source? *Letters in Applied Microbiology* 52(2), pp. 109–115.

Vivacqua-Gomes, N., Gurgel-Filho, E., Gomes, B., Ferraz, C., Zaia, A. and Souza-Filho, F. 2005. Recovery of enterococcus faecalis after single-or multiple-visit root canal treatments carried out in infected teeth ex vivo. *International Endodontic Journal* 38(10), pp. 697–704.

Vyas, S., Sihorkar, V. and Mishra, V. 2000. Controlled and targeted drug delivery strategies towards intraperiodontal pocket diseases. *Journal of Clinical Pharmacy and Therapeutics* 25(1), pp. 21–42.

Wang, Q.-Q., Zhang, C.-F., Chu, C.-H. and Zhu, X.-F. 2012. Prevalence of enterococcus faecalis in saliva and filled root canals of teeth associated with apical periodontitis. *International Journal of Oral Science* 4(1), pp. 19–23.

Washington, C. 1989. Evaluation of non-sink dialysis methods for the measurement of drug release from colloids: effects of drug partition. *International Journal of Pharmaceutics* 56(1), pp. 71–74.

Weis, M. V., Parashos, P. and Messer, H. 2004. Effect of obturation technique on sealer cement thickness and dentinal tubule penetration. *International Endodontic Journal* 37(10), pp. 653–663.

Wichterle, O. and Lim, D. 1960. Hydrophilic gels for biological use. *Nature* 185(4706), pp. 117–118.

Wilcox, L. R., Roskelley, C. and Sutton, T. 1997. The relationship of root canal enlargement to finger-spreader induced vertical root fracture. *Journal of Endodontics* 23(8), pp. 533–534.

Williams, G. J. and Stickler, D. J. 2008. Effect of triclosan on the formation of crystalline biofilms by mixed communities of urinary tract pathogens on urinary catheters. *Journal of Medical Microbiology* 57(9), pp. 1135–1140.

Wright, P. P. and Walsh, L. J. 2017. Optimizing antimicrobial agents in endodontics. In: Kumavath, R. N., ed., *Antibacterial Agents*, Rijeka: InTech, chap. 05.

Xu, Y., Li, L., Zheng, P., Lam, Y. C. and Hu, X. 2004. Controllable gelation of methylcellulose by a salt mixture. *Langmuir* 20(15), pp. 6134–6138.

Zanini, M., Meyer, E. and Simon, S. 2017. Pulp inflammation diagnosis from clinical to inflammatory mediators: A systematic review. *Journal of Endodontics* .

Zehnder, M. and Guggenheim, B. 2009. The mysterious appearance of enterococci in filled root canals. *International Endodontic Journal* 42(4), pp. 277–87.

Zehnder, M., Kosicki, D., Luder, H., Sener, B. and Waltimo, T. 2002. Tissue-dissolving capacity and antibacterial effect of buffered and unbuffered hypochlorite solutions. *Oral Surgery, Oral Medicine, Oral Pathology, Oral Radiology, and Endodontology* 94(6), pp. 756–762.

Zeiger, A. S., Hinton, B. and Van Vliet, K. J. 2013. Why the dish makes a difference: quantitative comparison of polystyrene culture surfaces. *Acta Biomaterialia* 9(7), pp. 7354–7361.

Zero, D., Van Houte, J. and Russo, J. 1986. The intra-oral effect on enamel demineralization of extracellular matrix material synthesized from sucrose by streptococcus mutans. *Journal of Dental Research* 65(6), pp. 918–923.

Zhang, L., Pornpattananangkul, D., Hu, C.-M. and Huang, C.-M. 2010. Development of nanoparticles for antimicrobial drug delivery. *Current Medicinal Chemistry* 17(6), pp. 585–594.

Zuidema, J. M., Rivet, C. J., Gilbert, R. J. and Morrison, F. A. 2014. A protocol for rheological characterization of hydrogels for tissue engineering strategies. *Journal of Biomedical Materials Research Part B: Applied Biomaterials* 102(5), pp. 1063–1073.

Appendix A

Protocol used for bacterial DNA extraction

Extract taken from QIAmp DNA Mini and Blood Mini Handbook. Full handbook available at: https://www.qiagen.com/gb/shop/sample-technologies/dna/genomic-dna/qiaamp-dna-mini-kit/#resources - accessed 30/05/2017.

Protocol: DNA Purification from Tissues (QIAamp DNA Mini Kit)

This protocol is for purification of total (genomic, mitochondrial, and viral) DNA from tissues using the QIAamp DNA Mini Kit.

Important points before starting

- All centrifugation steps are carried out at room temperature (15–25°C).
- Use carrier DNA if the sample contains <10,000 genome equivalents (see page 17).
- Avoid repeated freezing and thawing of stored samples, since this leads to reduced DNA size.
- Transcriptionally active tissues, such as liver and kidney, contain high levels of RNA which will copurify with genomic DNA. RNA may inhibit some downstream enzymatic reactions, but will not inhibit PCR. If RNA-free genomic DNA is required, include the RNase A digest, as described in step 5a of the protocol.

Things to do before starting

- Equilibrate the sample to room temperature (15–25°C).
- Heat 2 water baths or heating blocks: one to 56°C for use in step 3, and one to 70°C for use in step 5.
- Equilibrate Buffer AE or distilled water to room temperature for elution in step 11.
- Ensure that Buffers AW1 and AW2 have been prepared according to the instructions on page 16.
- If a precipitate has formed in Buffer ATL or Buffer AL, dissolve by incubating at 56°C.

Procedure

1. **Excise the tissue sample or remove it from storage. Determine the amount of tissue. Do not use more than 25 mg (10 mg spleen).**

   Weighing tissue is the most accurate way to determine the amount.

   If DNA is prepared from spleen tissue, no more than 10 mg should be used.

   The yield of DNA will depend on both the amount and the type of tissue processed.

   1 mg of tissue will yield approximately 0.2–1.2 µg of DNA.

2. **Cut up (step 2a), grind (step 2b), or mechanically disrupt (step 2c) the tissue sample.**

   The QIAamp procedure requires no mechanical disruption of the tissue sample, but lysis time will be reduced if the sample is ground in liquid nitrogen (step 2b) or mechanically homogenized (step 2c) in advance.

2a. **Cut up to 25 mg of tissue (up to 10 mg spleen) into small pieces. Place in a 1.5 ml microcentrifuge tube, and add 180 µl of Buffer ATL. Proceed with step 3.**

   It is important to cut the tissue into small pieces to decrease lysis time.

   2 ml microcentrifuge tubes may be better suited for lysis.

2b. **Place up to 25 mg of tissue (10 mg spleen) in liquid nitrogen, and grind thoroughly with a mortar and pestle. Decant tissue powder and liquid nitrogen into 1.5 ml microcentrifuge tube. Allow the liquid nitrogen to evaporate, but do not allow the tissue to thaw, and add 180 µl of Buffer ATL. Proceed with step 3.**

2c. **Add up to 25 mg of tissue (10 mg spleen) to a 1.5 ml microcentrifuge tube containing no more than 80 µl PBS. Homogenize the sample using the TissueRuptor or equivalent rotor–stator homogenizer. Add 100 µl Buffer ATL, and proceed with step 3.**

   Some tissues require undiluted Buffer ATL for complete lysis. In this case, grinding in liquid nitrogen is recommended. Samples cannot be homogenized directly in Buffer ATL, which contains detergent.

3. **Add 20 µl proteinase K, mix by vortexing, and incubate at 56°C until the tissue is completely lysed. Vortex occasionally during incubation to disperse the sample, or place in a shaking water bath or on a rocking platform.**

   Note: Proteinase K must be used. QIAGEN Protease has reduced activity in the presence of Buffer ATL.

   Lysis time varies depending on the type of tissue processed. Lysis is usually complete in 1–3 h. Lysis overnight is possible and does not influence the preparation. To ensure efficient lysis, a shaking water bath or a rocking platform should be used. If not available, vortexing 2–3 times per hour during incubation is recommended.

4. **Briefly centrifuge the 1.5 ml microcentrifuge tube to remove drops from the inside of the lid.**

5. **If RNA-free genomic DNA is required, follow step 5a. Otherwise, follow step 5b.**

   Transcriptionally active tissues, such as liver and kidney, contain high levels of RNA which will copurify with genomic DNA. RNA may inhibit some downstream enzymatic reactions, but will not inhibit PCR.

5a. First add 4 µl RNase A (100 mg/ml), mix by pulse-vortexing for 15 s, and incubate for 2 min at room temperature (15–25°C). Briefly centrifuge the 1.5 ml microcentrifuge tube to remove drops from inside the lid before adding 200 µl Buffer AL to the sample. Mix again by pulse-vortexing for 15 s, and incubate at 70°C for 10 min. Briefly centrifuge the 1.5 ml microcentrifuge tube to remove drops from inside the lid.

It is essential that the sample and Buffer AL are mixed thoroughly to yield a homogeneous solution.

A white precipitate may form on addition of Buffer AL. In most cases it will dissolve during incubation at 70°C. The precipitate does not interfere with the QIAamp procedure or with any subsequent application.

5b. Add 200 µl Buffer AL to the sample, mix by pulse-vortexing for 15 s, and incubate at 70°C for 10 min. Briefly centrifuge the 1.5 ml microcentrifuge tube to remove drops from inside the lid.

It is essential that the sample and Buffer AL are mixed thoroughly to yield a homogeneous solution.

A white precipitate may form on addition of Buffer AL, which in most cases will dissolve during incubation at 70°C. The precipitate does not interfere with the QIAamp procedure or with any subsequent application.

6. Add 200 µl ethanol (96–100%) to the sample, and mix by pulse-vortexing for 15 s. After mixing, briefly centrifuge the 1.5 ml microcentrifuge tube to remove drops from inside the lid.

It is essential that the sample, Buffer AL, and the ethanol are mixed thoroughly to yield a homogeneous solution.

A white precipitate may form on addition of ethanol. It is essential to apply all of the precipitate to the QIAamp Mini spin column. This precipitate does not interfere with the QIAamp procedure or with any subsequent application.

Do not use alcohols other than ethanol since this may result in reduced yields.

7. Carefully apply the mixture from step 6 (including the precipitate) to the QIAamp Mini spin column (in a 2 ml collection tube) without wetting the rim. Close the cap, and centrifuge at 6000 x *g* (8000 rpm) for 1 min. Place the QIAamp Mini spin column in a clean 2 ml collection tube (provided), and discard the tube containing the filtrate.*

Close each spin column to avoid aerosol formation during centrifugation.

It is essential to apply all of the precipitate to the QIAamp Mini spin column.

Centrifugation is performed at 6000 x *g* (8000 rpm) to reduce noise. Centrifugation at full speed will not affect the yield or purity of the DNA. If the solution has not completely passed through the membrane, centrifuge again at a higher speed until all the solution has passed through.

* Flow-through contains Buffer AL or Buffer AW1 and is therefore not compatible with bleach. See page 6 for safety information.

8. **Carefully open the QIAamp Mini spin column and add 500 µl Buffer AW1 without wetting the rim. Close the cap, and centrifuge at 6000 x *g* (8000 rpm) for 1 min. Place the QIAamp Mini spin column in a clean 2 ml collection tube (provided), and discard the collection tube containing the filtrate.***
9. **Carefully open the QIAamp Mini spin column and add 500 µl Buffer AW2 without wetting the rim. Close the cap and centrifuge at full speed (20,000 x *g*; 14,000 rpm) for 3 min.**
10. **Recommended: Place the QIAamp Mini spin column in a new 2 ml collection tube (not provided) and discard the old collection tube with the filtrate. Centrifuge at full speed for 1 min.**

    This step helps to eliminate the chance of possible Buffer AW2 carryover.
11. **Place the QIAamp Mini spin column in a clean 1.5 ml microcentrifuge tube (not provided), and discard the collection tube containing the filtrate. Carefully open the QIAamp Mini spin column and add 200 µl Buffer AE or distilled water. Incubate at room temperature for 1 min, and then centrifuge at 6000 x *g* (8000 rpm) for 1 min.**
12. **Repeat step 11.**

    A 5 min incubation of the QIAamp Mini spin column loaded with Buffer AE or water, before centrifugation, generally increases DNA yield.

    A third elution step with a further 200 µl Buffer AE will increase yields by up to 15%.

    Volumes of more than 200 µl should not be eluted into a 1.5 ml microcentrifuge tube because the spin column will come into contact with the eluate, leading to possible aerosol formation during centrifugation.

    Elution with volumes of less than 200 µl increases the final DNA concentration in the eluate significantly, but slightly reduces the overall DNA yield (see Table 5, page 25). Eluting with 4 x 100 µl instead of 2 x 200 µl does not increase elution efficiency.

    For long-term storage of DNA, eluting in Buffer AE and placing at –30 to –15°C is recommended, since DNA stored in water is subject to acid hydrolysis.

    Yields of DNA will depend both on the amount and the type of tissue processed. 25 mg of tissue will yield approximately 10–30 µg of DNA in 400 µl of water (25–75 ng/µl), with an A_{260}/A_{280} ratio of 1.7–1.9.

    For more information about elution and how to determine DNA yield, length, and purity, refer to pages 24–25 and Appendix A, page 50.

* Flow-through contains Buffer AL or Buffer AW1 and is therefore not compatible with bleach. See page 6 for safety information.

Appendix B

DNA sequences of 16S rRNA region of *E. faecalis* and *S. anginosus*

***E. faecalis* RB17**

D88

G C A C C C A G G G C A T G C G G G C T A T A A T G C A G T C G A C G C T T
C T T T C C T C C C G A G T G C T T G C A C T C A A T T G G A A A G A G G A
G T G G C G G A C G G G T G A G T A A C A C G T G G G T A A C C T A C C C
A T C A G A G G G G G A T A A C A C T T G G A A A C A G G T G C T A A T A
C C G C A T A A C A G T T T A T G C C G C A T G G C A T A A G A G T G A A A
G G C G C T T T C G G G T G T C G C T G A T G G A T G G A C C C G C G G T
G C A T T A G C T A G T T G G T G A G G T A A C G G C T C A C C A A G G C
C A C G A T G C A T A G C C G A C C T G A G A G G G T G A T C G G C C A C
A C T G G G A C T G A G A C A C G G C C C A G A C T C C T A C G G G A G G
C A G C A G T A G G G A A T C T T C G G C A A T G G A C G A A A G T C T G
A C C G A G C A A C G C C G C G T G A G T G A A G A A G G T T T T C G G A
T C G T A A A A C T C T G T T G T T A G A G A A G A A C A A G G A C G T T
A G T A A C T G A A C G T C C C C T G A C G G T A T C T A A C C A G A A A G
C C A C G G C T A A C T A C G T G C C A G C A G C C G C G G T A A T A C G T
A G G T G G C A A G C G T T G T C C G G A T T T A T T G G G C G T A A A G
C G A G C G C A G G C G G T T T C T T A A G T C T G A T G T G A A A G C C
C C C G G C T C A A C C G G G G A G G G T C A T T G G A A A C T G G G A G
A C T T G A G T G C A G A A G A G G A G A G T G G A A T T C C A T G T G T
A G C G G T G A A A T G C G T A G A T A T A T G G A G G A A C A C C A G T
G G C G A A G G C G G C T C T C T G G T C T G T A A C T G A C G C T G A G
G C T C G A A A G C G T G G G G A G C A A A C A G G A T T A G A T A C C C
T G G T A G T C C A C G C C G T A A A C G A T G A G T G C T A A G T G T T
G G A G G G T T T C C C G C C C T T T C A G T G C T G C A G C A A A C G C A
T T A A G C A C T C C G C C C T G G G G A G T A C G A C C C G C A A G G T
T G A A C T C A A A G G A T G A C G G G G G G C C C G C C A C A G C G T G C
A G C A T G T G A T T A A T T C G A G C A A C G C G A G G A T C T A C A G
T C T T G G A A C A T C G T T G G A A C C A C T C T C C C T T G G G G A G G A

E94

A A T G T G A C C C G T A G G T C T T G T A G A C T T C A C C C C A A T C A

T C T A T C C C A C C T T A G G C G G C T G G C T C C A A A A A G G T T A
C C T C A C C G A C T T C G G G T G T T A C A A A C T C T C G T G G T G T
G A C G G G C G G T G T G T A C A A G G C C C G G G A A C G T A T T C A C
C G C G G C G T G C T G A T C C G C G A T T A C T A G C G A T T C C G G C
T T C A T G C A G G C G A G T T G C A G C C T G C A A T C C G A A C T G A
G A G A A G C T T T A A G A G A T T T G C A T G A C C T C G C G G T C T A
G C G A C T C G T T G T A C T T C C C A T T G T A G C A C G T G T G T A G
C C C A G G T C A T A A G G G G C A T G A T G A T T T G A C G T C A T C C
C C A C C T T C C T C C G G T T T G T C A C C G G C A G T C T C G C T A G A
G T G C C C A A C T A A A T G A T G G C A A C T A A C A A T A A G G G T T
G C G C T C G T T G C G G G A C T T A A C C C A A C A T C T C A C G A C A
C G A G C T G A C G A C A A C C A T G C A C C A C C T G T C A C T T T G T C
C C C G A A G G G A A A G C T C T A T C T C T A G A G T G G T C A A A G G
A T G T C A A G A C C T G G T A A G G T T C T T C G C G T T G C T T C G A
A T T A A A C C A C A T G C T C C A C C G C T T G T G C G G G C C C C C G T
C A A T T C C T T T G A G T T T C A A C C T T G C G G T C G T A C T C C C C
A G G C G G A G T G C T T A A T G C G T T T G C T G C A G C A C T G A A G
G G C G G A A A C C C C T C C A A C A C T T A G C A C T C A T C G T T T A C G
G C G T G G A C T A C C A G G G T A T C T A A T C C T G T T T G C T C C C
C A C G C T T T C G A G C C T C A G C G T C A G T T A C A G A C C A G A G
A G C C G C C T T C G C C A C T G G T G T T C C T C C A T A T A T C T A C
G C A T T T C A C C G C T A C A C A T G G A A A T T C C A C T C T C C T C
T T C T G C A C T C A A G T C T C C A G T T T C C A A T G A C C C T C C C
C G G G T T G A G C C G G G G G C T T T C A C A T C A G A C T T A A G A A
A C C G C T G C G C T C G C T T T A C G C C C A A T A A T C T G A C C A C
G C T G C C A C C T A C G T A A T T A C C C G G C C G G G C T G T G C C C T T G

***S. anginosus* 39/2/14A**
D88
T C A A C A G C G C T G C T A T A C A T G C A G T A G G A C G C A C A G T
T T A T A C C G T A G C T T G C T A C A C C A T A G A C T G T G A G T T G
C G A A C G G G T G A G T A A C G C G T A G G T A A C C T A C C T A T T A
G A G G G G G A T A A C T A T T G G A A A C G A T A G C T A A T A C C G C
A T A A C A G T A T G T A A C A C A T G T T A G A T G C T T G A A A G A T
G C A A T T G C A T C G C T A G T A G A T G G A C C T G C G T T G T A T T
A G C T A G T A G G T A G G G T A A T G G C C T A C C T A G G C A A C G A
T A C A T A G C C G A C C T G A G A G G G T G A T C G G C C A C A C T G G
G A C T G A G A C A C G G C C C A G A C T C C T A C G G G A G G C A G C A
G T A G G G G A A T C T T C G G C A A T G G G G G G A A C C C T G A C C G A
G C A A C G C C G C G T G A G T G A A G A A G G T T T T C G G A T C G T A
A A G C T C T G T T G T T A A G G A A G A A C G A G T G T G A G A A T G G
A A A G T T C A T G C T G T G A C G G T A C T T A A C C A G A A A G G G A
C G G C T A A C T A C G T G C C A G C A G C C G C G G T A A T A C G T A G
G T C C C G A G C G T T G T C C G G A T T T A T T G G G C G T A A A G C G
A G C G C A G G C G G T T A G A A A A G T C T G A A G T G A A A G G C A G
T G G C T C A A C C A T T G T A G G C T T T G G A A A C T G T T T A A C T
T G A G T G C A G A A G G G G A G A G T G G A A T T C C A T G T G T A G C
G G T G A A A T G C G T A G A T A T A T G G A G G A A C A C C G G T G G C
G A A A G C G G C T C T C T G G T C T G T A A C T G A C G C T G A G C T C
G A A A G C G T G G G G A G C G A A C A G G A T T A G A T A C C C T G G T

A G T C C A C G C C G T A T A C G A T G A G T G C T A G T G T T A G G T C
C T T T C C T G G A C T T A G T G C G C A G C T A C G C A T T A A G C A C T
C C C G C C T G G G G G A G T A C G A C C G C A A G G T T G A A C T T C A
A A G G A A A T G A A A C T G G G G G C C G C C C C A A C C G T G T G A G
A C A C A G T G G T T A T A T T C A G C A C A C C G C C G A A A C A T A C
A G C C G T G T G A C T T C C A C T G T A C A C T C G C G C T C T A C A G C G A

E94
G T G G C T A G C T C T G C T C G A C T T C A C C C C A T C A T C T A T C
C C A C C T T A G G C G G G C T G G C T C C T T A C G G T T A C C T C A C C
G A C T T C G G G T G T T A C A A A C T C T C G T G G T G T G A C G G G C
G G T G T G T A C A A G G C C C G G G G A A C G T A T T C A C C G C G G C G
T G C T G A T C C G C G A T T A C T A G C G A T T C C G A C T T C A T G T
A G G C G A G T T G C A G C C T A A C A A T C C G A A C T G A G A C T G G
C T T T C A G A G A T T A G C T T G C C G T C A C C G G C T T G C G A C T
C G T T G T A C C A G C C A T T G T A G C A C G T G T G T A G C C C A G G
T C A T A A G G G G G C A T G A T G A T T T G A C G T C A T C C C C A C C T
T C C T C C G G T T T A T T A C C G G C A G T C T C G C T A G A G T G C C
C A A C T C A A T G A T G G C A A C T A A C A A T A A G G G
T T G C G C T C G T T G C G G G A C T T A A C C C A A C A T C T C A C G
A C A C G A G C T G A C G A C A A C C A T G C A C C A C C T G T C A C C A
G T G C C C C G A A G G G G A A A C C C T A T C T C T A G G G C A G T C A C
T G G G A T G T C A A G A C C T G G T A A G G T T C T T C G C G T T G C T
T C G A A T T A A A C C A C A T G C T C C A C C G C T T G T G C G G G C C
C C C G T C A A T T C C T T T G A G T T T C A A C C T T G C G G T C G T A
C T C C C C A G G C G G A G T G C T T A A T G C G T T A G C T G C G G C A
C T A A G T C C C G G A G A G G A C C T A A C A C C T A G C A C T C A T C
G T T T A C G G C G T G T A C T A C C A G G T A T C T A A T C C T G T T C
G C T C C C C A C G C T T T C G A G C C T C A G C G T C A G T T A C A G A
C C A G A G A G C C G C T T T C G C C A C C G G T G T T C C T C C A T A T
A T C T A C G C A T T T C A C C G C T A C A C A T G G T A T T C C A C T C
T C C C C T T C T G C A C T C A G T T A A A C A G T T C C A A G C C T A C
A A T G G T T G G A G C A C T G C C T T T C A C T T C G A C A T T T T T T
T T A C G C C G C G C G C T C G C G T T T T T A T G C C A C A T A A T C C
G T A A C A A G C A T T G G A C G C T C G C T C T A T T A T A T A T C C G
G C T G C T C G T G G G C A

Appendix C

Phospholipid assay protocol

Accessed from:
http://www.sigmaaldrich.com/content/dam/sigma-aldrich/docs/Sigma/Bulletin/2/mak122bul.pdf
- 13/11/2017.

SIGMA-ALDRICH®

sigma-aldrich.com

3050 Spruce Street, St. Louis, MO 63103 USA
Tel (800) 521-8956 (314) 771-5765 Fax (800) 325-5052 (314) 771-5757
email: techservice@sial.com sigma-aldrich.com

Product Information

Phospholipid Assay Kit

Catalog Number **MAK122**
Storage Temperature –20 °C

TECHNICAL BULLETIN

Product Description

Phospholipids are a class of lipids, which constitute a major component of cell membranes and play important roles in signal transduction. Most phospholipids contain one diglyceride, a phosphate group, and one choline.

The Phospholipid Assay Kit provides a simple, direct, and high-throughput assay for measuring choline-containing phospholipids in biological samples. In this assay, phospholipids (such as lecithin, lysolecithin, and sphingomyelin) are enzymatically hydrolyzed to release choline, which is determined using choline oxidase and a H_2O_2 specific dye. This results in a colorimetric (570 nm)/fluorometric (λ_{ex} = 530/λ_{em} = 585 nm) product directly proportional to the phospholipid concentration in the sample. The range of linear detection is 3–200 µM for colorimetric assays and 0.6–20 µM for fluorometric assays.

Components

The kit is sufficient for 100 assays in 96 well plates.

Assay Buffer Catalog Number MAK122A	10 mL
Enzyme Mix Catalog Number MAK122B	1 vl
Phosphatidylcholine Standard, 2 mM Catalog Number MAK122C	400 µL
PLD Enzyme Catalog Number MAK122D	120 µL
Dye Reagent Catalog Number MAK122E	120 µL

Reagents and Equipment Required but Not Provided.

- 96 well flat-bottom plate – It is recommended to use black plates with clear bottoms for fluorescence assays and clear plates for colorimetric assays.
- Fluorescence or spectrophotometric multiwell plate reader

Precautions and Disclaimer

This product is for R&D use only, not for drug, household, or other uses. Please consult the Material Safety Data Sheet for information regarding hazards and safe handling practices.

Preparation Instructions

Use ultrapure water for the preparation of reagents. Equilibrate all components to room temperature before use. Briefly centrifuge vials before opening. Keep thawed tubes on ice during assay.

Enzyme Mix – Reconstitute in 120 µL of Assay Buffer. Mix well by pipetting, then aliquot and store at –20 °C. Use within 1 month of reconstitution and keep cold while in use.

A precipitate may be present in the reconstituted aliquot. Gently centrifuge the vial and use the supernatant in the Reaction Mixes.

Storage/Stability

The kit is shipped on dry ice and storage at –20 °C, protected from light, is recommended.

Use within 1 month of reconstitution and keep cold while in use.

2

Procedure
All samples and standards should be run in duplicate.

Standards for Colorimetric Detection
Add 24 µL of the 2 mM Phosphatidylcholine Standard to 216 µL of water to prepare a 200 µM standard working solution. Add 0, 30, 60, and 100 µL of the 200 µM standard working solution into tubes. Add water to each tube to bring the volume to 100 µL, generating 0 (blank), 60, 120, and 200 µM standards. Transfer 20 µL of standards into separate wells of 96 well plate.

Standards for Fluorometric Detection
Prepare Standards as described for the Colorimetric Detection. Further dilute each standard 10-fold with water, generating 0 (blank), 6, 12, and 20 µM standards. Transfer 20 µL of standards into separate wells of 96 well plate.

Sample Preparation
Thiol (SH) group containing reagents (e.g., DTT, mercaptoethanol), sodium azide, EDTA, and sodium dodecyl sulfate may interfere with this assay and should be avoided in sample preparation.

Liquid samples such as serum and plasma can be assayed directly. Solid samples can be homogenized in the assay buffer. Aliquot 20 µL of each sample into two separate wells of a 96 well plate.

Notes: If a sample is known to contain choline, prepare a sample blank well with 20 µL of the sample.

For unknown samples, it is suggested to test several sample dilutions to ensure the readings are within the linear range of the standard curve.

Assay Reaction
1. Set up the Reaction Mixes according to the scheme in Table 1. 80 µL of the appropriate Reaction Mix is required for each reaction (well). Allow the Reaction Mixes to equilibrate to room temperature.

Table 1.
Reaction Mixes

Reagent	Sample and Standards	Sample Blank
Assay Buffer	85 µL	86 µL
Enzyme Mix	1 µL	1 µL
PLD Enzyme	1 µL	–
Dye Reagent	1 µL	1 µL

2. Add 80 µL of the appropriate Reaction Mix to each wells. Mix well using a horizontal shaker or by pipetting, and incubate the reaction 30 minutes at room temperature. Protect the plate from light during the incubation.

   Note: If precipitation occurs with certain samples, carry out the reaction in centrifuge tubes. After the 30 minute incubation, centrifuge for 5 minutes at 14,000 rpm. Transfer the supernatant into the wells to measure absorbance.

3. Measure the absorbance of the samples and standards at 570 nm for the colorimetric assay or the fluorescence intensity (λ_{ex} = 530/λ_{em} = 585 nm) for the fluorometric assay.

   Note: If the calculated phospholipid concentration of a sample is higher than 200 µM in the colorimetric assay or 20 µM in the fluorometric assay, dilute sample in 0.5% Triton™ X-100 and repeat the assay. Multiply result by the dilution factor.

Results

Calculations

Subtract blank value (0 standard) from the standard values and plot the absorbance or fluorescence measured for each standard against the standard concentrations. Determine the slope and use to calculate the phospholipid concentration of the sample.

Note: A new standard curve must be set up each time the assay is run.

Concentration of Phospholipid

The concentration of phospholipid in the sample can be calculated using the equation below.

$$\mu M = \frac{M_{sample} - M_{blank}}{Slope} \times n$$

M_{sample} = Absorbance or fluorescent intensity measured in unknown sample

M_{blank} = Absorbance or fluorescent intensity measured in blank (0 Standard, or sample blank if sample contains choline)

Slope = Determined from standard curve (μM^{-1})

n = Dilution factor (if used)

4

Troubleshooting Guide

Problem	Possible Cause	Suggested Solution
Assay not working	Cold assay buffer	Assay Buffer must be at room temperature
	Omission of step in procedure	Refer and follow Technical Bulletin precisely
	Plate reader at incorrect wavelength	Check filter settings of instrument
	Type of 96 well plate used	For fluorescence assays, use black plates with clear bottoms. For colorimetric assays, use clear plates
Samples with erratic readings	Samples prepared in different buffer	Use the Assay Buffer provided or refer to Technical Bulletin for instructions
	Cell/Tissue culture samples were incompletely homogenized	Repeat the sample homogenization, increasing the length and extent of homogenization step
	Samples used after multiple freeze-thaw cycles	Aliquot and freeze samples if needed to use multiple times
	Presence of interfering substance in the sample	If possible, dilute sample further
	Use of old or inappropriately stored samples	Use fresh samples and store correctly until use
Lower/higher readings in samples and standards	Improperly thawed components	Thaw all components completely and mix gently before use
	Use of expired kit or improperly stored reagents	Check the expiration date and store the components appropriately
	Allowing the reagents to sit for extended times on ice	Prepare fresh Master Reaction Mix before each use
	Incorrect incubation times or temperatures	Refer to Technical Bulletin and verify correct incubation times and temperatures
	Incorrect volumes used	Use calibrated pipettes and aliquot correctly
Non-linear standard curve	Use of partially thawed components	Thaw and resuspend all components before preparing the reaction mix
	Pipetting errors in preparation of standards	Avoid pipetting small volumes
	Pipetting errors in the Reaction Mix	Prepare a Master Reaction Mix whenever possible
	Air bubbles formed in well	Pipette gently against the wall of the plate well
	Standard stock is at incorrect concentration	Refer to the standard dilution instructions in the Technical Bulletin
	Calculation errors	Recheck calculations after referring to Technical Bulletin
	Substituting reagents from older kits/lots	Use fresh components from the same kit
Unanticipated results	Samples measured at incorrect wavelength	Check the equipment and filter settings
	Samples contain interfering substances	If possible, dilute sample further
	Sample readings above/below the linear range	Concentrate or dilute samples so readings are in the linear range

Triton is a trademark of The Dow Chemical Company or an affiliated company of Dow.

KVG,LS,MF,MAM 10/15-1